

UNIVERSITY OF NAPLES FEDERICO II



DEPARTMENT OF PHARMACY

PhD programme in Pharmaceutical Sciences

***TH17 AND IL-17 PATHWAY IN INFLAMMATION AND
INFLAMMATORY-RELATED DISEASES***

**PhD student
FEDERICA RAUCCI**

**Coordinator
Prof.
ROSARIA MELI**

**Tutor
Prof.
FRANCESCO MAIONE**

XXXV CYCLE (2019-2022)

*“Don’t be scared to miss the penalty kick:
it is not by these details that you judge a player;
you see a player by his courage, altruism, and fantasy”*
(Francesco De Gregori)

To me, who became a courageous, altruistic, and creative player
To all of you, who helped me become a good player

*“Non aver paura di sbagliare un calcio di rigore:
non è mica da questi particolari che si giudica un giocatore;
un giocatore lo vedi dal coraggio, dall’altruismo e dalla fantasia”*
(Francesco De Gregori)

A me, che sono diventata una giocatrice coraggiosa, altruista e fantasiosa
A tutti voi, che mi avete aiutata a diventare una buona giocatrice

INDEX

ABSTRACT	1
GRAPHICAL ABSTRACT	4
ABBREVIATIONS	5
CHAPTER 1: INTRODUCTION	8
1. IL-17 IN CHRONIC INFLAMMATION FROM DISCOVERY TO TARGET: FOCUS ON MPGES-1/PPAR- γ PATHWAY.....	8
1.1 IL-17 and IL-17R family members.....	8
1.2 IL-17 in acute and chronic inflammation.....	10
1.3 IL-17 and mPGES-1/PPAR- γ pathway.....	12
2. ROLE OF IL-17 IN GOUTY ARTHRITIS	15
3. THE ROLE OF IL-17 IN INFLAMMATORY DISEASES: PRE- CLINICAL ASSESSMENT OF A NOVEL MONOCLONAL ANTIBODY.....	18
3.1 Clinical results with inhibitors of IL-17 or IL-17R and pre- clinical assessment of a novel monoclonal antibody.....	18
EXPERIMENTAL SECTION	22
CHAPTER 2: MATERIALS AND METHODS	23
1. MATERIALS.....	23
2. HUMAN BLOOD SAMPLES.....	23
3. CELL CULTURE.....	24
3.1 Mouse macrophage cell line.....	24
3.2 Mouse embryonic fibroblast cell line.....	24
3.3 Human monocyte-derived macrophages (hMDMs) isolation and differentiation.....	25
3.4 Human dermal blood endothelial cells (HDBEC).....	26
3.5 Neutrophil isolation.....	26

3.6 Isolation of human fibroblasts.....	26
4. ANIMALS.....	27
5. <i>IN VIVO</i> MODELS.....	27
5.1 Air Pouch.....	27
5.2 Gouty Arthritis.....	28
5.2.1 Preparation of MSU crystals.....	28
5.2.2 Induction of MSU-induced knee joint inflammation.....	29
5.2.3 Joint scoring and evaluation.....	29
5.2.4 Isolation of joint-infiltrating cells.....	30
5.3 Antigen induced-arthritis.....	30
6. <i>IN VITRO</i> AND <i>EX VIVO</i> ANALYSIS.....	31
6.1 Myeloperoxidase assay.....	31
6.2 Elisa and ElisaSpot assay.....	31
6.3 Flow cytometry.....	32
6.4 Western blot analysis.....	34
6.5 Histology.....	35
6.6 Elisa-based binding assay.....	35
6.7 Transwell migration assay.....	36
7. DEVELOPMENT OF A NOVEL NEUTRALIZING ANTIBODY.....	36
7.1 Peptide synthesis and purification.....	36
7.2 Immunization and fusion protocols.....	38
8. STATISTICAL ANALYSIS.....	39
CHAPTER 3: RESULTS.....	40
1. IL-17-INDUCED INFLAMMATION MODULATES THE MPGES-1/PPAR- γ PATHWAY IN MONOCYTES/ MACROPHAGES.....	40

1.1 PF 9184 and Troglitazone, in a time- and dose-dependent manner, revert leukocytes accumulation and activation at the site of inflammation.....	40
1.2 mPGES-1 and PPAR- γ enzymatic pathway modulation on the onset of ongoing inflammation.....	44
1.3 PF 9184 and Troglitazone selectively modulate the recruitment of inflammatory monocytes	48
1.4 Co-administration of PF 9184 and Troglitazone with IL-17 into the air pouch decreases the release of cyto-chemokines in the inflammatory fluids.....	53
1.5 Protective effect of PF 9184 and Troglitazone on murine macrophages.....	56
2. IL-17 NEUTRALIZING ANTIBODY REGULATES MONOSODIUM URATE CRYSTAL-INDUCED GOUTY INFLAMMATION.....	59
2.1 Neutralization of IL-17 reduces the severity of MSU-induced gouty inflammation.....	59
2.2 IL-17Ab ameliorates MSU-induced leukocytes recruitment and activation in the knee joints	61
2.3 Injection of IL-17Ab into the knee joints reduces the recruitment of inflammatory monocytes	64
2.4 <i>In situ</i> administration of MSU and IL-17Ab influences systemic Th17 and Treg balance	68
3. DESIGN OF THE MOST ACTIVE SEQUENCE OF IL-17A/F AND BIOLOGICAL CHARACTERIZATION OF A NOVEL MONOCLONAL NEUTRALIZING ANTIBODY.....	71
3.1 Synthesis and biological characterization of the most active sequence of IL-17A/F.....	71

3.2 nIL-17 TM exerts a more prominent leukocytes recruitment and cyto-chemokines production next to IL-17 full-length protein on <i>in vivo</i> model of chronic inflammation.....	76
3.3 Biological characterization of a novel IL-17 neutralizing antibody (Ab-IPL-IL-17 TM).....	79
CHAPTER 4: DISCUSSION AND CONCLUSIONS.....	86
1. IL-17-INDUCED INFLAMMATION MODULATES THE MPGES-1/PPAR- γ PATHWAY IN MONOCYTES/MACROPHAGES.....	86
1.1 Conclusions.....	90
2. IL-17 NEUTRALIZING ANTIBODY REGULATES MONOSODIUM URATE CRYSTAL-INDUCED GOUTY INFLAMMATION.....	92
2.1 Conclusions.....	96
3. DESIGN OF THE MOST ACTIVE SEQUENCE OF IL-17A/F AND BIOLOGICAL CHARACTERIZATION OF A NOVEL MONOCLONAL NEUTRALIZING ANTIBODY.....	98
3.1 Conclusions.....	101
CHAPTER 5: GENERAL CONCLUSIONS.....	104
CHAPTER 6: SUPPLEMENTARY FIGURES.....	106
CHAPTER 7: SCIENTIFIC REPORTS.....	132
ACKNOWLEDGEMENTS.....	140
CONFLICT OF INTEREST.....	140
DATA AVAILABILITY STATEMENT.....	140
REFERENCES.....	141
PERSONAL ACKNOWLEDGEMENTS.....	156

ABSTRACT

IL-17 (IL-17A, originally called CTLA-8) was cloned in 1993, but its functions remained obscure for a decade. In 2005, IL-17 became prominent with the discovery of a new population of CD4⁺ T helper (Th) cells characterized by the expression of IL-17. This subset became known as Th17 cells, and a plethora of literature has since been devoted to understanding the mechanisms that direct the development, differentiation, and regulation of this lineage. Although Th17 cells are typically considered the principal source of IL-17, CD8⁺ cells have also been shown to make this cytokine. In addition, several innate immune cells produce this cytokine, including neutrophils, macrophages, innate-acting lymphocytes such as $\gamma\delta$ T cells, some natural killer T cells (NKT), and IL-17-expressing type 3 innate lymphoid cells (ILC3s). Collectively, IL-17-producing cells, whether adaptive or innate, are often termed type 17.

IL-17 is a cytokine that elicits protection against extracellular bacterial and fungal infections and plays an important role in inflammation. However, when produced in excess, it contributes to chronic inflammation associated with many inflammatory and autoimmune disorders. Indeed, the localized and prolonged release of IL-17 in specific tissues has been associated with increased severity of the inflammatory response that remains sustained over time. The cellular and molecular mechanisms behind these effects are far from being clear. This has made IL-17 an attractive therapeutic target.

Antibodies targeting IL-17 (secukinumab and ixekizumab) were approved in 2016 to treat moderate to severe plaque psoriasis. However, the efficacy of IL-17 blockade for other conditions has been less dramatic, although there are promising data from trials in ankylosing

spondylitis and psoriatic arthritis. Disappointingly and somewhat surprisingly, trials of secukinumab and brodalumab (anti-IL-17RA) in Crohn's disease were terminated early due to the worsening of the disease in the treatment group. An explanation for this paradox came from studies in mice showing a dominant protective role for IL-17 in maintaining intestinal barrier integrity that apparently outweighs its tissue-damaging potential in inflammatory bowel diseases. Thus, targeting IL-17 is an effective therapy for specific conditions, but its clinical use has revealed new insights into how Th17 cells function in humans.

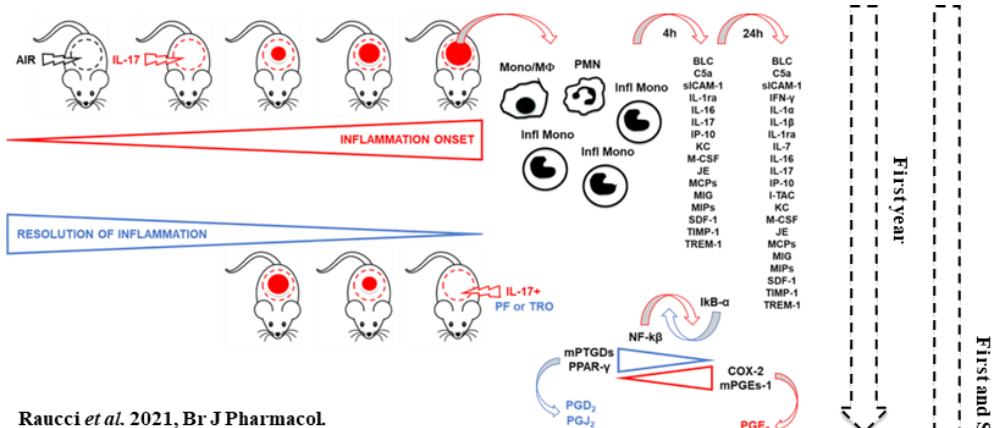
Since the IL-17 discovery, much attention has been given to mediators and factors responsible for the development of IL-17-producing cells, while very few studies have investigated the inflammatory properties of this cytokine. However, recent biochemical and pharmacological studies have reported that in several tissues and cell types, microsomal PGE₂ synthase (mPGES) and peroxisome proliferator-activated receptor γ (PPAR- γ) expression are modulated by a variety of inflammatory factors and stimuli. Considering that very little is known about the biological effects promoted by IL-17 in the context of mPGES-1/PPAR- γ modulation, this PhD thesis reports ours *in vitro* and *in vivo* evidence that defines the functional coordinate regulation between these two enzymes at the "crossroads of phlogistic pathway" involved in the induction and resolution of inflammation (the first and the second year of PhD).

The latter part of the thesis (the third year of PhD and PhD visiting program in the UK) is dedicated to the design of peptide molecules that could be easily synthesized and used as a stable surrogate of IL-17. Specifically, a 20 amino acid peptide (here referred to as nIL-17TM) that retains the primary biological function of the parental molecule has been

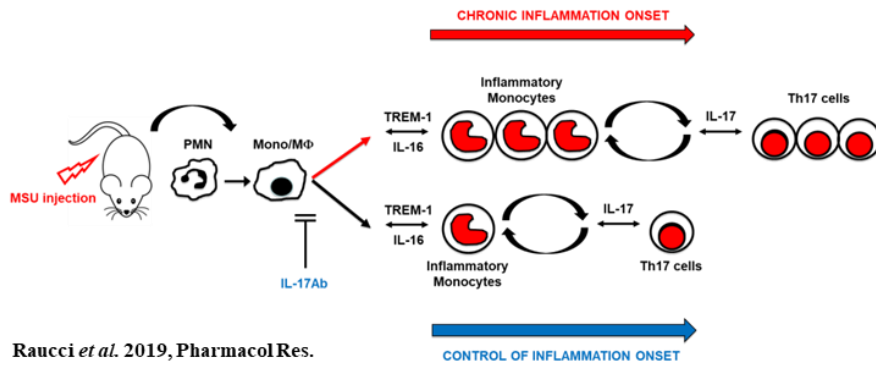
identified. The peptide was tested in both *in vitro* and *in vivo* models of inflammation, and it has been biologically validated in both murine and human cellular systems (neutrophils and macrophages). In addition, enzymatic binding assays were contextually performed to evaluate the peptide's binding affinity on IL-17 receptors (both IL-17RA and IL-17RC).

Finally, last but not least of importance, we describe the synthesis and main pharmacological properties of a novel patented IL-17 neutralizing antibody (here referred to as Ab-IPL-IL-17TM) that displayed significant activity on both murine and human biological systems. Also, we describe the efficacy of Ab-IPL-IL-17TM on fibroblasts from Rheumatoid Arthritis (RA) patients. Taken together, our evidence paves the way for discovering new therapeutic approaches to immune-based and inflammatory-related diseases.

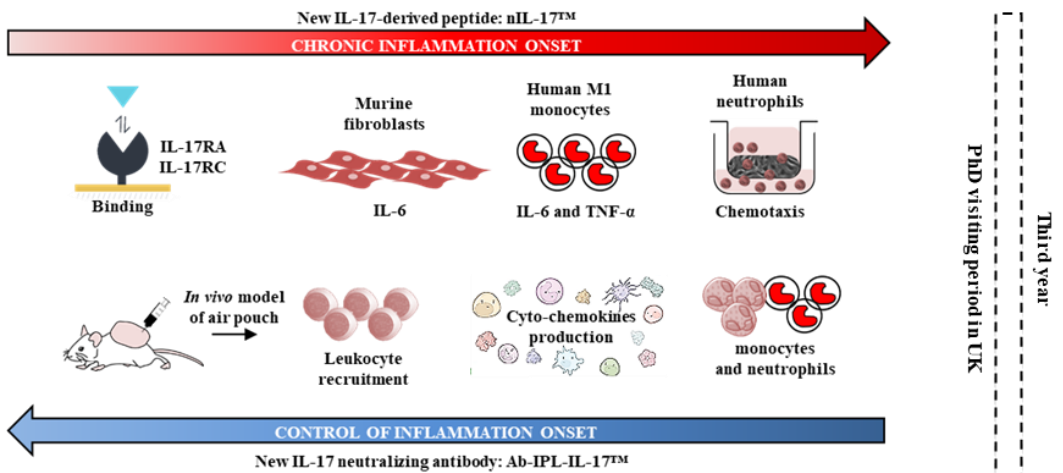
GRAPHICAL ABSTRACT



Rauci *et al.* 2021, Br J Pharmacol.



Rauci *et al.* 2019, Pharmacol Res.



Rauci *et al.* 2022, Data Submitted

ABBREVIATIONS

15d-PGJ₂, 15-deoxy- Δ 12,14-prostaglandin J₂;
Ab-IPL-IL-17TM, novel IL-17 neutralizing antibody;
AF, AF 3485;
AS, Ankylosing Spondylitis;
AUC, area under the curve;
BLC, B lymphocyte chemoattractant;
C5a, complement component 5a;
CD, Crohn's disease;
CD99, cluster of differentiation 99;
CFA, complete Freund's adjuvant;
CMC, carboxymethyl cellulose;
CoA, Certificate of Analysis;
COXs, cyclooxygenases;
cPGES, cytosolic prostaglandin E₂ synthase;
CTLA8, cytotoxic T lymphocyte-associated antigen 8;
CTRL, Control;
DMEM, Dulbecco's modified Eagle's medium;
DN, denatured;
EGF, epidermal growth factor;
FBS, fetal bovine serum;
fMLP, formyl-methionyl-leucyl-phenylalanine;
GA, gouty arthritis;
GRO- α , growth-regulated oncogene- α ;
G-CSF, granulocyte colony-stimulating factor;
H&E, haematoxylin and eosin;
HDBECs, human dermal blood endothelial cells;
hMDMs, human monocyte-derived macrophages;

i.a., intra-articular;
IBD, inflammatory bowel disease;
IFN γ , interferon gamma;
IL-, Interleukin-;
ILC3, 3 innate lymphoid cell;
IL-R, IL- Receptor;
IMIDs, immune-mediated inflammatory diseases;
IP-10, interferon γ -induced protein-10;
ITAC, interferon-inducible T-cell α chemoattractant;
I κ B- α , nuclear factor kappa-B inhibitor α ;
JE, junctional epithelium;
KC, keratinocyte chemoattractant;
LPS, lipopolysaccharides;
LTs, leukotrienes;
mAbs, monoclonal antibodies;
MAP, mitogen-activated protein;
mBSA, methylated bovine serum albumin;
MCP-, monocyte chemoattractant protein-;
MCSF, macrophage colony-stimulating factor;
MIG, monokine induced by interferon γ ;
MIPs, macrophage inflammatory proteins;
MMP-, matrix metalloproteinase;
mPGES, microsomal prostaglandin E₂ synthase;
MPO, myeloperoxidase;
mPTGDS-1, microsomal prostaglandin D₂ synthase-1;
MSU, monosodium urate;
NF- κ B, nuclear factor kappa B;
nIL-17TM, novel IL-17-derived peptide;

NKT, natural killer T cells;
NSAID, nonsteroidal anti-inflammatory drugs;
OA, Osteoarthritis;
PBMC, peripheral blood mononuclear cell;
PECAM-1, platelet endothelial cell adhesion molecule 1;
PF, PF 9184;
PGs, prostaglandins;
PMN, polymorphonuclear leukocyte;
PPAR- γ , peroxisome proliferator-activated receptor- γ ;
Ps, Psoriasis;
PsA, Psoriatic Arthritis;
PUFA, polyunsaturated fatty acid;
RA, Rheumatoid Arthritis;
Res, resolving arthritis;
SC, scrambled;
SDF-1, stromal cell-derived factor-1;
SEFIR, SEF/IL-17R;
sICAM-1, soluble intercellular adhesion molecular-1;
SMDs, Small molecule drugs;
SpA, spondylarthritis;
Th, T helper;
TIMP-1, metallopeptidase inhibitor-1;
Traf6, tumor necrosis factor (TNF) receptor-associated factor 6;
Tregs, regulatory T cells;
TREM-1, triggering receptor expressed on myeloid cells-1;
TRO, Troglitazone;
US-SPPS, ultrasound-assisted solid-phase peptide synthesis;
WT, wild-type.

CHAPTER 1: INTRODUCTION

1. IL-17 IN CHRONIC INFLAMMATION FROM DISCOVERY TO TARGET: FOCUS ON MPGES-1/PPAR- γ PATHWAY

1.1 IL-17 and IL-17R family members

Human cytotoxic T lymphocyte-associated antigen 8 (CTLA8) was identified in 1993 and named Interleukin- (IL-)17 in 1995 [1]. The first bioactivity of human IL-17 was described in 1996 by showing the production of IL-6 and IL-8 from RA synoviocytes in response to IL-17. This immediately linked IL-17 to inflammation through IL-6 and to neutrophil recruitment through IL-8 [2].

Sequence screening identified an IL-17 family comprising six members from IL-17A (here referred to as IL-17) to IL-17F (Fig. 1). IL-17A and F are the closest members, with 50% homology. They are secreted as IL-17A and IL-17F homodimers and as IL-17A/F heterodimers [3, 4]. They share most of their activities, with IL-17A being more potent than IL-17F and IL-17A/F having an intermediate activity [5]. IL-17B, IL-17C, and IL-17D are classified as pro-inflammatory cytokines, but their role is not fully known. By contrast, IL-17E, also known as IL-25, has the lowest homology and is involved in T helper (Th)₂ cell responses against parasites and allergies [4]. IL-25 regulates IL-17 function, and this could possibly occur via competition at the receptor level [6].

IL-17 Receptor (IL-17R) was identified in 1995 as a new type of cytokine receptor [7]. The IL-17R family was later described with five subunits, from IL-17RA to IL-17RE (Fig. 1). IL-17A, IL-17F, and IL-17A/F bind the same receptor complex comprising IL-17RA and IL-17RC subunits [8, 9]. IL-17RA is also a receptor subunit of the receptor for IL-25, comprising IL-17RA and IL-17RB. This is important when targeting IL-17RA, which blocks the pro-inflammatory pathways

mediated by IL-17A, -17F, and -17A/F but also the anti-inflammatory response mediated by IL-25 (Fig. 1). All receptor subunits have a single transmembrane domain, and the binding of IL-17 to the IL17RA/RC complex recruits the ubiquitin ligase Act1 via the SEF/IL-17R (SEFIR) domain [8]. Act1 recruits tumor necrosis factor (TNF) receptor-associated factor 6 (Traf6), leading to the activation of nuclear factor kappa B (NF- κ B) and the mitogen-activated protein (MAP) kinase pathways. Such activation up-regulates many inflammatory genes, particularly the neutrophil-specific CXC chemokines [10, 11].

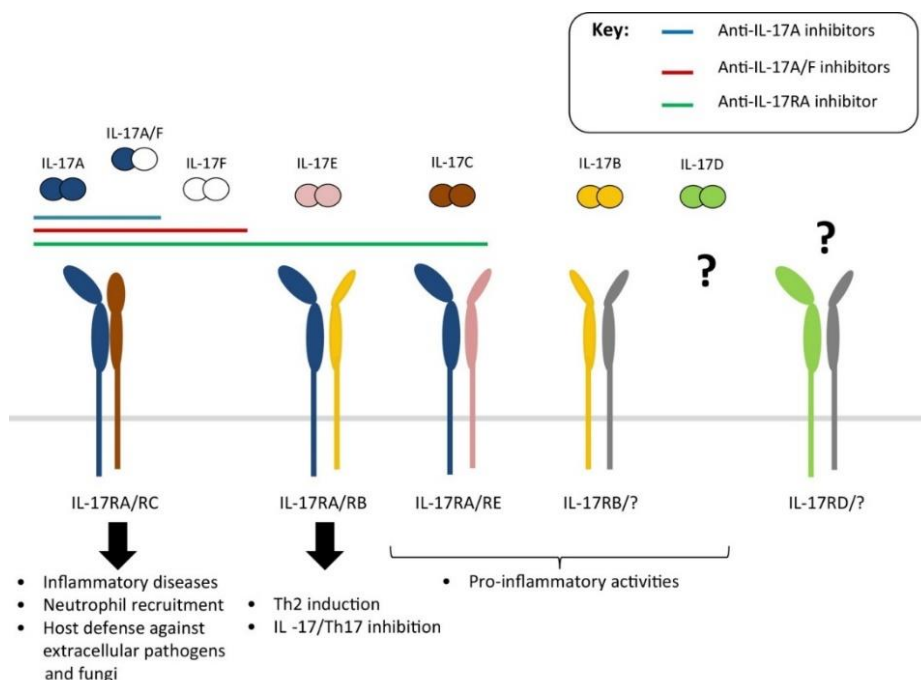


Fig. 1. Interleukin (IL)-17 cytokine and receptor family. IL-17 homodimer or heterodimer ligands bind various receptor complexes. IL-17A and IL-17F bind the IL-17 receptor (IL-17R)A and IL-17RC complex. IL-17E or IL-25 binds the IL-17RA and IL-17RB complex. Bars represent the various antibodies in clinical development that target IL-17A (blue), IL17A and IL-17F (red), or IL-17RA (green). From Beringer *et al.* [12].

1.2 IL-17 in acute and chronic inflammation

In the last few years, the scientific community has focused on IL-17 due to its pivotal role in the ongoing events typical of some inflammatory-based chronic diseases [13, 14]. Indeed, this cytokine is implicated in the mechanisms involved in cell activation, growth, and proliferation [15, 16]. Specifically, current studies have shown a close correlation, in the early stages of the inflammatory response, between IL-17 and the recruitment of polymorphonuclear cells (PMNs) [17, 18]. Indeed, both preclinical and clinical data have underlined the importance of IL-17 as a regulator of PMNs infiltration due to its chemotactic activity [19, 20]. In this context, it has been shown that IL-17 plays a main role in neutrophil maturation and differentiation. This is due to its ability to increase granulocyte-colony stimulating factor (G-CSF) release [21], thereby fostering the differentiation of the progenitors hematopoietic CD34⁺ towards neutrophils [2]. In addition, IL-17 can also induce other granulopoiesis markers and chemokines, such as growth-regulated oncogene- α (GRO- α), that regulate neutrophil penetration into tissues [20, 22]. Furthermore, IL-17 also promotes cyto-chemokines release, namely IL-1, IL-6, TNF α , macrophage inflammatory protein 2 (MIP-2), IL-8, Interferon-inducible protein 10 (IP-10), all used by neutrophils in chemotaxis [23-25].

The involvement of neutrophils and PMNs during the early phase of acute inflammation involves cyto-chemokines released by macrophages/monocytes subset [26]. It has been reported that the release of macrophage-related cytokines, including IL-1, TNF α and IL-6, is prompted by IL-17 to propagate and amplify the inflammatory onset [27]. Indeed, IL-17 induces monocyte adhesion, increasing the release of soluble intercellular adhesion molecule-1 (sICAM-1), integrin α 4,

platelet endothelial cell adhesion molecule 1 (PECAM-1) and cluster of differentiation 99 (CD99), representing one of the main stimuli for monocytes maturation and activation [28]. Further, our recent study has reported that IL-17 may constitute a specific modulator of inflammatory monocytes during later phases of the inflammatory response [29].

The biological effects exerted by IL-17 also include its synergistic activity with other pro-inflammatory “inducers”. IL-17, in combination with IL-1 β and TNF α , enhances the inflammatory reaction in cartilage, synovium and meniscus [30, 31]. IL-17 is also associated with the degradation of articular cartilage and destruction of bone due to the production of the matrix metalloproteinase- (MMP-)1 and MMP-13 collagenases in chondrocytes, the degradation of proteoglycans, and the expression of IL-6 and leukaemia inhibitory factor in fibroblast-like cells of the synovium [32, 33]. As schematically reported in Fig. 2, IL-17 can be considered a "*not canonical*" pro-inflammatory cytokine considering the variety of its actions. Indeed, it plays a unique role in the context of ongoing inflammatory diseases by exacerbating cellular and biochemical events activated during the acute phase of the inflammatory response. Although predominantly acting at the local site, IL-17 can also circulate in the bloodstream and thus may indirectly affect endothelial cell function inducing vascular inflammation, increasing the risk of atherosclerosis and/or cardiac and thrombotic events in patients with certain inflammatory-based diseases [34]. Moreover, IL-17, in combination with TNF α , is also responsible for a pro-coagulant and pro-thrombotic state [35, 36], thus providing evidence for its implication in the cardiovascular events associated with autoimmune diseases [37, 38].

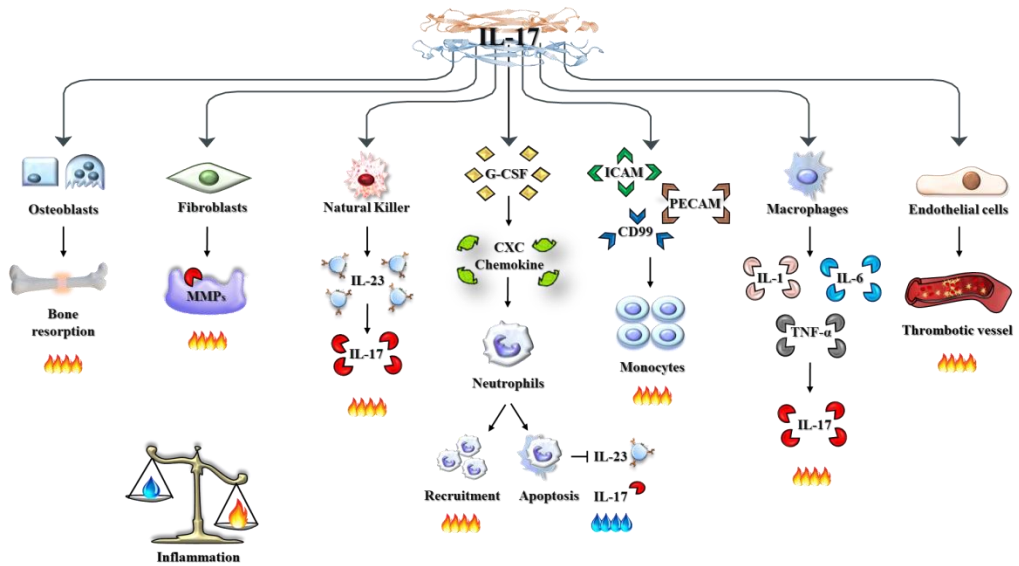


Fig. 2. Biological function of IL-17. Scheme of the main biological function of IL-17A on different cells and soluble factors. Taking into account the variety of its actions, IL-17A can be considered a "not canonical" pro-inflammatory cytokine since it plays a unique role in the context of ongoing inflammatory diseases by exacerbating cellular and biochemical events activated during the acute phase of the inflammatory response. From Maione *et al.* [39].

1.3 IL-17 and mPGES-1/PPAR- γ pathway

Inflammation is a complex defence mechanism characterized by leukocyte extravasation from the vasculature to local tissue damage resulting from injurious and noxious agents/stimuli [40]. Neutrophils dominate the initial influx of leukocytes, followed by monocytes and macrophages. The recruitment of inflammatory monocytes is correlated with a transient increase of pro-inflammatory mediators, including cytokines, chemokines, prostaglandins (PGs), and leukotrienes (LTs) [13, 41]. Indeed, inappropriate monocyte/macrophage survival or

overactivation perpetuates inflammatory pathways and strengthens disease activity/duration [42]. Therefore, regulating the function of monocytes/macrophages during inflammation is critical to promote resolution and healing. PGs and LTs are potent bioactive lipid mediators involved in the onset of inflammation and numerous homeostatic functions [43]. Their biosynthesis is initialized by cyclooxygenases (COXs) isoenzymes (COX-1 and COX-2) that convert arachidonic acid to PGH₂ [44] and subsequently isomerized, by three different PGE₂ synthases (situated downstream of COXs in the prostaglandin synthesis pathway), to PGE₂ [45]. The cytosolic prostaglandin E₂ synthase (cPGES) and the microsomal prostaglandin E₂ synthase (mPGES)-2 are constitutive enzymes, whereas mPGES-1 is an inducible isoform [46]. PGE₂ production can also be indirectly modulated by the alternative pathway of peroxisome proliferator-activated receptor- γ (PPAR- γ), a member of the nuclear receptor superfamily of ligand-dependent transcription factors activated by 15-deoxy- Δ 12,14-prostaglandin J₂ (15d-PGJ₂) [47]. Anti-inflammatory effects related to PPAR- γ activation have previously been demonstrated in several studies [48, 49] through its ability to increase the expression of nuclear factor kappa-B inhibitor α (I κ B- α), an endogenous inhibitor which interferes with the activation of p65 NF- κ B [50], via its natural ligand 15d-PGJ₂. Although a large body of work has been carried out to elucidate the biological function of PPAR- γ activation, this nuclear receptor's role remains poorly defined in the context of monocytes/macrophages activation via the arachidonic pathway.

Several biochemical and pharmacological studies recently demonstrated a molecular interaction between COXs and PGES isoenzymes, resulting in preferential functional coupling activity. Specifically, mPGES-2 was

shown to utilize COX-1 to generate PGH₂ in contrast to mPGES-1, which uses COX-2 [46]. Moreover, studies with PGES deficient mice have shown that induced PGE₂ synthesis is largely and preferentially dependent on mPGES-1 enzyme [51]. Consistently, the up-regulation of mPGES-1 expression and the involvement of COX-2/mPGES-1/PGE₂ cascade in terms of PGs production has been extensively reported in pathological settings in which PGE₂ is implicated, such as fever, pain and inflammatory based diseases [52, 53]. In line with these observations, it has been reported that in several tissues and different cell types, including fibroblasts, osteoblasts, chondrocytes and osteoarthritic cartilage, mPGES-1 expression is enhanced by a variety of inflammatory factors, including lipopolysaccharides (LPS), IL-1 β , TNF- α and IL-17, the latter of which was used in this study [54, 55]. In this context, IL-17 has received much attention as a significant driver of autoimmune and autoinflammatory conditions [38, 56, 57]. This cytokine is mainly produced by Th17 lymphocytes, but it also released by natural killer T cells (NKT), macrophages, neutrophils, monocytes, CD8⁺ T cells, $\gamma\delta$ T cells and innate lymphoid cells [3]. We have previously demonstrated that IL-17, compared to other pro-inflammatory cytokines such as IL-1 α and TNF α , sustains chronic inflammation and tissue remodelling rather than initiating it [19] through its ability to prime monocytes/macrophages towards an inflammatory phenotype [36, 56]. Considering that very little is known about the biological effects promoted by IL-17 both *in vitro* and *in vivo* in the context of mPGES-1/PPAR- γ modulation, here we sought to investigate and characterize the role of IL-17 on this pathway during an ongoing inflammatory response.

2. ROLE OF IL-17 IN GOUTY ARTHRITIS

Gout is a paradigm of acute, self-limiting inflammation caused by increased blood uric acid levels and damaging effects of monosodium urate (MSU) crystals accumulation within intra-and/or peri-articular areas [58]. Under long-standing hyperuricemia, MSU crystals deposits, usually associated with tophi, further induce a chronic inflammatory response that may lead to joint structure damage, often referred to as gouty arthritis (GA) or chronic gout [59].

During the progression of the inflammatory response and gouty attack, MSU crystals induce a significant leukocyte infiltration into the joint cavity [60]. This early pathologic hallmark is mainly characterized by neutrophil influx into the joint fluid followed by monocytes/macrophages that, in turn, phagocytose MSU crystals resulting in membranolytic and inflammasome activation [61, 62], generation of oxygen-derived free radicals, the release of lysosomal enzymes, pro-inflammatory interleukins (mainly IL-1, IL-6 and TNF α) and PGE₂ [63, 64].

PGs and leukotrienes are powerful bioactive lipid mediators involved in numerous homeostatic functions and in the onset of inflammation [43]. Their biosynthesis is initialized by COXs and then finalised PGE₂ synthases (by the inducible isoform mPGEs-1) that convert PGH₂ [44] to PGE₂ [45, 46]. Recently, several biochemical and pharmacological studies demonstrated a molecular interaction between COX and PGEs isoenzymes [51, 65], resulting in preferential functional coupling activity of COX-2/mPGEs-1/PGE₂, which triggers the inflammatory response associated with conditions such as gout [52, 53, 66, 67]. However, it is still unclear how this process is being regulated and which molecular mechanisms are detrimental to gouty inflammation onset [68, 69].

In this context, emerging evidence supports the view that systemic differentiation and maturation of Th17 cells and local recruitment are potential mechanisms by which these cells cause damage to target tissues. Liu and coll. [70] reported significantly elevated levels of IL-17 in the serum of GA patients early in the onset of gout symptoms, gradually decreasing as symptoms diminished (Fig. 3). Moreover, recent work highlighted that, although the genetic variants in IL-17 do not appear to be involved in the development of gout [71], systemic Th17/Treg (regulatory T cells) imbalance changes over time during the development of acute gouty arthritis and a decrease in ratio, favouring Th17 cells is consistent with inflammation development in the joints [72].

We and others have also highlighted the importance of IL-17 (and IL-17-related cytokines) [19, 73, 74] in sustaining the release of multiple mediators such as IL-1, IL-6, IL-8, PGE₂ and monocyte chemoattractant protein- (MCP-)1 (also known as JE) by a wide variety of cells involved both directly and indirectly, on GA pathophysiology, including fibroblasts, endothelial cells, neutrophils and inflammatory monocytes. [75-77]. Collectively these findings suggested a detrimental role for IL-17 in GA onset and progression and helped us to hypothesise that targeting IL-17 by a neutralizing antibody strategy could provide a novel treatment strategy to target gouty inflammation and/or arthritis.

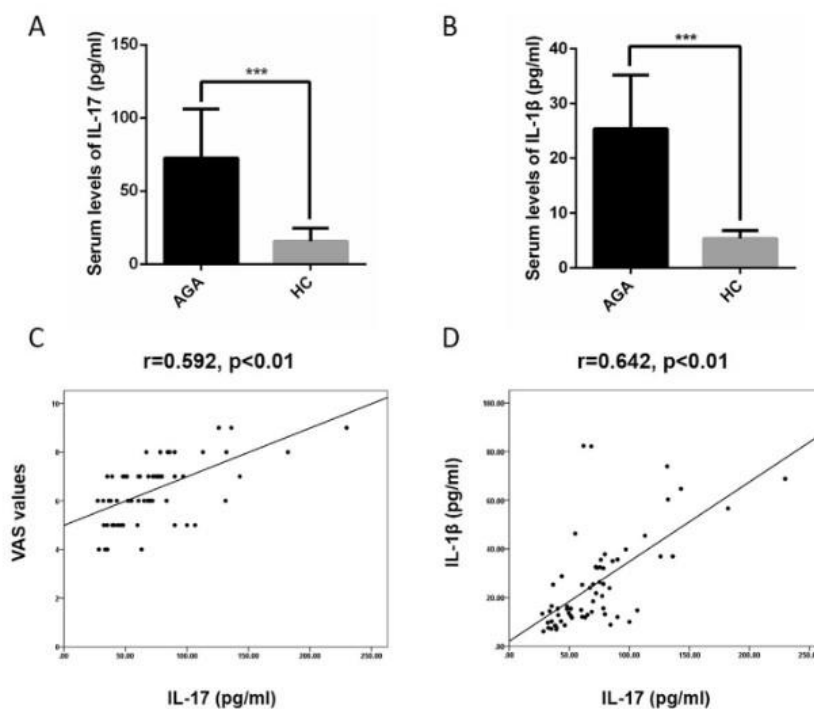
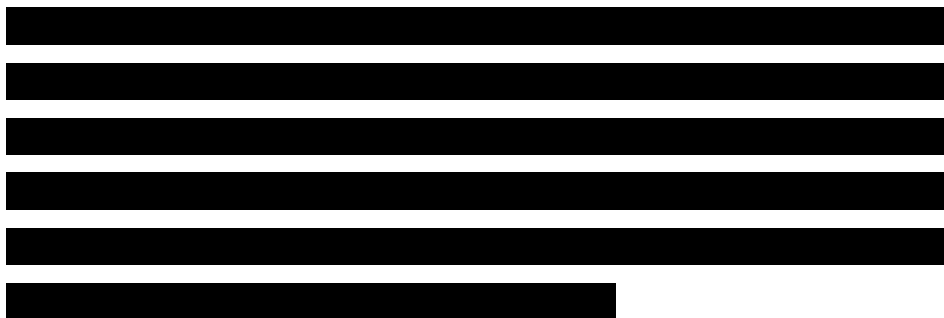


Fig. 3. IL-17 is a novel biomarker for GA with an acute flare. Serum IL-17 levels of GA patients with acute flares and healthy controls (A). Serum IL-1 β levels of GA patients with acute flares and healthy controls (B). Pearson's correlation analysis of IL-17 with VAS values in 64 GA patients with acute flares (C). Pearson's correlation analysis of IL-17 with IL-1 β levels in 64 GA patients with acute flares (D). GA, GA patients; HC, Healthy controls. Blood samples of GA patients were collected less than 12 h after a gout attack. All data are presented as mean \pm SD and were analyzed with the two-tailed unpaired t-test (*** $P < 0.001$). From Liu *et al.* [70].

[REDACTED]

Drug	Manufacturer					
		Psoriasis	PsA	AS	RA	Other Indications
<i>IL-17A Inhibitors</i>						
Secukinumab (AIN457), Cosentyx™	Novartis	Approved	Approved	Approved	Phase III	
Ixekizumab (LY2439821)	Lilly	Submitted	Phase III		Phase II	
CNTO 6785	Janssen				Phase II	COPD (Phase II)
CJM112	Novartis	Phase I/II				Hidradenitis suppurativa (Phase II)
BCD 085	Biocad					Healthy subjects (Phase I)
<i>IL-17A and IL-17F Inhibitors</i>						
Bimekizumab (UCB-4940)	UCB	Phase I	Phase I		Phase II	
ALX-0761 (MSB 0010841)	Merck Serono Ablynx	Phase I				
<i>IL-17A and TNFα Inhibitors</i>						
ABT-122	AbbVie		Phase II		Phase II	
COVA322	Janssen/Covagen	Phase I/II	Preclinical	Preclinical	Preclinical	
<i>IL-17RA Inhibitors</i>						
Brodalumab (AMG 827)	Valeant Pharmaceuticals	Phase III		Phase III	Phase II	

Table 1. Drug candidates targeting IL-17 or its receptor IL-17RA and their current clinical status. From Beringer *et al.* [12].



[REDACTED]

EXPERIMENTAL SECTION

CHAPTER 2: MATERIALS AND METHODS

1. MATERIALS

Mouse and human IL-6 Elisa kit, human TNF α Elisa kit, human IL-8 Elisa Kit, mouse PGE₂ Elisa kit, proteome profiler mouse cytokine array kit, recombinant mouse and human IL-17, recombinant human TNF α protein, murine and human IL-17 neutralizing antibodies were purchased from R&D System (Milan, Italy). PF 9184 (PF) and Troglitazone (TRO) were purchased from Tocris (Milan, Italy), AF 3485 (AF) from Cayman Chemical Company (Michigan, USA), whereas FACS buffer and all conjugated antibodies from BioLegend (London, UK). Ficoll-Paque Plus (endotoxin tested, ≤ 0.12 EU/ml) was obtained from GE Healthcare Bio-Sciences AB (Uppsala, Sweden). Collagenase (Type VIII), fetal bovine serum (FBS), hyaluronidase, monosodium urate crystals, E-Toxate™ reagent from Limulus Polyphemus and RPMI-1640 cell medium were purchased from Sigma-Aldrich Co. (Milan, Italy). PGD₂ Elisa kit and the primary antibodies for western blot analysis were obtained from Elabscience (Milan, Italy), whereas the HRP-conjugated IgG secondary antibodies from Dako (Copenhagen, Denmark). 15d-PGJ₂ Elisa kit was purchased from Abcam (Cambridge, UK). Unless otherwise stated, all the other reagents were from BioCell (Milan, Italy).

2. HUMAN BLOOD SAMPLES

Whole blood was collected from healthy donors with written informed consent and approval from the University of Birmingham Local Ethical Review Committee (ERN_18-0382). An equal proportion of male and female donors were used with an age range between 22-70 [94].

3. CELL CULTURE

3.1 Mouse macrophage cell line

Mouse macrophage cell line (J774A.1, ATCC[®] TIB-67[™]) was cultured in Dulbecco's modified Eagle's medium (DMEM) supplemented with FBS (ATCC[®] 30-2020[™]) to a final concentration of 10%. Cells were seeded in petri culture dishes (100 × 20 mm, Falcon[®]) at a density of 5×10^5 cells/dish and allowed to grow for 24 h. The medium was then replaced, and cells were treated for 4 and 24 h with recombinant mouse IL-17 (0.5-500 ng/ml). In another set of experiments, cells were treated with IL-17 (50 ng/ml) in the presence or absence of PF 9184 (50 μ M) or Troglitazone (50 μ M), according to previous *in vitro* studies [55]. Following incubations for 4 and 24 h, cells were collected with a cell scraper and pellets were lysed at 4°C for 10 min with a buffer containing 1g/100 ml Triton X-100, 5 mM EDTA in PBS (pH 7.4) containing protease inhibitors. After centrifugation at 14000×g for 10 min at 4°C, the supernatant was collected and stored at -80°C for future western blot analysis. Protein concentration was determined by the Bio-Rad protein assay (Bio-Rad, Milan, Italy).

3.2 Mouse embryonic fibroblast cell line

Mouse embryonic fibroblast cell line (NIH-3T3) was cultured in DMEM supplemented with FBS (ATCC[®] 30-2020[™]) to a final concentration of 10%. Cells were seeded in petri culture dishes (100 × 20 mm, Falcon[®]) at a density of 5×10^5 cells/dish and allowed to grow for 24 h. The medium was then replaced, and, at 70% confluency, cells, according to previous *in vitro* studies [55, 95], were treated for 24 h with recombinant mouse IL-17 (50 ng/ml), nIL-17[™] peptide (50 ng/ml) alone or in combination

with IL-17 or nIL-17TM neutralizing antibodies (MAB421 or Ab-IPL-IL-17TM; 750 ng/ml). Following incubations for 24 h, supernatants were collected and stored at -80°C for future Elisa analysis. Protein concentration was determined by the Bio-Rad protein assay (Bio-Rad, Milan, Italy) [96].

3.3 Human monocyte-derived macrophages (hMDMs) isolation and differentiation

Whole blood from healthy donors was separated using density gradients Histopaque 1119 and 1077 (Sigma-Aldrich, U.K.) to obtain the peripheral blood mononuclear cell (PBMC) fraction, accordingly to the procedure described by Krautter and coll. [94]. Monocytes were isolated from PBMC using PBS without Ca²⁺ and Mg²⁺ supplemented with 0.5 % BSA and 2 mM EDTA at 4 °C, by positive selection using anti-CD14 microbeads and MACS separation columns (Miltenyi Biotec, Germany). Purified monocytes (~95 %) were cultured at 37 °C in 5 % CO₂ in M199 media (Life Technologies, Paisley, U.K.) containing 10 ng/ml epidermal growth factor (EGF) (Sigma-Aldrich, Poole, UK) and 10% autologous human serum. To induce “pro-inflammatory” (M1) or “pro-resolution” (M2) phenotypes, previously established protocols were followed [97]. Briefly, M1 and M2 phenotypes were generated by treating human monocyte-derived macrophages (hMDMs) with LPS (100 ng/ml) and interferon gamma (IFN γ ; 20 ng/ml) or IL-4 (20 ng/ml), respectively, for 16h. hMDMs were supplemented with M199 media containing 10 ng/ml EGF and 10 % human autologous serum every two days for six days [94]. Then, cells, after polarization, were stained for IL-17Rs (RA or RC) or stimulated for 24 h with IL-17, nIL-17TM (100 ng/ml) alone or in combination with neutralizing antibodies (MAB317 or Ab-IPL-IL-17TM

at 10 µg/ml) [98, 99]. Finally, supernatants were collected and measured to evaluate IL-6 and TNFα levels.

3.4 Human dermal blood endothelial cells (HDBEC)

Primary human dermal blood endothelial cells (HDBECs) were purchased from PromoCell and cultured in cell growth medium MV (PromoCell, Heidelberg, Germany) [100]. HDBECs were seeded into 12-well tissue culture plates until yielding confluent monolayers. HDBEC monolayers were washed in endothelial cell growth medium MV warmed to 37°C and simulated with TNFα (100 U/ml) or IFNγ (10 ng/ml) for 24 h at 37°C.

3.5 Neutrophil isolation

Neutrophils were isolated using a double-density histopaque gradient and hypotonic lysis, as described previously [101]. Briefly, PMN were isolated using a single density histopaque gradient and, after a first dilution (1:1 w/w) with PBS, were layered with histopaque 1077 (Sigma Chem. Co., Poole, U.K.) and histopaque 1119 (Sigma). After centrifugation at 400 g for 30 min at RT, the bottom layer was harvested and washed twice in sterile PBS. Contaminating erythrocytes were removed by hypotonic lysis.

3.6 Isolation of human fibroblasts

Synovial tissue samples were obtained by ultrasound-guided biopsy [102] from resolving arthritis (Res) or fulfilled RA classification criteria patients [103]. RA was classified according to 2010 American College of Rheumatology criteria [104]. Isolated fibroblasts were cultured accordingly to the protocol described by Salmon and coll. [105] and

treated with IL-17 (10 ng/ml) and TNF α (100 U/ml) alone or in combination with MAB317 or Ab-IPL-IL-17TM (10 μ g/ml).

4. ANIMALS

Experimental procedures were carried out on 8-12-week-old male CD1 mice in compliance with international and national law and policies and approved by the Italian Ministry of Health. Animal studies were performed in compliance with the ARRIVE guidelines and with the recommendations made by BJP (EU Directive 2010/63/EU for animal experiments, ARRIVE guidelines, and the Basel declaration, including the 3Rs concept; [106, 107]). Mice, purchased from Charles River (Milan, Italy), were housed with *ad libitum* access to food and water and maintained on a 12 h light/dark cycle. Experimental study groups were randomized and blinded. All procedures were carried out to minimize the number of animals used (n=7 per group) and their suffering.

5. IN VIVO MODELS

5.1 Air Pouch

Dorsal air pouches were induced by injection of 2.5 ml of air on day 0 and day 3, as previously described [74]. On day 6, mice received the following treatments: i) Control (CTRL) 0.25 ml of 0.5% carboxymethyl cellulose (CMC); ii) IL-17 (1 μ g) in 0.25 ml of 0.5% CMC; iii) IL-17 (1 μ g) in 0.25 ml of 0.5% CMC co-administrated with PF 9184 (1-9 μ g/pouch); iv) IL-17 (1 μ g) in 0.25 ml of 0.5% CMC co-administrated with Troglitazone (1-9 μ g/pouch) accordingly to previous studies [19, 55]. In another set of experiments, the inhibitory effect of PF 9184 was compared to AF 3485 (9 μ g/pouch). In all experimental conditions, mice

were sacrificed after 4, 24, and 48 h from the injection and air pouches were washed thoroughly with 2 ml of PBS containing 50 U/ml heparin and 3 mM EDTA. In the last set of experiments, mice received the following treatments: i) CTRL 0.25 ml of 0.5% CMC; ii) IL-17 (1 µg) in 0.25 ml of 0.5% CMC; iii) nIL-17TM (1 µg) in 0.25 ml of 0.5% CMC; iv) IL-17 (1 µg) plus MAB421 or Ab-IPL-IL-17TM (10 µg) in 0.25 ml of 0.5% CMC; v) IL-17 (1 µg) plus Anti-JE (10 µg) in 0.25 ml of 0.5% CMC; vi) IL-17 (1 µg) plus Anti-KC (10 µg) in 0.25 ml of 0.5% CMC. Animals were sacrificed after 24 h, and the lavage fluids were centrifuged at 220×g for 10 min at 4°C to separate the exudates from the recruited cells. Inflammatory exudates were collected and measured to evaluate the level of inflammatory cyto-chemokines, whereas the cellular pellet was subjected to western blot and FACS analysis as described below. Cell number was determined by TC20 automated cell counter (Bio-Rad, Milan, Italy) using Bio-Rad's automated cell counter uses disposable slides, TC20 trypan blue dye (0.4% trypan blue dye w/v in 0.81% sodium chloride and 0.06% potassium phosphate dibasic solution) and a CCD camera to count cells based on the analyses of capture images [74, 108].

5.2 Gouty Arthritis

5.2.1 Preparation of MSU crystals

The MSU crystals were prepared as previously described [109]. Briefly, 800 mg of MSU were dissolved in 155 ml of boiling milli-Q water containing 5 ml of NaOH, and after the pH was adjusted to 7.2, the solution was cooled gradually by stirring at room temperature and crystals collected after centrifugation at 3.000 g for 5 min at 4°C. Obtained crystals were washed twice with 100% ethanol, dried,

autoclaved (180°C for 2 hours), and weighed under sterile conditions. Crystals were resuspended in PBS by sonication and stored in a sterile environment until use. MSU crystals were confirmed as endotoxin-free by a commercial test kit of limulus polyphemus lysate assay (<0.01 EU/10 mg).

5.2.2 Induction of MSU-induced knee joint inflammation

Joint inflammation was induced by the intra-articular (i.a.) administration of MSU crystals (200 µg/20 µl) into the right knee joint of mice under isoflurane anaesthesia. Control animals received an i.a. injection of PBS (20 µl) or 20 µl of IL-17Ab isotype control. Animals from IL-17Ab-treated groups received 1, 3 and 10 µg (i.a.) in 20 µl of IL-17 neutralizing antibodies (IL-17Ab) 30 minutes after MSU crystals administration.

5.2.3 Joint scoring and evaluation

In a preliminary experiment finalized to evaluate the dose-responsive effect of IL-17 neutralizing antibodies (IL-17Ab), the joints from different experimental conditions were scored macroscopically on a scale from 0 to 3, where 0 = no inflammation, 1 = mild inflammation, 2 = moderate inflammation, and 3 = severe inflammation, in increments of 0.25. A score of 0.25 was given when the first signs of swelling and redness were present. Joint swelling scoring was performed by two authors without knowledge of the experimental groups [110]. After macroscopic scoring, knee joint oedema was determined with a calliper (Mitutoyo) before (zero time) and after the i.a. injection with MSU crystals or MSU crystals plus IL-17Ab at times indicated. Knee joint oedema was determined for each mouse by subtracting the initial paw

value from the paw value measured at each time point and presented as Δ mm/joint [109].

5.2.4 Isolation of joint-infiltrating cells

According to the protocol described by Akitsu and colleagues [111], ankle joints were cut out and digested with hyaluronidase (2.4 mg/ml) and collagenase (1 mg/ml) in RPMI 1640 plus 10% FBS for 1 h at 37 °C. Then, the cells were filtered through a cell strainer with a 70- μ m nylon mesh (Becton Dickinson, Franklin Lakes, NJ, USA) and washed with RPMI 1640 plus 10% FBS. After that, collected cells were washed in PBS for total cell count before flow cytometry analysis.

5.3. Antigen induced-arthritis

Eight-week-old male C57Bl/6J wild-type (WT) mice were purchased from Charles River and were maintained in a specific pathogen-free facility with free access to food. Environmental conditions were: 21 ± 2 °C, $55 \pm 10\%$ relative humidity and a 12h light-dark cycle. Mice were immunised with methylated bovine serum albumin (mBSA, 10 μ g s.c., Sigma-Aldrich) in complete Freund's adjuvant (CFA, Fisher Scientific). On day 21, monoarthritis was induced by intraarticular injection of mBSA (100 μ g) into the knee. Mice were treated therapeutically at 24 h or 72h post disease onset by i.p injection with either infliximab (Anti-TNF α , 50 μ g/mice) or a neutralizing antibody to IL-17 (Ab-IPL-IL-17TM, 50 μ g/mice). Joint thickness (mm) was measured by callipers daily for up to 7 days. Data are expressed as a percentage change from baseline measurement taken on day 21 or area under the curve (AUC).

6. IN VITRO AND EX VIVO ASSAYS

6.1 Myeloperoxidase assay

Leukocytes myeloperoxidase (MPO) activity was assessed by measuring the H₂O₂-dependent oxidation of 3,3',5,5'-tetramethylbenzidine as previously reported [19]. Cellular lysate (from air pouch experiments) and tissues (from knee joint) were homogenized in a solution composed of hexadecyltrimethylammonium bromide (0.5% w/v) in 50 mM sodium phosphate buffer at pH 5.4. After homogenization, samples were centrifuged at 1008 × g for 10 min, and the supernatant was used for the assay. Aliquots of 20 µl were incubated with 160 µl of 3,3',5,5' - tetramethylbenzidine and 20 µl of H₂O₂ (in 80 mM phosphate buffer, pH 5.4) in 96-well plates. Plates were incubated for 5 min at room temperature, and OD was read at 620 nm using a plate reader (Biorad, Italy). The assay was performed in duplicates and normalized for protein content.

6.2 Elisa and ElisaSpot assay

Enzyme-linked immunosorbent assays for IL-17, PGE₂, PGD₂, and 15d-PGJ₂ were carried out on inflammatory pouch exudates and on whole knee joint homogenates. The levels of IL-6, IL-8 and TNFα were analyzed on cell supernatants accordingly to the procedure described by Raucci and coll. [29]. Briefly, 100 µl of samples, diluted standards, quality controls and dilution buffer (blank) were added to a pre-coated plate with monoclonal anti-IL-17, PGE₂, PGD₂, 15d-PGJ₂, IL-6, IL-8 and TNFα for 2 h. After washing, 100 µl of biotin-labelled antibody was added for 1 h. The plate was washed, and 100 µl of the streptavidin-HRP

conjugate was added, and the plate was incubated for a further 30 min period in the dark. The addition of 100 µl of the substrate and stop solution represented the last steps before the reading of absorbance (measured at 450 or 405 nm) on a microplate reader. Antigen levels in the samples were determined using a standard curve and expressed as pg/pouch or pg/ml [86]. For cyto-chemokines protein array, equal volumes (1.5 ml) of pouch inflammatory fluids and knee joint homogenates in all described experimental conditions were incubated with the pre-coated proteome profiler array membranes according to the manufacturer's instructions. Dot plots were detected by using the enhanced chemiluminescence detection kit and Image Quant 400 GE Healthcare software (GE Healthcare, Italy) and successively quantified using GS 800 imaging densitometer software (Biorad, Italy) as previously described [73].

6.3 Flow cytometry

Cells collected from the pouch cavities were first washed with PBS and then re-suspended in FACS buffer (PBS containing 1% FCS and 0.02% NaN₂) containing CD16/CD32 FcγIIR blocking antibody (clone 93; eBioscience, London, UK) for 30 min at 4°C. Thereafter, cells were labelled for 30 min at 4°C with the following conjugated antibodies (all from BioLegend, London, UK): CD45 (1:100; clone 30-F11), LY6C (1:100; clone HK1.4), LY6G (1:100; clone 1A8), CD115 (1:100; clone AFS98), CD11b (1:100; clone M1/70), F4/80 (1:100; clone BM8), CD206 (1:100; clone C068C2), prior to analysis by FACS calibre using CellQuest software (Becton Dickinson, Franklin Lakes, NJ). Neutrophils, macrophages, and resident/inflammatory monocytes were defined

according to the previously described flow cytometry procedure [74, 112, 113]. Lymphocytes isolated from whole blood (collected by intracardiac puncture) by Ficoll-Paque Plus gradient method were washed in FACS buffer (PBS containing 1% BSA and 0.02% NaN₂) and directly stained with the following conjugated antibodies (all from BioLegend, London, UK): CD4 (1:200; clone GK1.5), CD8 (1:200; clone 5H10-1), CD25 (1:200; clone 3C7) for 60 minutes at 4°C. After washing, cells were fixated, permeabilized, and stained intracellularly with IL-17 (1:200; clone TC11-18H10.1) and Foxp3 antibody (1:200; clone MF-14). Th17 and Treg population were defined as CD4⁺IL-17⁺ and CD4⁺CD25⁺Foxp3⁺ cells respectively. For the characterization of joint-infiltrating cells we adopted a similar procedure followed by the incubation with GR1 (1:300; clone RB6-8C5), F480 (1:300; clone BM8), B220 (1:200; clone RA3-6B2), CD115 (1:200; clone AFS98) for 60 minutes at 4°C. T cells, neutrophils, macrophages, and resident/inflammatory monocytes were defined according to the flow cytometry procedure previously described [74, 114]. At least 1×10⁴ cells were analysed per sample, and positive and negative populations were determined based on the staining obtained with related IgG isotypes. Flow cytometry was performed on BriCyte E6 flow cytometer (Mindray Bio-Medical Electronics, Nanshan, China) using MRFlow and FlowJo software operation [115]. hMDMs were washed with PBS without Ca²⁺ and Mg²⁺ containing 25 mM lactose for 20 min at RT. Cells were then incubated with FcR blocking agents (Miltenyi) in PBS without Ca²⁺ and Mg²⁺ containing lactose before staining with IL-17 Receptor A (1:100; clone 133617) and IL-17 Receptor C (1:100; clone 309822). Protein expression was analysed by flow cytometry on a Dako CyAn (Beckman Coulter, High Wycombe, UK), and data were analysed using MRFlow

and FlowJo software operation. The unspecific binding of antibodies was quantified by using corresponding isotype controls.

6.4 Western blot analysis

Whole cellular pellets from fibroblasts and knee joints homogenates (50 µg of protein) were subjected to SDS-PAGE (10 and 12% gel) using standard protocols as previously described [116]. The proteins were transferred to nitrocellulose membrane (0.2 µm nitrocellulose membrane, Trans-Blot® Turbo™, Transfer Pack, Bio-Rad Laboratories, Hercules, CA, USA) in transfer buffer (25 mM Tris-HCl pH 7.4 containing 192 mM glycine and 20% v/v methanol) at 400 mA for 2 h. The membranes were saturated by incubation for 2 h with non-fat dry milk (5% wt/v) in PBS supplemented with 0.1% (v/v) Tween 20 (PBS-T) for 2 h at RT and then incubated with 1:1000 dilution of primary antibodies over-night at 4°C such as mouse monoclonal anti-actin (E-AB-20094), mouse monoclonal anti-COX-2 (E-AB-27666), mouse monoclonal anti-IκB-α (4814), rabbit polyclonal anti-IL-17 Receptor (E-AB-63080), mouse monoclonal anti-NFκB (MAB3026), rabbit polyclonal anti-mPTGDS-1 (TA301420), rabbit polyclonal anti-mPGES-1 (E-AB-32563), rabbit polyclonal anti-PPAR-γ (NBP2-22106), and then washed 3 times with PBS-T.

In all cases, blots were then incubated with a 1:3000 dilution of related horseradish peroxidase-conjugated secondary antibody for 2 h at RT and finally washed 3 times with PBS-T. Protein bands were detected by using the enhanced chemiluminescence method (Clarity™ Western ECL Substrate, Bio-Rad Laboratories, Hercules, CA, USA) and Image Quant 400 GE Healthcare software (GE Healthcare, Italy). Finally, protein

bands were quantified using the GS 800 imaging densitometer software (Biorad, Italy) and normalized with respective actin.

6.5 Histology

Histological analysis was conducted at the 18 h time-point. Joints were trimmed, placed in a decalcifying solution (EDTA 0.1 mM in PBS) for 14 days and then embedded in paraffin. Sections (5 μm) were deparaffinized with xylene and stained with haematoxylin and eosin (H&E) as previously described [19] for conventional morphological evaluation. A dimension used for the analysis of the slices was 569 x 633 pixels and magnification $\times 20$. In all cases, a minimum of ≥ 3 sections per animal were evaluated. Phase-contrast digital images were taken using the Image Pro image analysis software package.

6.6 Elisa-based binding assay

IL-17RA-Fc and IL-17RC-Fc were plated in 96 well plates at 2 $\mu\text{g/ml}$ and 1 $\mu\text{g/ml}$, respectively. Plates were incubated overnight at 4°C, and then washed 3 times with PBST wash buffer and blocked for 1h with 200 μL of protein-free T20 blocking buffer. Cytokines were biotinylated with EZ Link NHS-Biotin according to the manufacturer's instructions. Plates were incubated for 30 min at RT before 3 washes with PBST and a 30 min incubation with Streptavidin-HRP. The colourimetric signal was developed with TMB, and the reaction stopped with sulfuric acid (stop solution). OD values were read on a SpectraMax M3 (Molecular Devices). The percentage of binding or inhibition was calculated as previously described [117].

6.7 Transwell migration assay

Chemotaxis was assessed using a transwell assay, as previously described [118]. M199 media (final volume 700 μ l) were added to the bottom well of a Transwell-24 permeable support with 3.0 μ m pores (Corning, NY, USA) with IL-17 (10-500 ng/ml), nIL-17TM (10-500 ng/ml), and formyl-methionyl-leucyl-phenylalanine (fMLP; 10⁻⁶ M as positive control) alone or in combination with IL-17 neutralizing antibodies (MAB317 or Ab-IPL-IL-17TM) (10 μ g/ml). Then 2 \times 10⁵ neutrophils in a final volume of 200 μ l were added to the top chamber, which had a confluent HDBEC monolayer activated with TNF α (100 U/ml) and IFN γ (10 ng/ml) for 24 h. After 2 h of incubation at 37 $^{\circ}$ C, neutrophils were collected from the bottom of the wells and quantified by flow cytometry using CountBrightTM Absolute Counting Beads (Thermofisher, Rugby, UK) as previously described [119, 120].

7. DEVELOPMENT OF A NOVEL IL-17 NEUTRALIZING ANTIBODY

7.1 Peptide synthesis and purification

[REDACTED]

[Redacted text block]

[REDACTED]

7.2 Immunization and fusion protocols

The immunization protocol and the synthesis of a novel IL-17 neutralizing antibody (Ab-IPL-IL-17TM) were commissioned to ProteGenix (France). All experimental details and procedures are reported in Scientific Reports 1 and 2.

8. STATISTICAL ANALYSIS

Statistical analysis complies with the international recommendations on experimental design and analysis in pharmacology [122, 123], and data sharing and presentation in preclinical pharmacology [124, 125]. All data are presented as means \pm S.D. and analysed using one- or two-way ANOVA followed by Bonferroni's or Dunnett's for multiple comparisons. GraphPad Prism 8.0 software (San Diego, CA, USA) was used for analysis. Differences among groups were considered significant when $P \leq 0.05$ was achieved. The sample size was chosen to ensure alpha 0.05 and power 0.8. Animal weight was used for randomization and group allocation to reduce unwanted sources of variations by data normalization. No animals and related *ex vivo* samples were excluded from the analysis. *In vivo* study was carried out to generate groups of equal size ($n = 5-7$ of independent values) using randomization and blinded analysis.

CHAPTER 3: RESULTS

1. IL-17-INDUCED INFLAMMATION MODULATES THE mPGES-1/PPAR- γ PATHWAY IN MONOCYTES/MACROPHAGES

1.1 PF 9184 and Troglitazone, in a time- and dose-dependent manner, revert leukocytes accumulation and activation at the site of inflammation

We knew from our previous studies [19, 74] that the single administration of IL-17 (1 μ g/pouch) into a 6-day-old air pouch causes a transient infiltration of leukocytes by 4 h, which peaks at 24 h and then declines by 48 h. To test the potential dose-responsive effect of an mPGES-1 inhibitor and a PPAR- γ agonist at this local site of inflammation, we administered PF 9184 (1-9 μ g/pouch) and Troglitazone (1-9 μ g/pouch) concomitantly with IL-17. All mice were sacrificed at 4, 24 and 48 h time points. Consistent with our previous findings, 4 and 24 h after IL-17 administration, mice showed significant differences in the number of inflammatory leukocytes compared to vehicle-treated (Fig. 1A-B). No significant differences were observed at 48 h (Fig. 1C). Interestingly, mice receiving PF at a dose of 9 μ g/pouch showed a marked decrease (~40%) in inflammatory infiltrates, compared to IL-17-treated mice, at both 4 and 24 h (Fig. 1A-B). A similar anti-inflammatory profile was observed after TRO administration (9 μ g/pouch), with a marked reduction in infiltrating leukocytes at 4 and 24 h (Fig. 1A-B). No biological effects were observed at 48 h (Fig. 1C). The inhibitory effect of PF was also compared to AF (another selective mPGES-1 inhibitor) a similar reduction in total leukocyte infiltration was observed (Supplementary Fig. 1). Based on these results, we selected the most

active PF and TRO (9 $\mu\text{g/pouch}$) dose for all subsequent analyses. The level of MPO (Fig. 1D-F), a peroxidase enzyme most abundantly expressed in polymorphonuclear leukocytes, and different prostaglandins such as PGE_2 , PGD_2 and 15-d-PGJ_2 were then measured in pouch fluid. Administration with IL-17 (still present in the air pouch at 48 hours after a single injection, Supplementary Fig. 2) was correlated with increased levels of MPO (Fig. 1D-E) and PGE_2 (Fig. 2A-B) at both 4 and 24 h. Conversely, a reduction in PGD_2 at both 4 and 24 h (Fig. 2C-D) and 15-d-PGJ_2 (Fig. 2F) only at 24 h was observed. When co-injected in the presence of PF and TRO, the opposite profile was observed with a marked reduction in MPO (Fig. 1E) activity and PGE_2 (Fig. 2A-B) and reversal in PGD_2 (Fig. 2C-D) and 15-d-PGJ_2 levels (Fig. 2F). Collectively these data indicate time- and dose-dependent protective effects of a selective mPGES-1 inhibitor and a PPAR- γ agonist on inflammatory cell recruitment and activation in response to IL-17 induced inflammation.

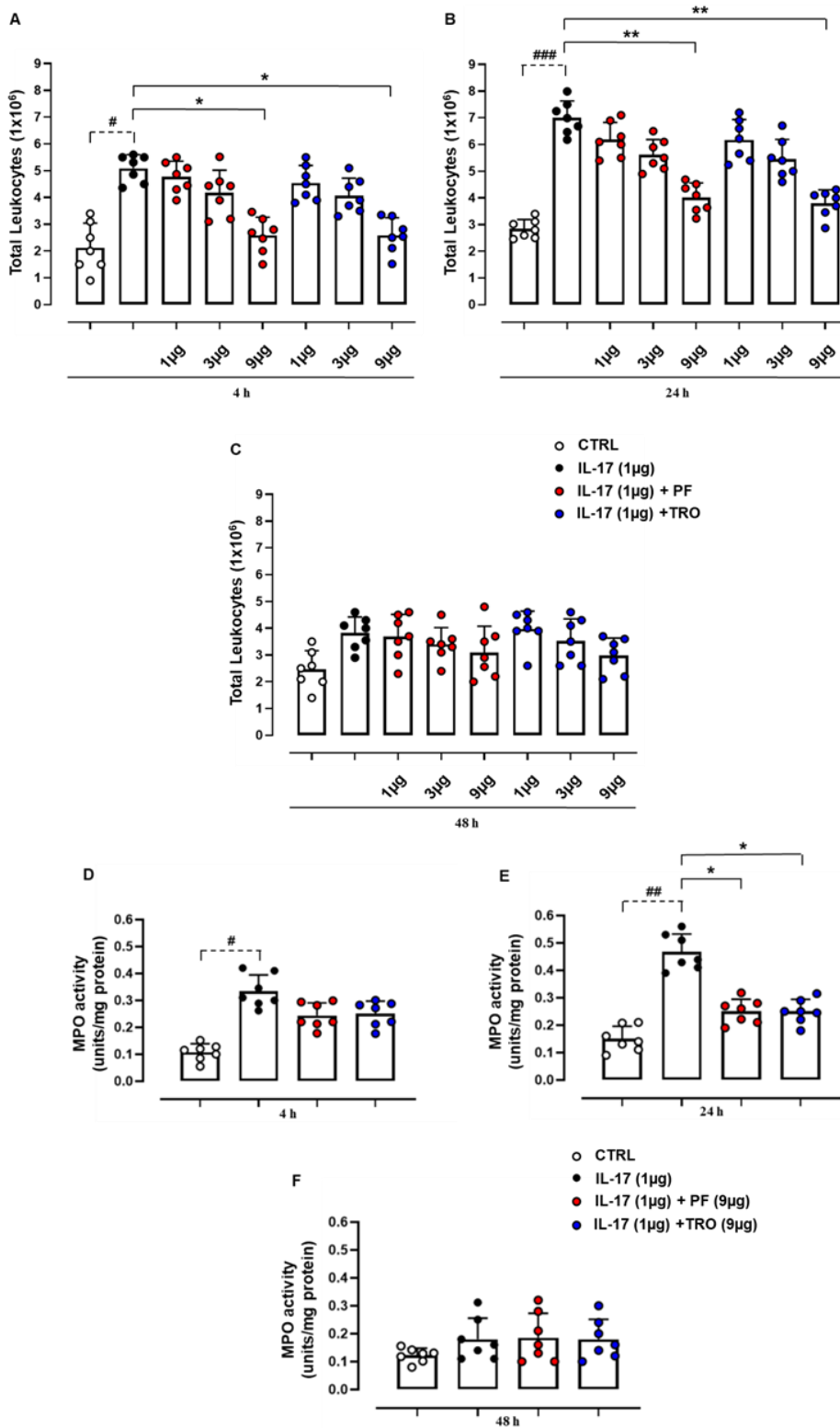


Fig. 1. PF and TRO, in a time- and dose-dependent manner, revert leukocyte accumulation and activation at the site of inflammation. Mice were treated with IL-17 vehicle (CTRL), IL-17 (1 $\mu\text{g/pouch}$) alone (IL-17) or co-administrated with PF 9184 (PF, 1-9 $\mu\text{g/pouch}$) and Troglitazone (TRO, 1-9 $\mu\text{g/pouch}$) and thereafter total cell number from pouches inflammatory exudates were evaluated at 4 (A), 24 (B) and 48 (C) h. At the same time point (D-F), supernatants from cell pellet lysate were tested for myeloperoxidase activity. Data were expressed as millions of cells for the pouch (A-C) or units/mg of protein (D-F) and presented as means \pm S.D. of $n=7$ mice per group. Statistical analysis was conducted by one-way ANOVA followed by Bonferroni's for multiple comparisons. # $P\leq 0.05$, ## $P\leq 0.01$, ### $P\leq 0.005$ vs CTRL group; * $P\leq 0.05$, ** $P\leq 0.01$ vs IL-17 group. From Raucci *et al.* [29]

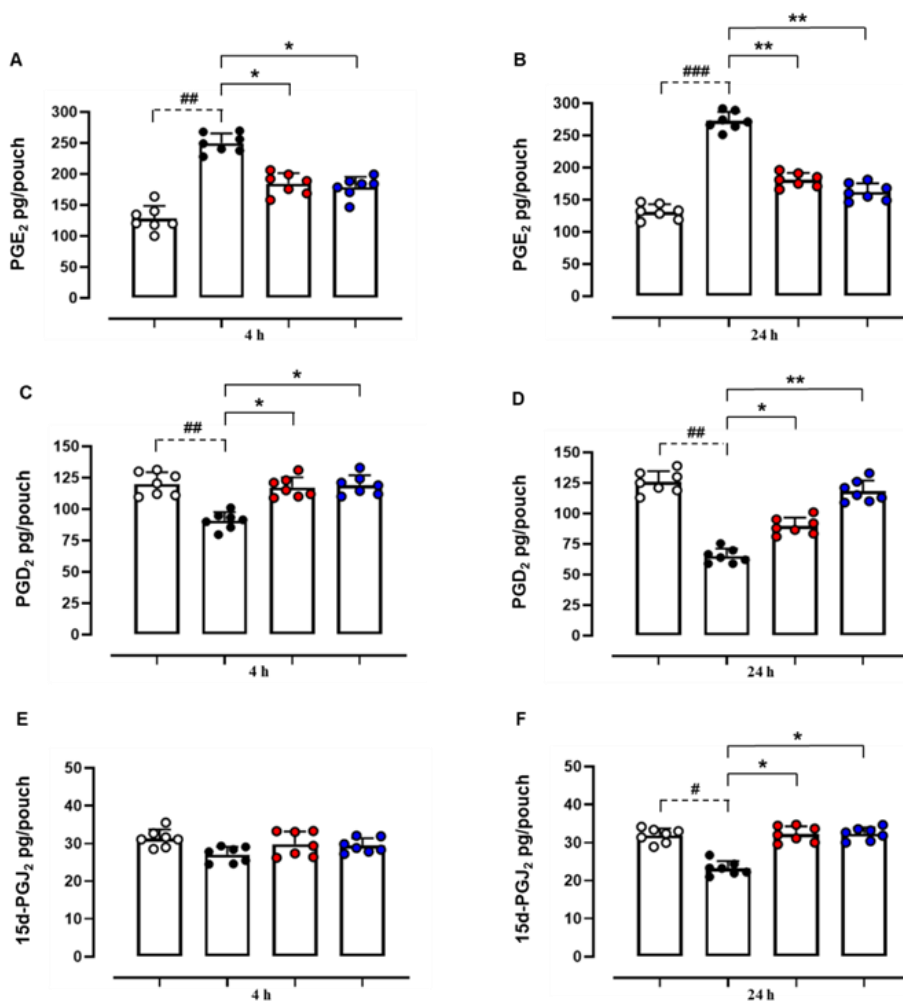
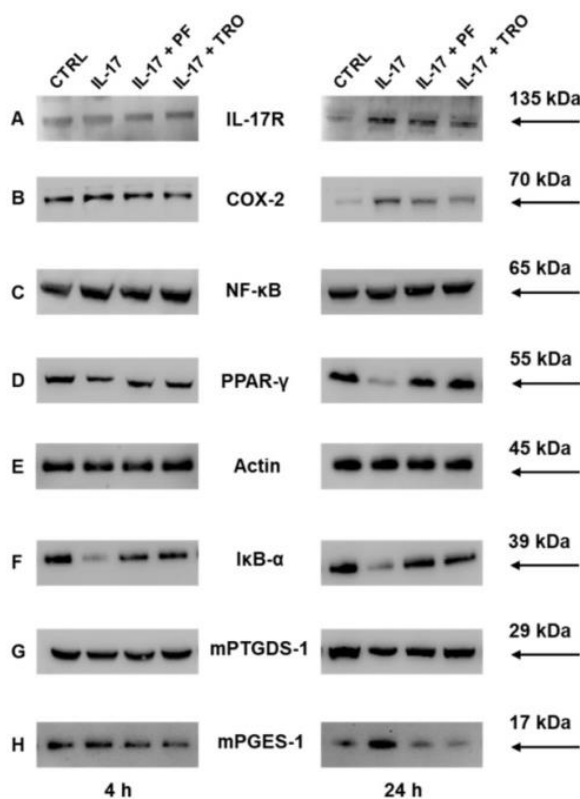


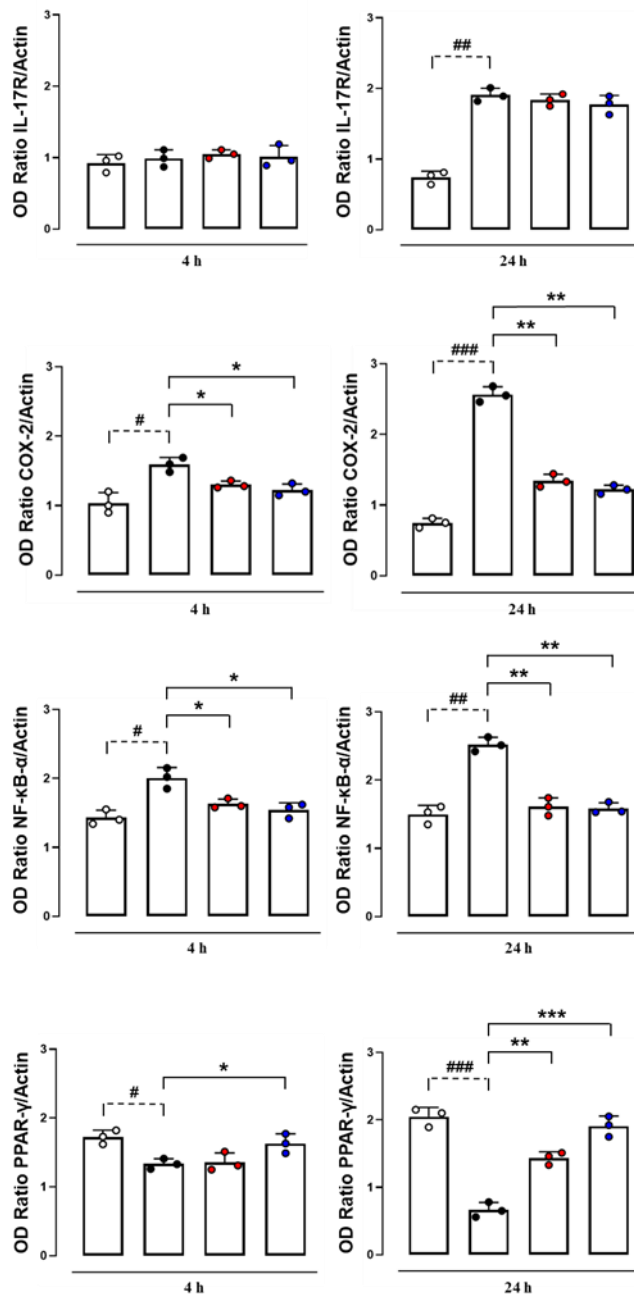
Fig. 2. PF and TRO selectively modulate the release of pro- and/or anti-inflammatory prostaglandins at the site of inflammation. Mice were treated with IL-17 vehicle (CTRL), IL-17 (1 μ g/pouch) alone (IL-17) or co-administrated with PF 9184 (PF, 9 μ g/pouch) and Troglitazone (TRO, 9 μ g/pouch). Inflammatory fluids from all experimental conditions were assayed by Elisa for PGE₂ (A-B), PGD₂ (C-D), and 15d-PGJ₂ (E-F) levels at both 4 and 24 h. Data were expressed as pg/pouch and presented as means \pm S.D. of n=7 mice per group. Statistical analysis was conducted by one-way ANOVA followed by Bonferroni's for multiple comparisons. #P \leq 0.05, ##P \leq 0.01, ###P \leq 0.005 vs CTRL group; *P \leq 0.05, **P \leq 0.01 vs IL-17 group. From Raucci *et al.* [29].

1.2 mPGES-1 and PPAR- γ enzymatic pathway modulation on the onset of ongoing inflammation

Previous studies have shown that in various tissues and cell types, both COX-2 and mPGES-1 expression are enhanced in response to a range of inflammatory mediators, including LPS, IL-1 β , TNF- α , and IL-17 [86]. Therefore, we carried out western blot analysis on recruited cells and found that COX-2 (Fig. 3B) and mPGES-1 (Fig. 3H) were up-regulated following IL-17-induced inflammation and were both significantly reduced at 4 and, in particular, 24 h post PF and TRO treatment. Moreover, we found that IL-17R expression (increased in IL-17-treated animals compared to CTRL group at 24 h) was not influenced by either PF or TRO administration (Fig. 3A). We also observed a substantial increase in NF- κ B expression in mice treated with IL-17 (Fig. 3C). The natural inhibitor of NF- κ B (I κ B- α) was also measured, and the converse was observed in mice treated with PF or TRO at 4, and 24 h (Fig. 3F). Notably, microsomal prostaglandin D₂ synthase-1 (mPTGDS-1) and PPAR- γ expression were weakly present in IL-17 group, whereas it significantly increased in PF (only at 24 h) and TRO-treated mice (at

both 4 and 24 h), confirming the hypothesis of the activation of an alternative molecular pathway following thiazolidinedione administration (Fig. 3D,G respectively). The inhibitory effect of PF was also compared to AF, and similar levels of inhibition in COX-2/mPGES-1 and PPAR- γ expression were observed (Supplementary Fig. 3). Densitometric values (at the bottom of Fig. 3) are expressed as OD Ratio with actin (Fig. 3E) for both 4 and 24 h. Uncropped and original western blots are presented in Supplementary Fig. 4-15.





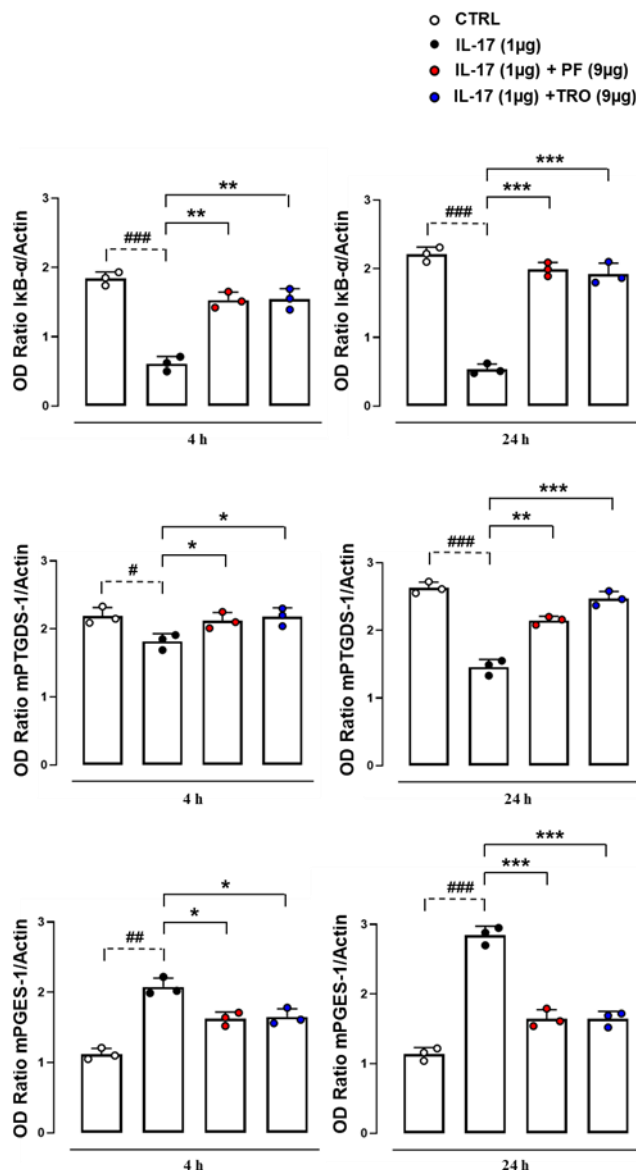


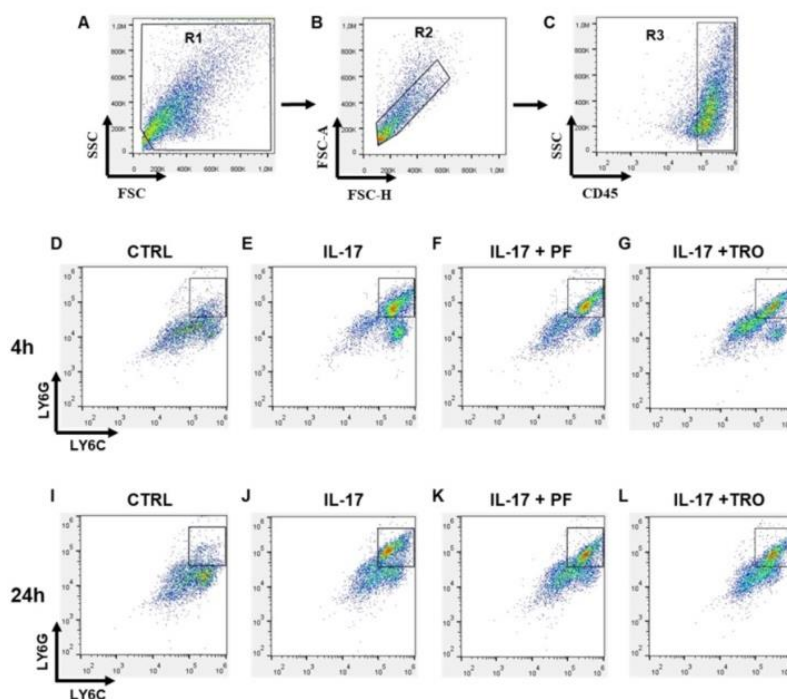
Fig. 3. mPGES-1 and PPAR- γ enzymatic pathway modulation on the onset of ongoing inflammation. Whole cellular pellets homogenates from air pouch experiments in all experimental conditions were assayed by western blot for IL-17 Receptor (IL-17R) (A), COX-2 (B), NF- κ B (C), PPAR- γ (D), IkB- α (F), mPTGDS-1 (G), mPGES-1 (H) expression at 4 and 24 h. Western blot images are representative of three separate experiments with similar results. Cumulative densitometric values (at the

bottom of the Figure) are expressed as OD Ratio with actin (E) for both 4 and 24 h. Values are presented as means \pm S.D. of three separate independent experiments run each with n=7 mice per group pooled. Statistical analysis was conducted by one-way ANOVA followed by Bonferroni's for multiple comparisons. #P \leq 0.05, ##P \leq 0.01, ###P \leq 0.005 vs CTRL group; *P \leq 0.05, **P \leq 0.01, ***P \leq 0.005 vs IL-17 group. From Raucci *et al.* [29].

1.3 PF 9184 and Troglitazone selectively modulate the recruitment of inflammatory monocytes

We further characterize the phenotype of recruited cells at different time points. Flow cytometry was employed to determine neutrophil and monocyte/macrophage subsets. Specifically, to identify potential differences in leukocyte sub-populations, total cells were gated (Fig. 4A, 5A, and 5N, *gate* R1), followed by single cells (Fig. 4B, 5B, and 5O, *gate* R2). CD45 (pan leukocyte/immune cell marker; Fig. 4C) and CD11b (myeloid marker; Fig. 5C,P) were selected (^{+ve}, *gate* R3). Neutrophils were identified as CD45^{+ve}/Ly6G^{hi}/Ly6C^{hi} as shown both at 4 (Fig. 4D-G) and 24 h (Fig. 4I-L). Monocytes and macrophages were further delineated based on a range of markers. CD11b^{+ve} cells were plotted for Ly6C and CD115 at 4 (Fig. 5D-G) and 24 h (Fig. 5I-L) to distinguish CD11b^{+ve}/CD115^{+ve}/Ly6C^{lo} patrolling monocytes (*gate* R4) from CD11b^{+ve}/CD115^{+ve}/Ly6C^{hi} inflammatory monocytes (*gate* R5) [86, 112, 126], and for CD206 and F4/80 (Fig. 5Q-T and 5V-Y at 4 and 24 h respectively) to identify CD11b^{+ve}/F480^{+ve}/CD206^{+ve} reparative macrophages [113]. Our results show that in IL-17-injected mice, at 4 h, the majority of cells recovered were neutrophils (Fig. 4H) which were largely replaced by inflammatory monocytes (Fig. 5M) and a lower proportion of reparative macrophages (Fig. 5Z) at 24 h. Interestingly,

both PF and TRO treatments significantly inhibited this selective and time-dependent recruitment of neutrophils and inflammatory monocytes (Fig. 4H,M and 5H,M). Moreover, TRO administration at 24 h maintained similar levels of reparative macrophages as the control group (Fig. 5Z). No significant differences were found in resident monocyte recruitment in all experimental conditions (*gate R4*). Reported values were strengthened by a low percentage of positive cells found in the staining for the isotype control antibodies (Supplementary Fig. 16). These results suggest that PF and TRO treatment significantly disrupts the recruitment of inflammatory cells in the first phase of the response and that TRO selectively promotes resolution in the subsequent reparative phase.



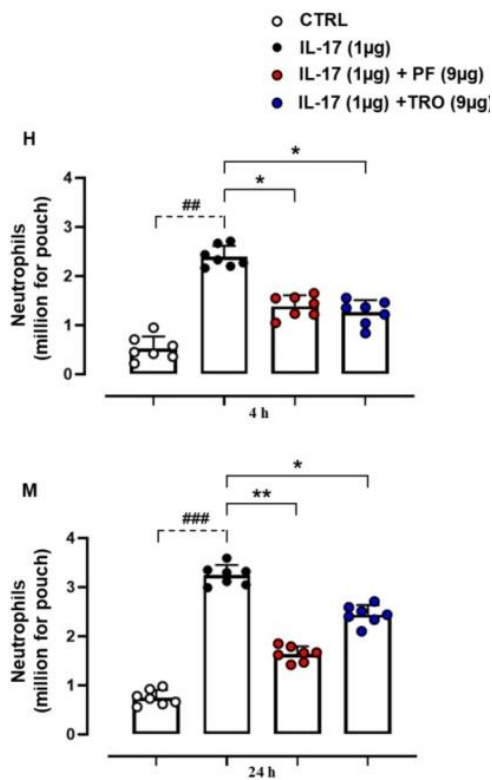
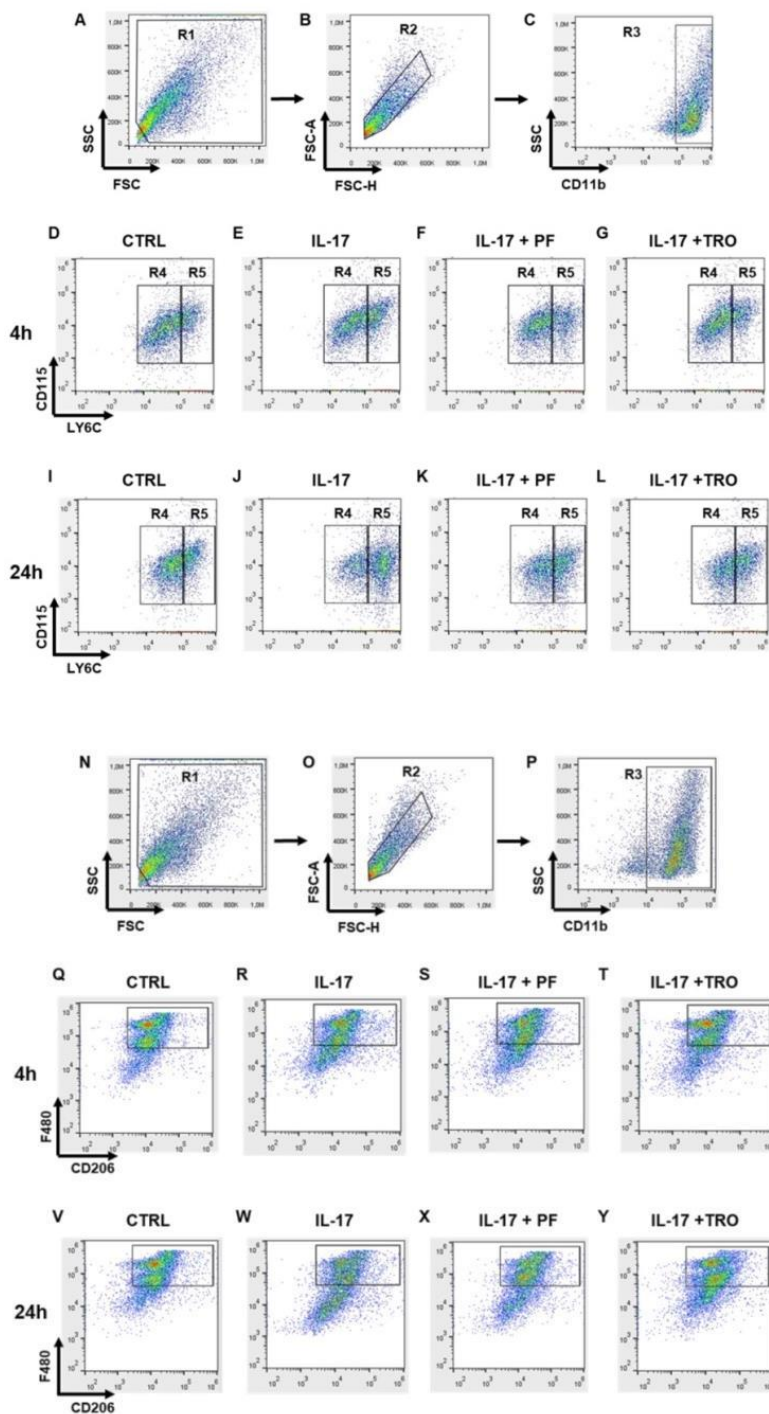


Fig. 4. Flow cytometry strategy applied to identify neutrophils' modulation after IL-17 stimulation. Mice were treated with IL-17 vehicle (CTRL), IL-17 (1 µg/pouch) alone (IL-17) or co-administrated with PF 9184 (PF, 9 µg/pouch) and Troglitazone (TRO, 9 µg/pouch). Cells collected from the pouch cavities were washed and gated in their totality (A, gate R1) and singlet (B, gate R2) before the identification of CD45 positive (C, CD45⁺) population (gate R3). CD45⁺ cells (C) were then plotted for Ly6C and Ly6G expression at 4 (D-G) and 24 h (I-L) to identify CD45⁺/Ly6C⁺/Ly6G⁺ as neutrophils. Histogram values (expressed as million for pouch) indicate the total positive cells, in the different experimental conditions, of CD45⁺/Ly6C⁺/Ly6G⁺ (H,M) at 4 and 24 h. FACS pictures are representative of independent experiments with similar results. Values are presented as means ± S.D. of n=7 mice per group. Statistical analysis was conducted by one-way ANOVA followed by Bonferroni's for multiple comparisons. ###P≤0.01, ####P≤0.005 vs CTRL group; *P≤0.05, **P≤0.01 vs IL-17 group. From Raucci *et al.* [29].



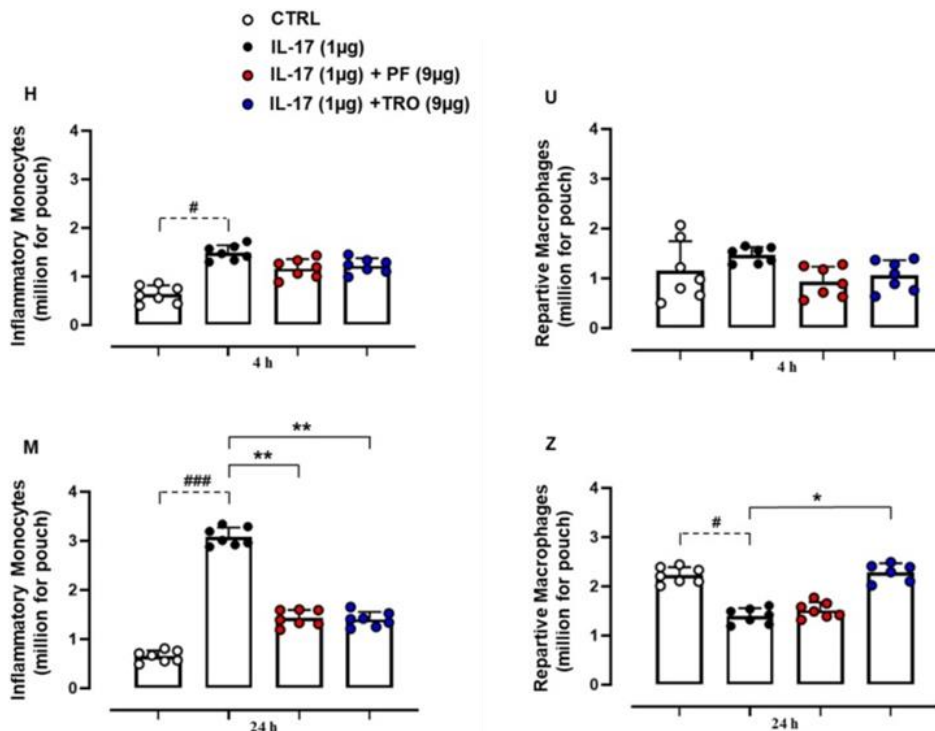
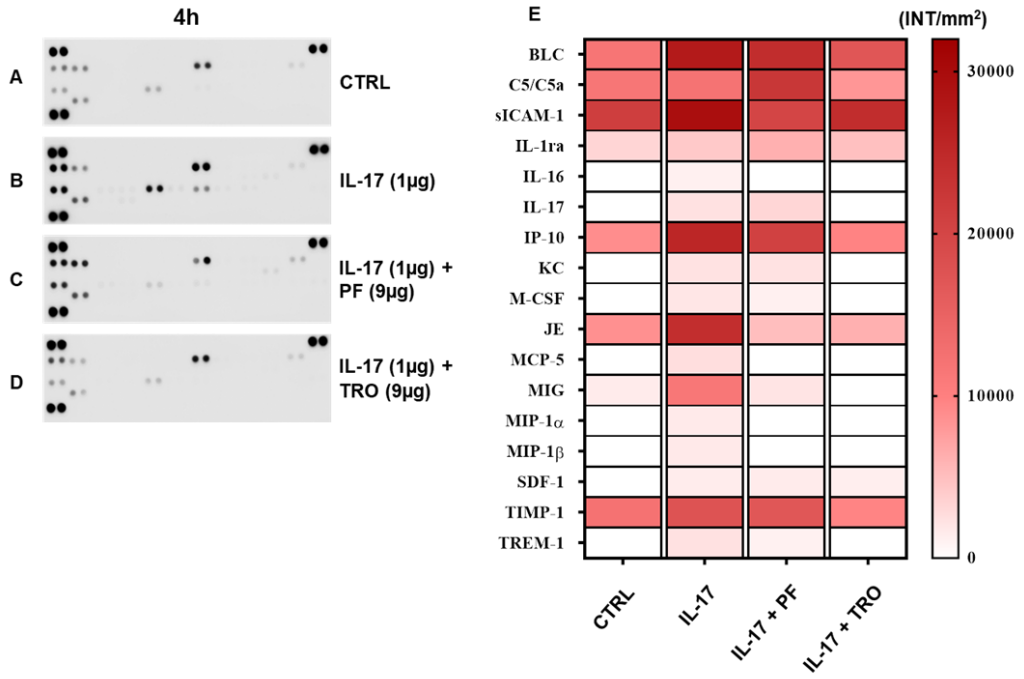


Fig. 5. PF and TRO selectively modulate the recruitment of inflammatory monocytes and reparative macrophages. Mice were treated with IL-17 vehicle (CTRL), IL-17 (1 µg/pouch) alone (IL-17) or co-administrated with PF 9184 (PF, 9 µg/pouch) and Troglitazone (TRO, 9 µg/pouch). Cells collected from the pouch cavities were washed, gated in their totality (A,N, *gate* R1) and singlet (B,O, *gate* R2) before the identification of CD11b positive (C,P CD11b^{+ve}) population (*gate* R3). CD11b^{+ve} (C) cells were then plotted for Ly6C and CD115 expression at 4 (D-G) and 24 h (I-L) to distinguish CD11b^{+ve}/CD115^{+ve}/Ly6C^{low} patrolling monocytes (*gate* R4) from CD11b^{+ve}/CD115^{+ve}/Ly6C^{hi} inflammatory monocytes (*gate* R5). Therefore, CD11b^{+ve} cells were then plotted for CD206 and F480 expression at both 4 (Q-T) and 24 h (V-Y) to identify CD206^{+ve}/F480^{+ve} population. Histograms values (expressed as million for pouch) indicate the total positive cells, in the different experimental conditions, of CD11b^{+ve}/CD115^{+ve}/Ly6C^{hi} (H,M) and CD11b^{+ve}/CD206^{+ve}/F480^{+ve} (U,Z) at 4 and 24 h. FACS pictures are representative of independent experiments with similar results. Values are presented as means ± S.D. of n=7 mice per group. Statistical analysis was conducted by one-way ANOVA followed by Bonferroni's for multiple comparisons. #P<0.05, ###P<0.005 vs CTRL group; *P<0.05, **P<0.01 vs IL-17 group. From Raucci *et al.* [29].

1.4 Co-administration of PF 9184 and Troglitazone with IL-17 into the air pouch decreases the release of cyto-chemokines in the inflammatory fluids

To gain some insights into other possible differences in the inflammatory response caused by the co-administration of an mPGES-1 inhibitor or a PPAR- γ agonist with an IL-17 inflammatory stimulus, we used an unbiased approach (pre-made protein array) based on profiling cytokines and chemokines present in the inflammatory fluids. As shown in Figure 6, the pouch fluid obtained from IL-17-administered mice showed a large increase, at 4 (Fig. 6A-D) and, in particular, 24 h (Fig. 6F-I), of cyto-chemokines compared to vehicle (CTRL group). When comparing pouch fluids from PF and TRO-treated groups with IL-17 (alone), we observed a selective decrease in a range of mediators (Fig. 6A-D and Fig. 6F-I at 4 and 24 h, respectively). Densitometric analysis revealed that the PF-treated group had a specific modulation, at 4 h (Fig. 6E), in the following factors: B lymphocyte chemoattractant (BLC), sICAM-1, IL-16, IP-10, keratinocyte chemoattractant (KC), macrophage colony-stimulating factor (MCSF), junctional epithelium (JE), MCP-5, monokine induced by interferon γ (MIG), MIPs, metalloproteinase inhibitor-1 (TIMP-1) and triggering receptor expressed on myeloid cells-1 (TREM-1) compared to IL-17 group (Fig. 6E). This profile was confirmed at the 24 h time-point (Fig. 6J) in addition to complement component 5a (C5a), INF- γ , IL-1 α , IL-1 β , IL-7, interferon-inducible T-cell α chemoattractant (ITAC) and stromal cell-derived factor-1 (SDF-1) (Fig. 6J). A similar inhibitory profile was found in TRO-injected mice, but surprisingly we observed a more prominent modulation of BLC, C5a, IL-17, IP-10, SDF-1 and TIMP-1 at 4 h (Fig. 6E) and of BLC, sICAM-1, IL-16, IL-17, JE, MCP-5 and MIG at 24 h time-point (Fig. 6J). Δ increase/decrease of cyto-

chemokines in all experimental conditions are reported in Supplementary Fig. 17.



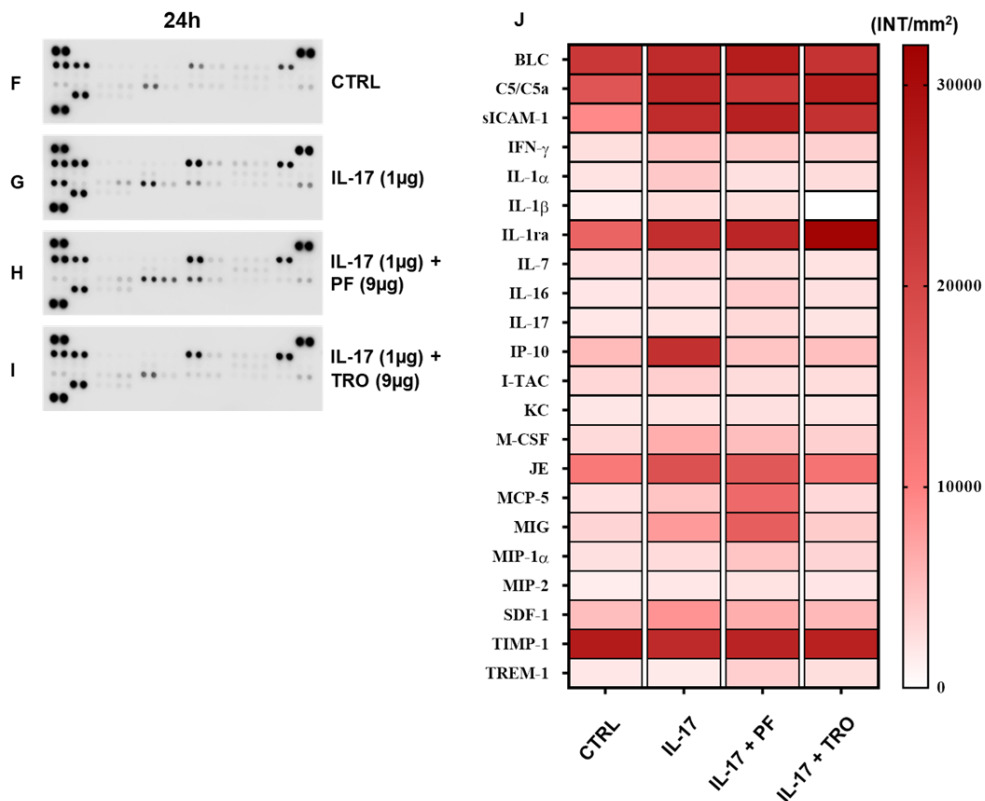
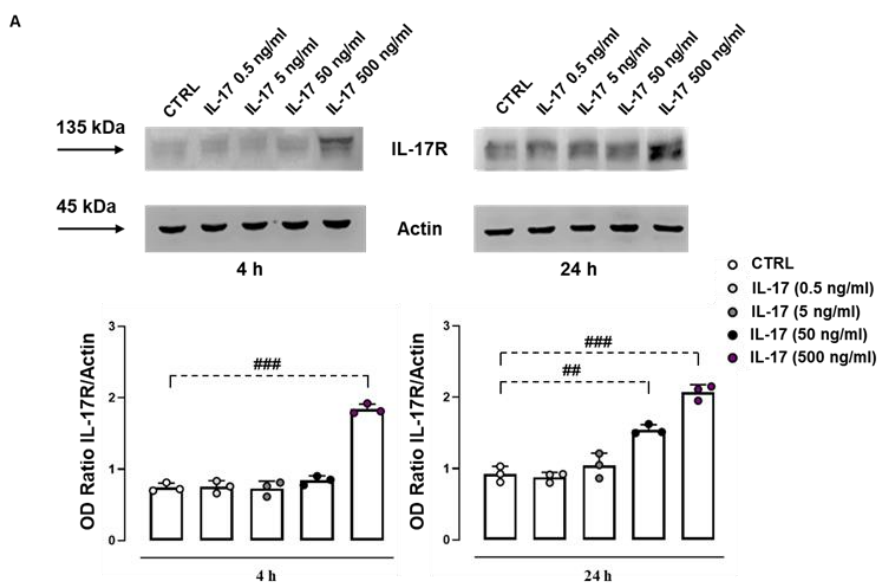


Fig. 6. Co-administration of PF and TRO with IL-17 into the air pouch decreases the release of cyto-chemokines in the inflammatory fluid. Inflammatory supernatants obtained from the pouch cavities were assayed using a Proteome Profiler cytokine array at both 4 and 24 h for CTRL (respectively **A**, **F**), IL-17 (1 µg/pouch, respectively **B**, **G**), IL-17 + PF (9 µg/pouch, respectively **C**, **H**) and IL-17 + TRO (9 µg, respectively **D**, **I**). Densitometric analysis is presented as heat map at 4 (**E**) and 24 h (**J**). Data (expressed as INT/mm²) are presented as means ± S.D. of positive spots of three separate independent experiments run each with n=7 mice per group pooled. From Raucci *et al.* [29].

1.5 Protective effect of PF 9184 and Troglitazone on murine macrophages

To further confirm the validity of our *in vivo* findings, we carried out *in vitro* studies using a murine macrophage cell line J774. Stimulation of macrophages with increasing concentrations of IL-17 (0.5-500 ng/ml) induced a significant increase in IL-17R expression at both 4 and 24 h (Fig. 7A). Notably, pre-treatment of IL-17 (50 ng/ml)-stimulated macrophages with PF or TRO (50 μ M) reverted the expression of COX-2 and mPGES-1 at 4 and 24 h (Fig. 7B). Moreover, PPAR- γ expression was weakly present in IL-17 group, whereas it significantly increased in PF (only at 24 h) and TRO-treated mice (at both 4 and 24 h), further strengthening our hypothesis of activation of an alternative pathway following thiazolidinedione administration (Fig. 7B). Densitometric values (at the bottom of the Fig. 7A,B) are expressed as OD Ratio with actin for both 4 and 24 h. Original western blots are presented in Supplementary Fig. 18-23.



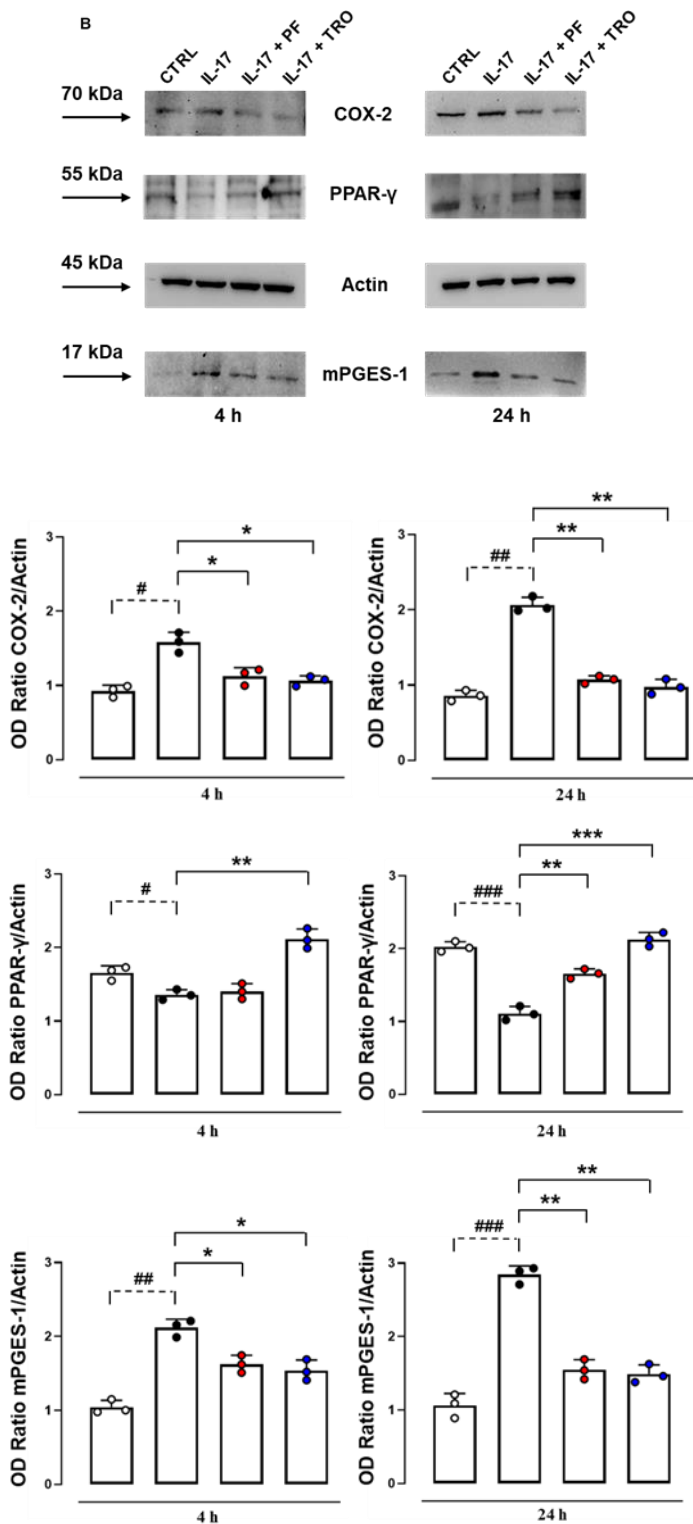


Fig. 7. Protective effect of PF and TRO on murine isolated and IL-17-stimulated macrophage. Whole cellular pellets homogenates from murine macrophages stimulated with increasing concentration of IL-17 (0.5-500 ng/ml) (**A**) or with IL-17 at 50 ng/ml in the presence or absence of PF 9184 (PF, 50 μ M) and Troglitazone (TRO, 50 μ M) at 4 and 24 h (**B**) were analyzed, by western blot, for IL-17R, COX-2, PPAR- γ , mPGES-1 and actin expression. Western blot images are representative of three separate experiments with similar results. Cumulative densitometric values (at the bottom of Figure **A,B**) are expressed as OD Ratio with actin for both 4 and 24 h. Values are presented as means \pm S.D. of three separate independent experiments run each with n=7 mice per group pooled. Statistical analysis was conducted by one-way ANOVA followed by Bonferroni's for multiple comparisons. #P \leq 0.05, ##P \leq 0.01, ###P \leq 0.005 vs CTRL group; *P \leq 0.05, **P \leq 0.01, ***P \leq 0.005 vs IL-17 group. From Raucci *et al.* [29].

2. IL-17 NEUTRALIZING ANTIBODY REGULATES MONOSODIUM URATE CRYSTAL-INDUCED GOUTY INFLAMMATION

2.1 Neutralization of IL-17 reduces the severity of MSU-induced gouty inflammation

I.a. injection of MSU crystals into mouse knee joints was used to mimic the etiologic cause of human gouty inflammation [127]. MSU crystals injection produced an intense and reproducible joint inflammatory score (that peaked between 18 and 24 h) that was dose-dependently attenuated by the administration of IL-17Ab (1-10 $\mu\text{g}/20 \mu\text{l}$), with a maximum inhibition rate observed at the dose of 10 μg . A significant, but lesser, effect was observed when IL-17Ab was administrated at a dose of 3 μg , then abrogated at a dose of 1 μg (Fig. 8A). Administration of IL-17Ab isotype control (IgG_{2A}) had no significant effects on clinical scores (data not shown).

Based on these results, we evaluated joint swelling in a time-course experiment with the most active dose of IL-17Ab (10 μg). As shown in Fig. 8B, neutralization of IL-17 remarkably decreased joint swelling between 18 and 24 h. All inflammatory parameters subsided by 24–48h after MSU crystals injection.

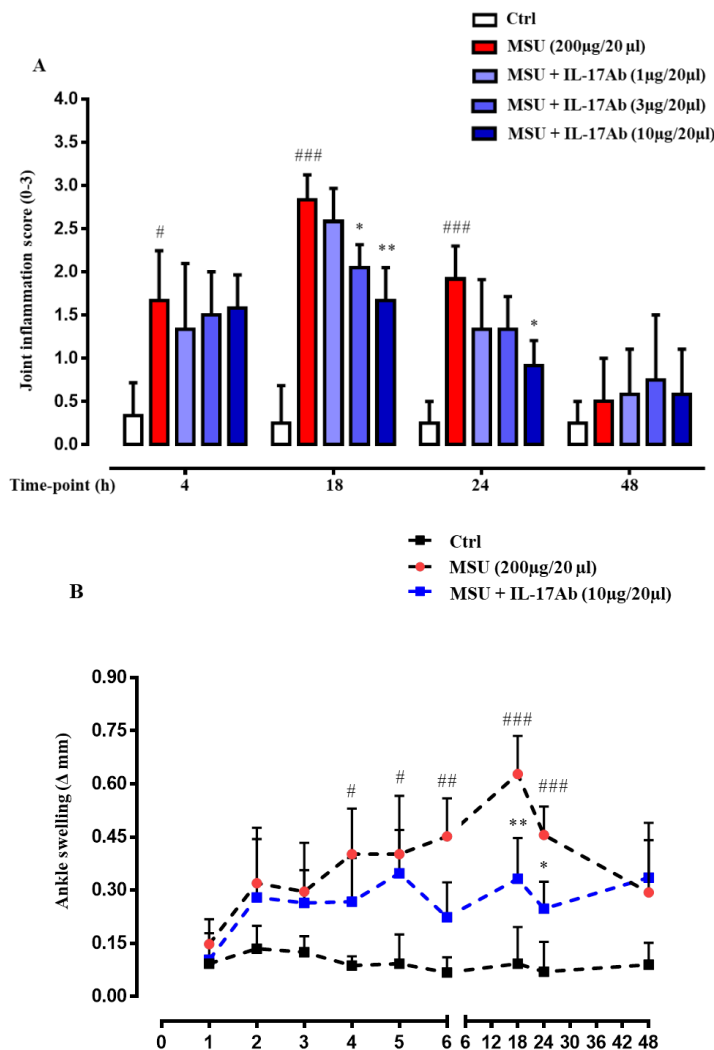


Fig. 8. IL-17Ab modulates MSU crystals-induced gouty inflammation and oedema. Mice were treated with IL-17Ab (1.0, 3.0 and 10µg/20µl) or IL-17Ab vehicle (20µl PBS) 30 min after intra-articular stimulation with MSU crystals (200µg/20µl) in the right knee joint. **(A)** Joint inflammation score (0-3 in increments of 0.25) was evaluated at 4, 18, 24 and 48 h, and **(B)** joint inflammation oedema was evaluated at 1,2,3,4,5,6,18, 24 and 48 h after the stimulus with MSU. Data (expressed as joint inflammation score and Δ increase of knee joint mm) are presented as means \pm SD of n=6 mice per group. Statistical analysis was conducted by one-way ANOVA followed by Bonferroni's multiple comparisons. [#]P<0.05, ^{##}P<0.01, ^{###}P<0.005 vs Ctrl group; ^{*}P<0.05, ^{**}p<0.01 vs MSU group. From Raucci *et al.* [86].

2.2 IL-17Ab ameliorates MSU-induced leukocytes recruitment and activation in the knee joints

Leukocyte recruitment into the knee joint is a hallmark of gout inflammation and arthritis pathology [128, 129]. Thus, based on previous results, we selected the most active doses (10 μ g) of IL-17Ab to test the modulation of leukocyte recruitment and activation. The histopathological (H&E) findings (Fig. 9) show that IL-17Ab reduced inflammatory cell recruitment to the knee joint (Fig. 9C) compared to MSU crystals-treated mice (Fig. 9B), suggesting a reduction in synovitis. In addition, we also observed a significant reduction in MPO activity (a surrogate marker for granulocyte infiltration) in the knee joints of IL-17Ab-treated mice compared to MSU crystals group alone (Fig. 9D).

In line with these observations, it has been reported that in several tissues and different cell types, including leukocytes, fibroblasts, osteoblasts and chondrocytes, mPGEs-1 expression is enhanced by a variety of inflammatory factors, including LPS, IL-1 β , TNF α , and IL-17, the latter of which was targeted in this study [54, 55, 130]. Western blot analysis performed on whole knee joint homogenates showed that COX-2 (Fig. 10A) and mPGEs-1 (Fig. 10B) were up-regulated during MSU crystals condition and were both significantly decreased after IL-17Ab treatment (Fig. 10E,F, respectively). Moreover, we observed that IL-17R expression (increased in MSU-treated animals compared to the Ctrl group) was not influenced after IL-17Ab administration (Fig. 10C,G). Uncropped and original western blots are presented in Supplementary Fig. 24-25. Notably, we observed a strong reduction of soluble PGE₂ levels in the IL-17Ab-treated group compared to MSU-treated animals (Fig. 10H).

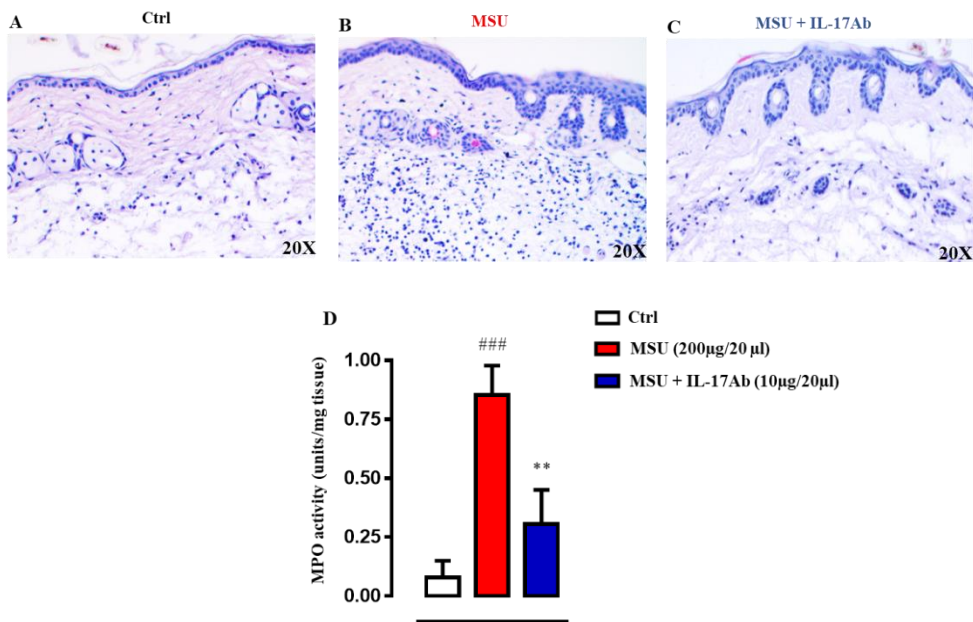


Fig. 9. IL-17Ab treatment moderates leukocyte infiltration in the mouse knee joint. Mice were treated with IL-17Ab (10µg/20µl) or IL-17Ab vehicle (20µl PBS) 30 min after intra-articular stimulation with MSU crystals (200µg/20µl) in the right knee joint. Thereafter, at 18h time-point, knee joint tissues were stained for haematoxylin-eosin (A-C) and tested for myeloperoxidase activity (D). H&E pictures are representative of three independent experiments with similar results. Data of MPO activity (expressed as Units for mg of tissue) are presented as means \pm SD of n=6 mice per group. Statistical analysis was conducted by one-way ANOVA followed by Bonferroni's multiple comparisons. ### $P \leq 0.005$ vs Ctrl group; ** $p \leq 0.01$ vs MSU group. From Raucci *et al.* [86].

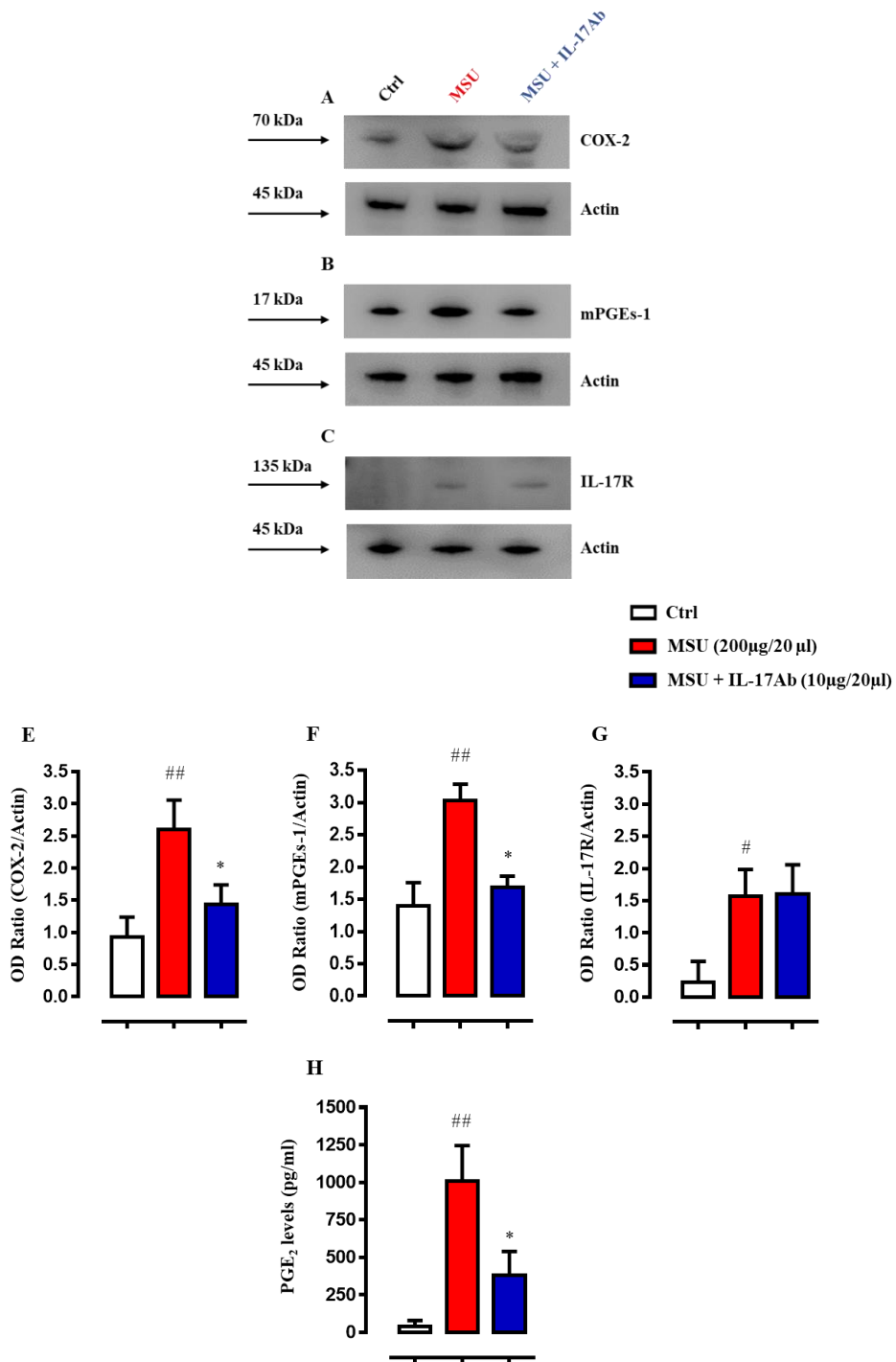


Fig. 10. IL-17Ab modulates COX-2 and mPGEs-1 expression in MSU crystals-induced gouty inflammation. Whole knee joints homogenates from Ctrl, MSU and MSU + IL-17Ab group were analysed by western blot for COX-2 (A), mPGEs-1 (B), IL-17R (C) and their actin expression with related cumulative densitometric values (E-G). WB pictures are representative of three separate experiments with similar results. Thereafter, whole homogenates from different experimental conditions were assayed by Elisa for PGE₂ levels (E). Data of Elisa assay (expressed as pg/ml) are presented as means \pm SD of n=6 mice per group. Statistical analysis was conducted by one-way ANOVA followed by Bonferroni's multiple comparisons. ^{##}P \leq 0.01 vs Ctrl group; *p \leq 0.05 vs MSU group. From Raucci *et al.* [86].

2.3 Injection of IL-17Ab into the knee joints reduces the recruitment of inflammatory monocytes

To investigate and compare the phenotype of inflammatory leukocytes recruited by MSU injection, we stained cells with anti-B220, anti-CD115, anti-F480, and anti-GR1 antibodies and analysed them by flow cytometry. Specifically, to identify potential differences in monocyte subpopulations, we first gated on the B220⁻ population (Gate R1, Fig. 11A,D,G) and then determined GR1 and F480 expression (Fig. 11B,E,H). A double positive population for these markers (Gate R2) was then further interrogated for CD115 (Fig. 11C,F,I) as their expression level is commonly correlated with the degree of maturation of inflammatory monocytes [131, 132]. Our results show that in MSU-injected mice, the majority of cells recovered were B220⁻/GR1^{hi}-F480^{hi}/CD115⁺ (88.30 \pm 2.48 compared to 71.70 \pm 2.57 of Ctrl) with a significant lower expression in IL-17Ab-treated group (75.30 \pm 2.29) (Fig. 11J). These values were strengthened by an irrelevant percentage of positive cells found in the staining for the isotype control antibodies (data not shown).

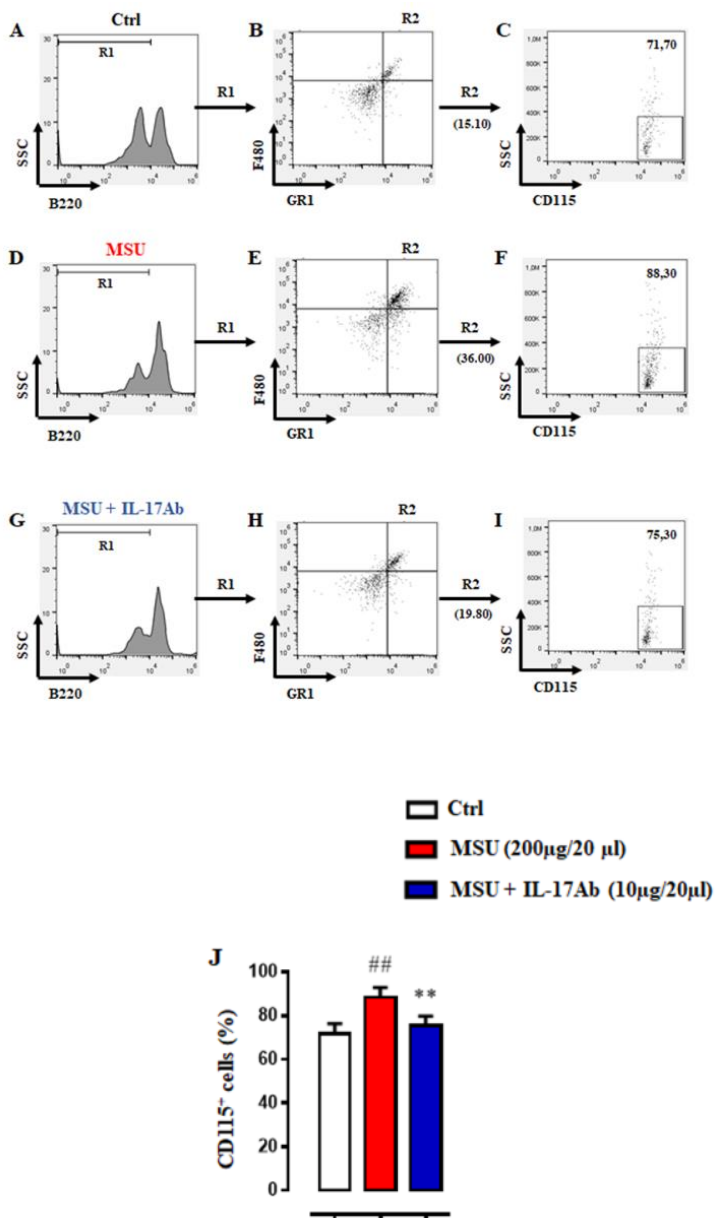


Fig. 11. Flow cytometry strategy applied to identify the modulation of inflammatory monocytes in MSU and MSU + IL-17Ab-treated groups. Ankle joints were digested, and single cell suspensions were obtained. Cells were washed and stained with the following panel of antibodies: anti-B220, anti-CD115, anti-F480, and anti-GR1. Cells negative for B220 (R1, **A**, **D**, **G**) were plotted for GR1-F480 (**B**, **E**, **H**) in

order to get a double positive population (R2) followed by further characterization based on CD115 (C, F, I). The numbers in the dot plots indicated the percentage of positively stained cells after the gating strategy, whereas histogram values (J) indicated the percentage of CD115 positive stained cells. FACS plots are representative of three independent experiments with similar results. Data are presented as means \pm SD of n=6 mice per group. Statistical analysis was conducted by one-way ANOVA followed by Bonferroni's multiple comparisons. ##P \leq 0.01 vs Ctrl group; **p \leq 0.01 vs MSU group. From Raucci *et al.* [86].

We next sought to determine the effect of IL-17Ab on MSU crystals-induced pro-inflammatory cyto-chemokines production (Fig. 12A), given the importance of pro-inflammatory mediators to gout pathology onset [133]. MSU crystals administration induced a robust increase of JE, IL-1 α , IL-1 β , IL-16, IL-17, C5a, BLC and, with a less (but still significant) extent IP-10, Rantes, KC, TIMP-1, SDF-1 and metalloproteinases (Fig. 12C) compared to Ctrl group (Fig. 12B). Interestingly, treatment with IL-17Ab (Fig. 12D) reverted this cyto-chemokines over-production next to MSU crystals-treated mice (Fig. 12E). IL-17Ab isotype control did not alter the levels of any of the mediators measured (data not shown).

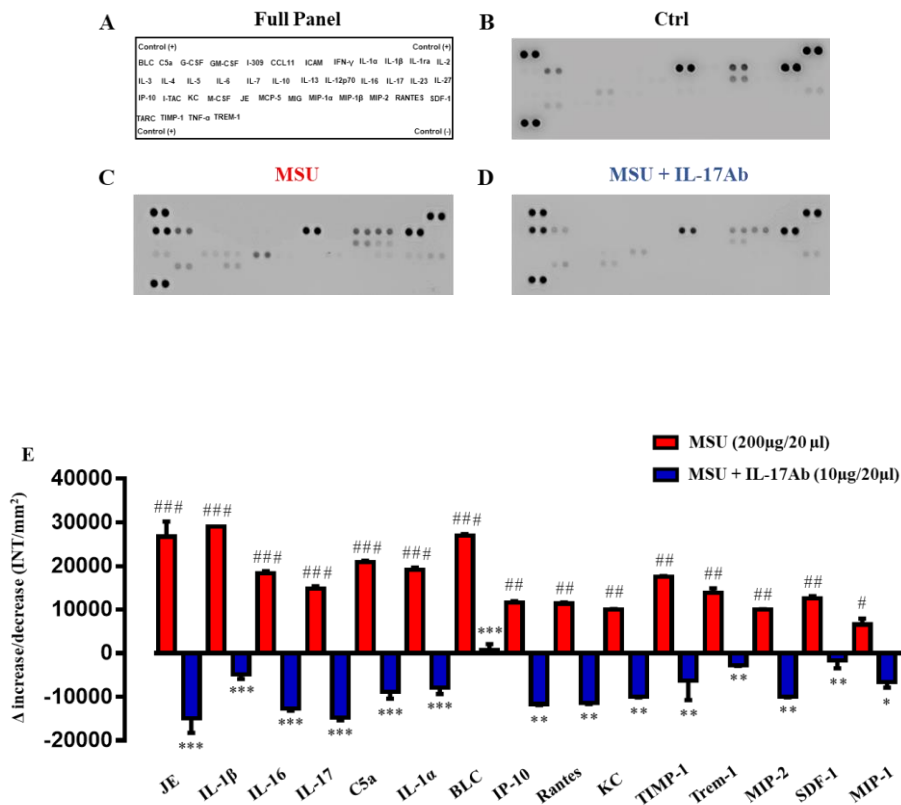
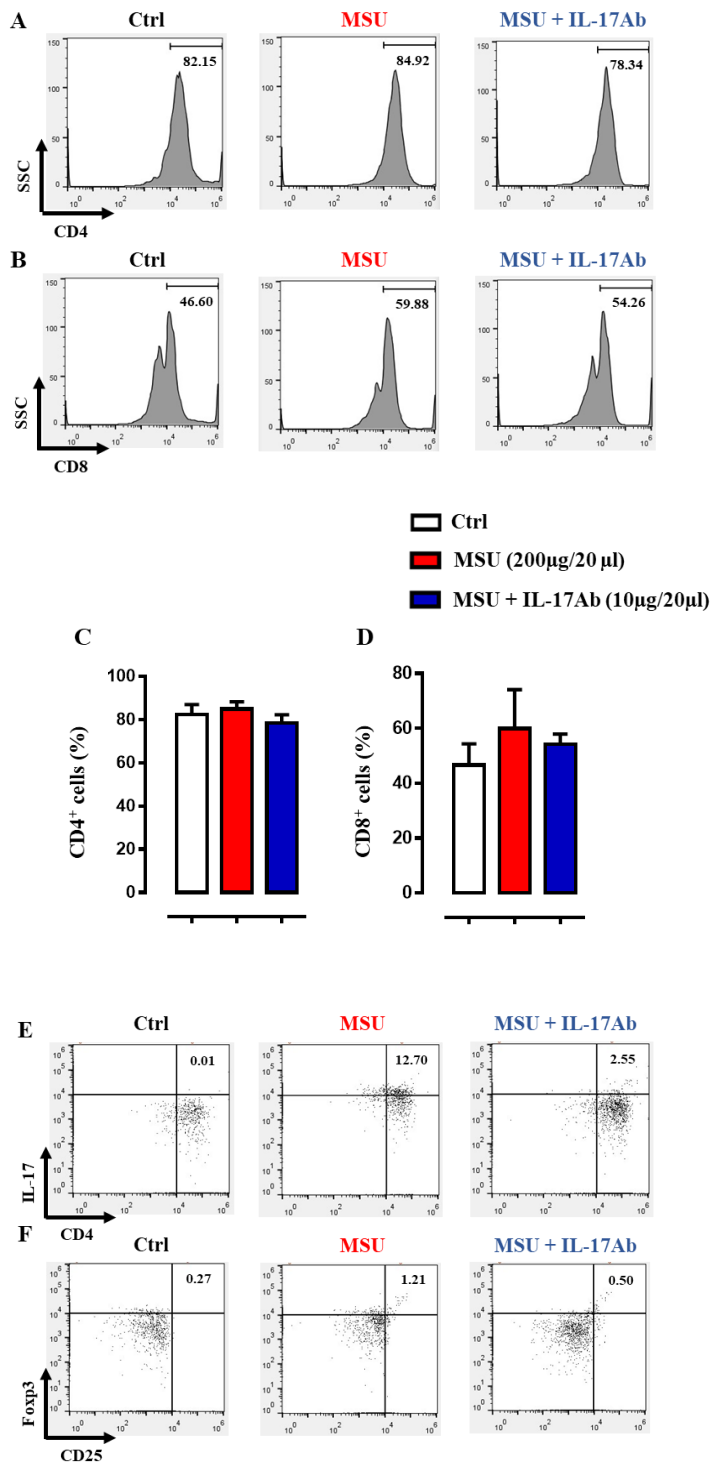


Fig. 12. Survey of inflammatory mediators collected from mice receiving MSU and IL-17Ab injection in the knee joint. Inflammatory fluids obtained from homogenates knees joints were assayed using a Proteome Profiler cytokine array (A) for Ctrl (B), MSU (C) and MSU + IL-17Ab (D) group. The bar graph (E) shows the densitometric analysis of the arrays in B–D. Bars show mean changes \pm SD. of positive spots of three independent experiments with $n=6$ mice obtained as a Δ of increase/decrease in the INT/mm² between MSU and Ctrl (red bar) and MSU + IL-17Ab and MSU (blue bar). Statistical analysis was conducted by one-way ANOVA followed by Bonferroni’s multiple comparisons. # $P \leq 0.05$, ## $P \leq 0.01$, ### $P \leq 0.005$ vs Ctrl group; * $P \leq 0.05$, ** $p \leq 0.01$, *** $p \leq 0.005$ vs MSU group. From Raucci *et al.* [86].

2.4 *In situ* administration of MSU and IL-17Ab influences systemic Th17 and Treg balance

In order to clarify whether the differing inflammatory profiles observed in the knee joints were correlated to different systemic Th17 and Treg balance, we stained isolated lymphocytes cells with an anti-CD4, an accessory protein for MHC class-II antigen/T-cell receptor interaction, an anti-CD8, a marker that identifies cytotoxic/suppressor T-cells that interact with MHC class I and then with an anti-CD4/IL-17 and anti-CD4/CD25/Foxp3 in order to identify Th17 and Treg population respectively according to previous protocols [134, 135].

The results did not reflect any significant difference in the levels of CD4⁺ and CD8⁺ cells in all experimental conditions (Fig. 13A-D). However, as shown in Fig. 13E and G, MSU crystals-treated mice displayed a strong increase in the percentage of Th17⁺ cells (12.70 ± 3.85) compared to the Ctrl group (0.01 ± 0.002), which was significantly reduced after IL-17Ab treatment (2.55 ± 1.10). This systemic lymphocyte profile change (Fig. 13G) did not affect the Treg repertoire, given that we did not observe any significant difference in terms of CD4⁺CD25⁺Foxp3⁺ cells (Fig. 13F,H). These values were strengthened by an irrelevant percentage of positive cells found in all the staining for the isotype control antibodies (data not shown).



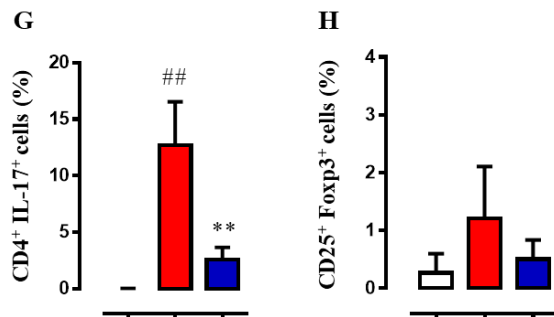


Fig. 13. IL-17Ab influences Th17 and Treg ratio in peripheral blood.

Lymphocytes isolated from whole blood by Ficoll-Paque Plus gradient method were washed and stained with CD4 (A), CD8 (B) and CD4/IL-17 (E). Finally, CD4⁺ cells were plotted for CD25/Foxp3 (F) and analyzed by FACS. Histogram values (C, D, G and H) indicated the percentage of positively stained cells in the different experimental conditions. FACS pictures are representative of three independent experiments with similar results. Data are presented as means \pm SD of n=6 mice per group. Statistical analysis was conducted by one-way ANOVA followed by Bonferroni's multiple comparisons. ^{##}P \leq 0.01 vs Ctrl group; ^{**}p \leq 0.01 vs MSU group. From Raucci *et al.* [86].

3. DESIGN OF THE MOST ACTIVE SEQUENCE OF IL-17A/F AND BIOLOGICAL CHARACTERIZATION OF A NOVEL MONOCLONAL NEUTRALIZING ANTIBODY

3.1 Synthesis and biological characterization of the most active sequence of IL-17A/F

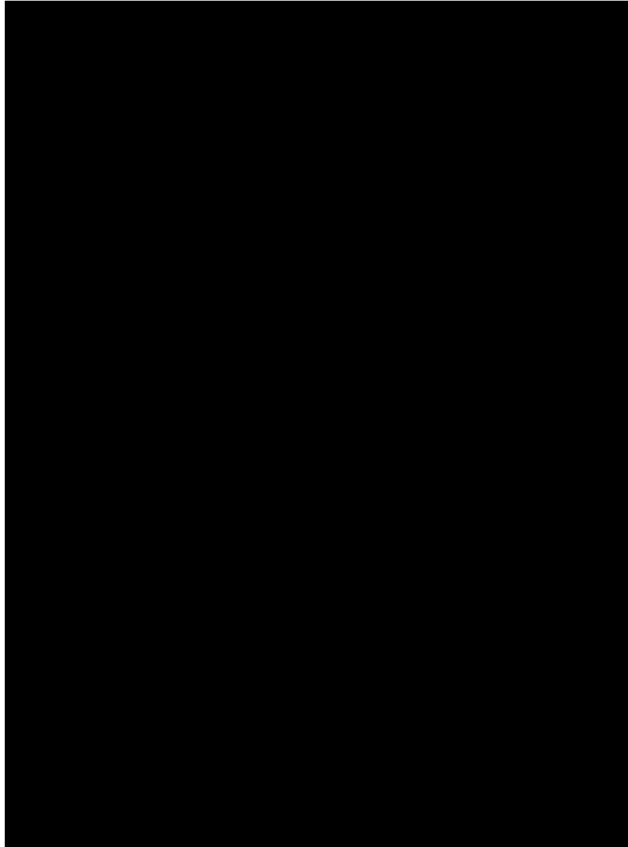
[REDACTED]

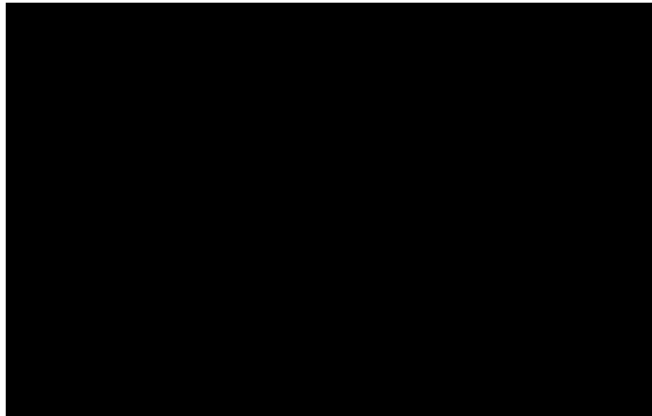
[REDACTED]

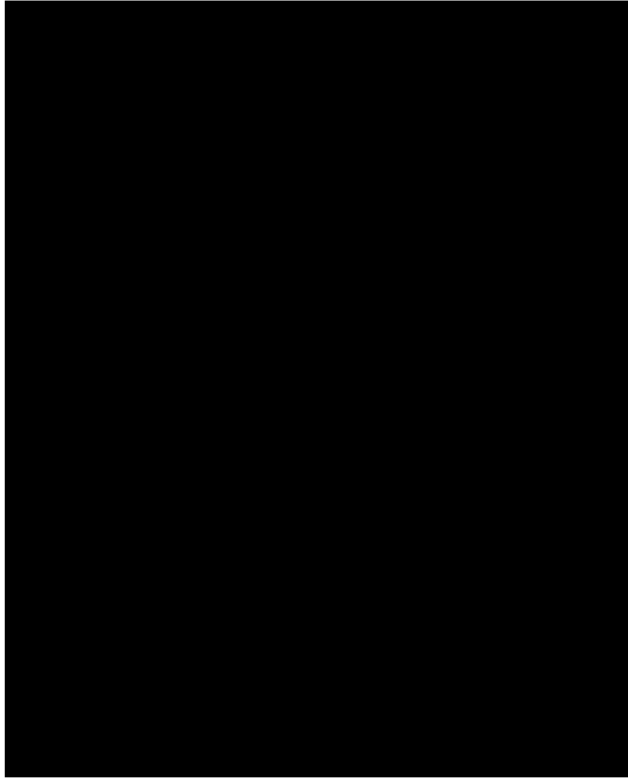
A

[REDACTED]

[REDACTED]

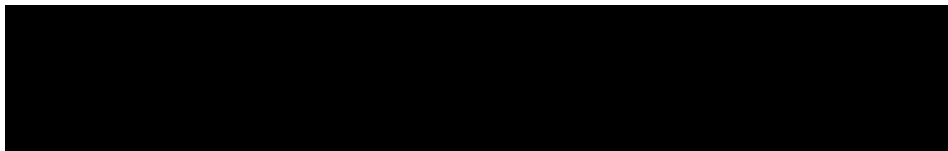
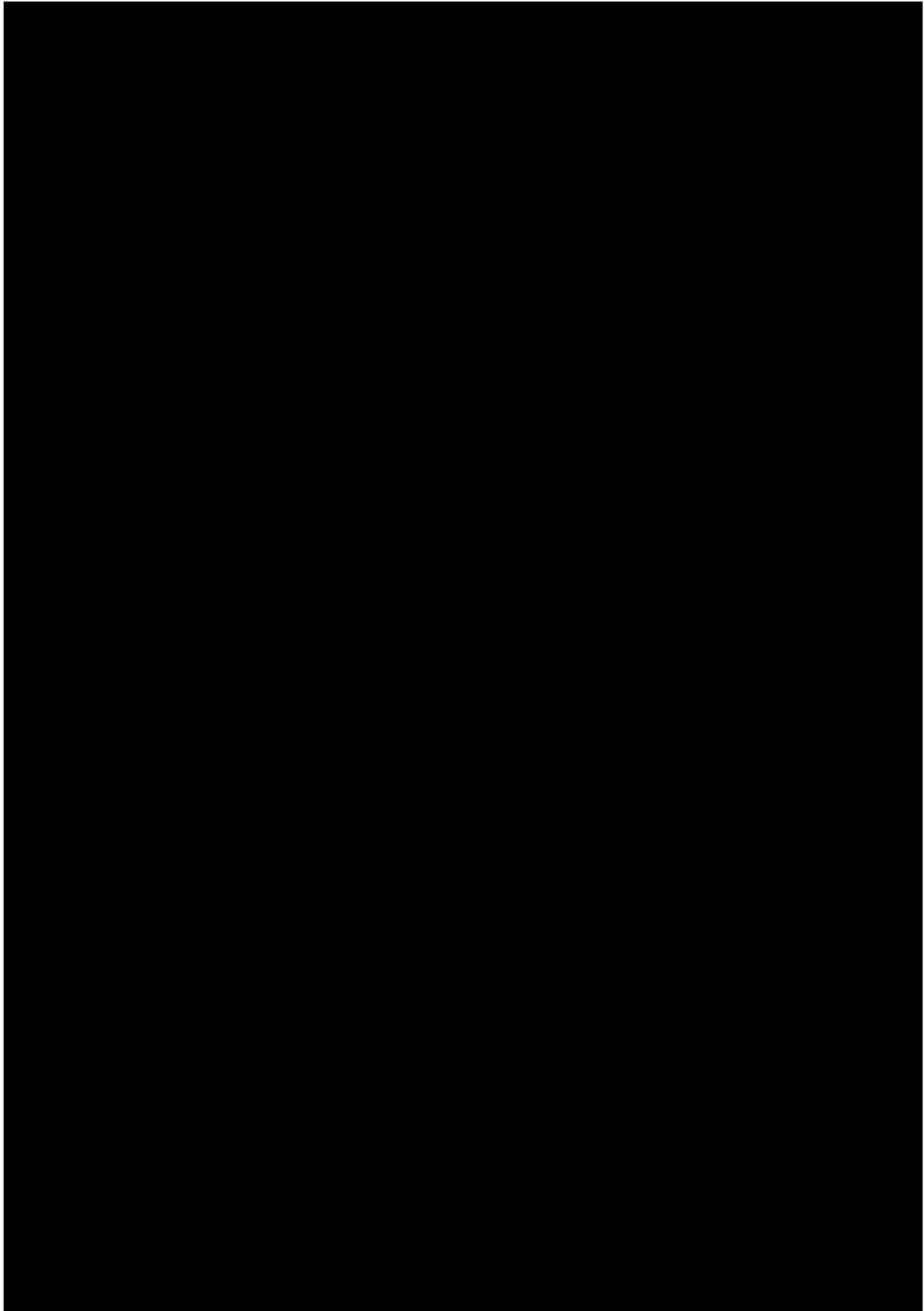






3.2 nIL-17TM exerts a more prominent leukocytes recruitment and cyto-chemokines production next to IL-17 full-length protein on *in vivo* model of chronic inflammation

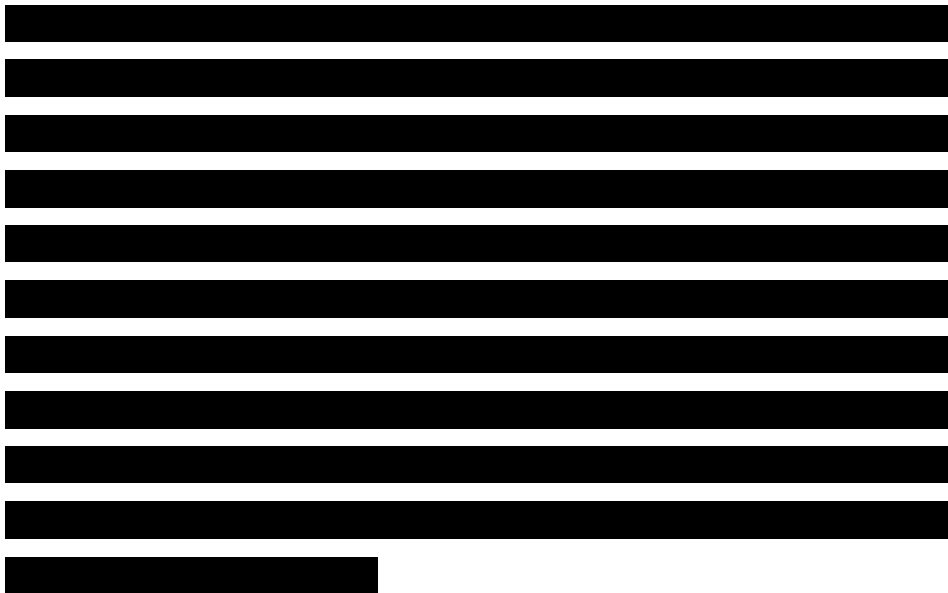
[REDACTED]







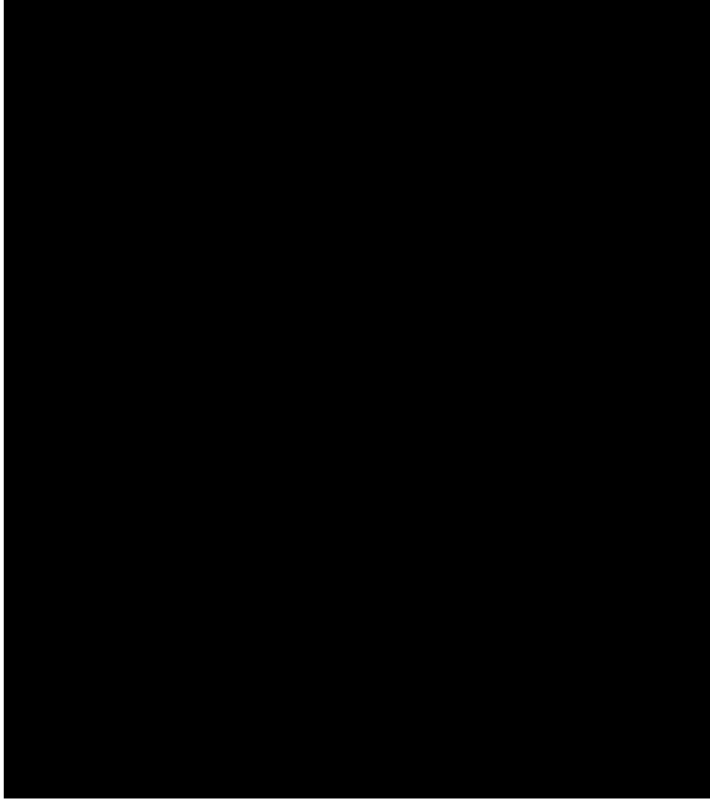
3.3 Biological characterization of a novel IL-17 neutralizing antibody (Ab-IPL-IL-17TM)





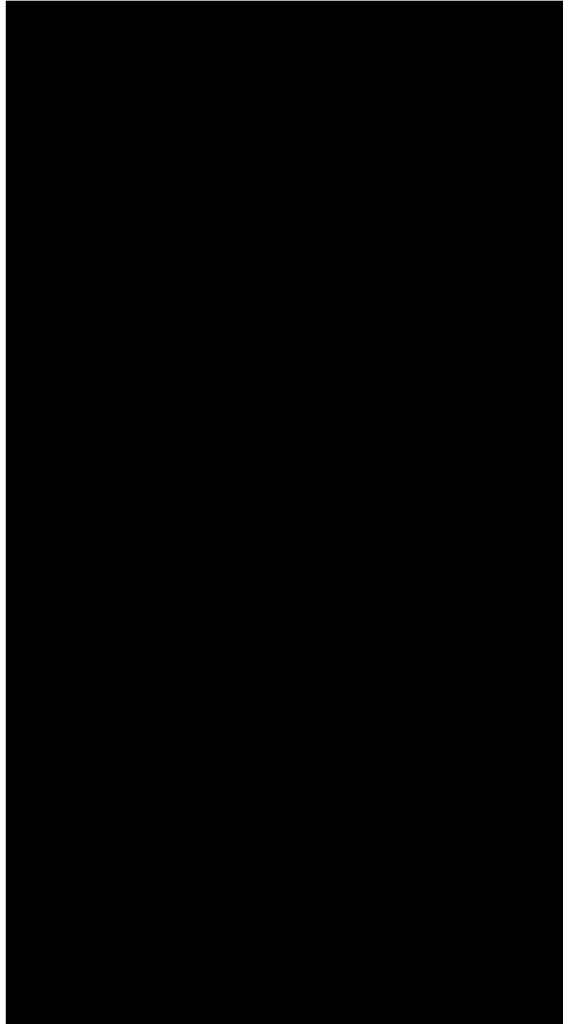
[REDACTED]

[REDACTED]



[REDACTED]

[REDACTED]



CHAPTER 4: DISCUSSION AND CONCLUSIONS**1. IL-17-INDUCED INFLAMMATION MODULATES THE mPGES-1/PPAR- γ PATHWAY IN MONOCYTES/MACROPHAGES**

The integration of inflammatory signals is paramount to controlling the intensity and duration of the immune response. Eicosanoids, particularly PGE₂, are critical molecules in the initiation of inflammation and transition from innate to acquired immune responses. mPGES-1, an integral membrane enzyme functionally coupled to COX-2, whose regulated expression controls PGE₂ levels at sites of inflammation [137, 138], has pleiotropic effects on many immune system cells, influencing both the innate and acquired immune responses [139, 140]. PGE₂ can promote the influx and activation of neutrophils, macrophages and mast cells [141, 142] but can also suppress NKT cytolytic and granulocyte functions [143]. *In vitro* evidence from several groups has shown that the induction of mPGES-1 is increased in response to the pro-inflammatory cytokines IL-1 β , TNF, or LPS and that its expression in certain immune-mediated inflammatory diseases (IMIDs), maybe up-regulated by a wide range of stimuli [144]. Li and colleagues [55] have shown that the expression and regulation of mPGES-1 and PPAR- γ in human osteoarthritic cartilage and chondrocytes are regulated by pro-inflammatory stimuli such as IL-1 α and TNF α and that the concomitant presence of IL-17 displayed a synergistic effect reversed by Troglitazone or exogenous PGE₂. These data suggest that mPGES-1 may prove to be an interesting therapeutic target for controlling PGE₂ synthesis in certain IMIDs such as RA, PsA and spondylarthritis (SpA) [145, 146], where IL-17 levels are uniquely situated to amplify inflammation [56].

Self-regulation of the COXs pathway does not consist solely of positive feedback but also involves mechanisms that inhibit the inflammatory response. At the centre of the COXs auto-inhibitory pathway are PPARs. Activation of inflammatory responses causes an increase in the expression of PPAR- α and a decrease in PPAR- γ [147, 148]. PPARs are nuclear receptors activated by oxidized and nitrated fatty acid derivatives and cyclopentenone prostaglandins (PGA₂ and 15d-PGJ₂) during the inflammatory response. Other activators include nonsteroidal anti-inflammatory drugs (NSAID), fatty acids, especially polyunsaturated fatty acid (PUFA) (arachidonic acid, ALA, EPA, and DHA) and thiazolidinedione derivatives [149]. The primary function of PPARs during the inflammatory reaction is to promote the inactivation of NF- κ B (by direct binding of p65 NF- κ B) or the proteolytic degradation of p65 NF- κ B. PPARs also cause an increase in the expression of I κ B- α , SIRT1, and PTEN, which interfere with the activation and function of NF- κ B in inflammatory reactions [150]. From a pathological point of view, it should also be taken into account that IL-1 α , TNF α , IL-17 and PGE₂, which are involved in the pathogenesis and progression of certain IMIDS, also down-regulate PPAR- γ expression in a dose- and time-dependent manner [151, 152]. Several lines of evidence suggest that PPAR- γ activation may have therapeutic benefits in RA, PsA and possibly other chronic articular diseases [50, 153], where all these mediators, particularly IL-17, are up-regulated [56, 86].

IL-17 is an archetype molecule for the entire family of IL-17 cytokines. Currently believed to be produced by a specific subset of CD4⁺ T cells, named Th17 cells, but also by many innate cell components [13], this cytokine is functionally located at the interface of innate and adaptive immunity [56]. Specifically, IL-17 ability to induce the release of a range

of cyto-chemokines and growth factors has led to its emergence as an essential co-ordinator of local inflammatory reactions due to its ability to modulate neutrophil and monocyte accumulation in inflamed tissues. Furthermore, growing evidence suggests that targeting IL-17 signalling may prove helpful in various inflammatory-based diseases, including RA, Osteoarthritis (OA), asthma, Crohn's disease (CD), psoriatic like-disease and PsA. Here, using a well-established preclinical model of ongoing inflammation, the dorsal air pouch [19], we tested the hypothesis that pre-treatment with an mPGES-1 inhibitor or PPAR- γ agonist could retard the process of IL-17-induced inflammation. We confirmed the pro-inflammatory action (at 4 and 24 h) of IL-17 but also found a novel protective role for PF and TRO, as exemplified by a reduction in both PMN recruitment (at both 4 and in particular 24 h), MPO activity and modulation of crucial lipid mediators strictly related to mPGES-1 and PPAR- γ enzymatic activity (PGE₂, PGD₂, and PGJ₂). From a mechanistic basis, we demonstrated that IL-17 increased in a time-dependent manner, the levels of its receptor (IL-17R), COX-2, mPGES-1, and NF- κ B and decreased mPTGDS-1, PPAR- γ and I κ B- α expression, in pouch-recruited leukocytes. Moreover, co-administration with PF and TRO was shown to significantly revert PMN recruitment, MPO activity, and reduce the level of lipid mediators and, most importantly, modulate mPGES-1, mPTGDS-1, PPAR- γ and NF- κ B/I κ B- α expression, leaving unchanged IL-17R expression. Another exciting aspect of this thesis is that we provide the first reported evidence of an indirect, coordinated functional regulation in both neutrophils and monocytes by mPGES-1 and PPAR- γ . This is most likely related to complex mechanisms regulating COX-2/mPGES-1 *in vivo*, which impact PPAR- γ activity [57].

This hypothesis is consistent with previous studies showing that pre-adipocytes stably transfected with either COX-1 or COX-2 had lower PPAR- γ expression [154] and that mice genetically deficient for mPGES-1 had basal elevations in PPAR- γ expression and transcriptional activity [147]. The mechanisms by which the COX-2/mPGES-1/PGE₂ axis and the nuclear receptor PPAR- γ interact during the inflammatory process are not entirely delineated but may be linked to PGE₂ ability (mainly produced by neutrophils at the early stage of inflammation) to decrease the amount of well-known lipid mediators (such as PGD₂ and PGJ₂) which are implicated in the induction of PPAR- γ [57]. It is also possible that the reduction of COX-2/PGE₂ involves trans-repression, via SUMOylation, of PPAR γ [155, 156]. This “off-target” effect has been previously described for other mPGEs-1 inhibitors [157], such as AF 3485. In this thesis, AF displayed a similar anti-inflammatory profile compared to PF 9184.

This biological event is interconnected with a cellular shift from neutrophils to monocytes, as exemplified by the release of specific neutrophils (KC, C5a) and monocytes/macrophages (INF- γ , IL-16, IL-17, IP-10, JE, MIPs, TREM-1, sICAM-1, IL-1 α/β , MCPs, MIG, TIMP-1) cyto-chemokines. It is well-established in the literature that i) PPAR- γ acts as a negative regulator of macrophage activation [48] due to its ability to control the polarization of monocyte differentiation between pro-inflammatory (M1) and alternative anti-inflammatory (M2) macrophage phenotypes [158] and to reduce neutrophil migration to sites of injury [159]; ii) neutrophils are a primary cellular source of mPGES-1, with activated M1, rather than alternatively activated M2 macrophages, a secondary source [160, 161]. It is clear from these current results that the release of PGE₂ and PGD₂/PGJ₂ related to COX-2/mPGES-1 and PPAR-

γ /mPTGDS-1 expression follows the temporal shift from neutrophils to monocytes that are implicated in the potential resolution of inflammatory response. This was confirmed by our experiments performed in the presence of either PF or TRO's where both compounds were shown to revert the inflammatory response (Fig. 1). To further support this association between IL-17 and mPGEs-1/PPAR γ expression and modulation, and in light of the detrimental role of macrophages and macrophage-derived cytokines in RA and SpA synovium [162], we performed *in vitro* experiments where we used J774 cell line. Interestingly, we confirmed our *in vivo* results, demonstrating a direct involvement of mPGEs-1/PPAR- γ axis in IL-17-stimulated macrophages.

1.1 Conclusions

In conclusion, our results reveal a novel interaction between IL-17 and mPGEs-1/PPAR- γ generated by macrophages/inflammatory monocytes during inflammation. Therefore, we believe that the IL-17/mPGEs-1/PPAR- γ “axis” could represent a potential therapeutic target for inflammatory-based and immune-mediated diseases.

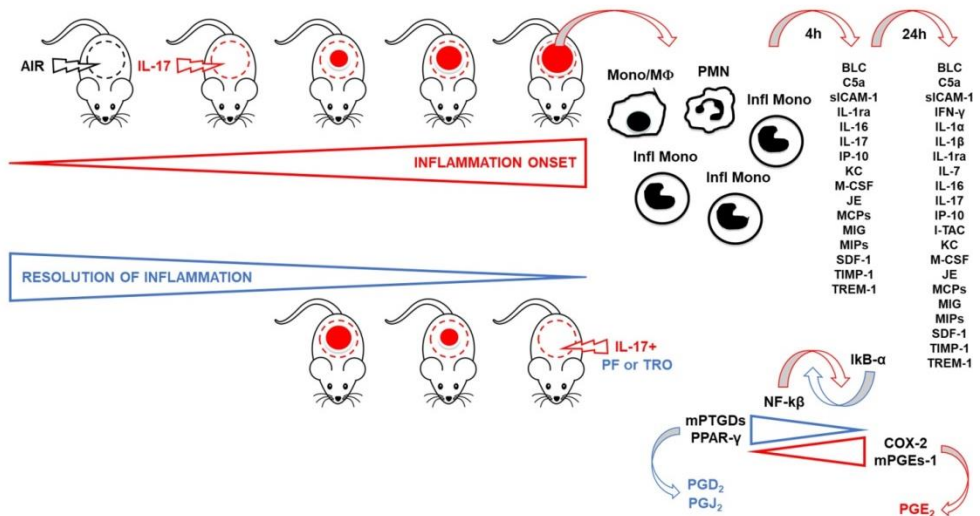


Fig. 1 Schematic representation IL-17/mPGES-1/PPAR- γ axis involvement on the onset and resolution of inflammation. IL-17 injection into the air pouch recruits neutrophils and, more specifically, inflammatory monocytes, producing a massive release of pro-inflammatory cyto-chemokines at 4 and 24 h. However, the co-administration of IL-17 with an mPGES-1 inhibitor (PF) or PPAR- γ agonist (TRO) shifts the *equilibrium* between COX-2/mPGES-1 and PPAR- γ /mPTGDS-1 pathways, down-regulating PGE₂ and up-regulating PGD₂/PGJ₂ levels via NF- κ B. From Raucci *et al.* [29].

2. IL-17 NEUTRALIZING ANTIBODY REGULATES MONOSODIUM URATE CRYSTAL-INDUCED GOUTY INFLAMMATION

The results of this thesis show, for the first time, that i.a. injection of MSU crystals stimulates *in vivo* production of Th17 cells and Th17-related inflammatory cyto-chemokines. In addition, we have provided evidence that the administration of a neutralizing antibody against IL-17 attenuates joint symptoms, swelling and leukocyte infiltration/activation to the inflamed tissues, possibly providing a new strategy for the treatment of gouty inflammation and/or arthritis.

Gout is characterized by the deposition of MSU crystals in joints, which is associated with increased serum urate content, leading to excruciating pain and inflammatory events [163, 164]. In addition, MSU crystals deposits induce chronic inflammatory responses that may lead to joint damage, often referred to as gouty arthritis or chronic gout [165]. Moreover, MSU crystals can also cause acute, self-limited, inflammatory flares, which are likely triggered by crystal shedding from the cartilage surface into the joint space, where they can interact with resident cells.

All these processes are mainly related to activated neutrophils and macrophages, which are responsible for the release of PGE₂, IL-1 β , TNF α , and activate nociceptor neurons and, thereby, producing pain [166-168]. Indeed, targeting IL-1 β , TNF α or PGE₂ in rheumatic diseases reduce neutrophil recruitment and associated pain [128].

Recent evidence has highlighted that serum IL-17 levels are significantly elevated in GA patients [70] and that systemic Th17/Treg imbalance is consistent with inflammation development in the joints. Accordingly, the changes in the Th17/Treg ratio decrease at an earlier stage, followed by

an increase at a later stage, suggesting a photogenic role of this specific CD4⁺ subset in gouty onset and development [72]. In line with these observations, we have demonstrated that MSU crystals injection in mice induces the up-regulation of different mediators strictly correlated with the biological activity of IL-17 and Th17 cells profile [13]. Furthermore, we found that MSU crystals administration induced the modulation of i) typical pro-inflammatory cytokines such as IL-1 α , IL-1 β , IL-16, IL-17 and TREM-1, ii) different chemokines such as BLC, IP-10, JE, SDF-1 and Rantes involved in leukocytes recruitment and activation and iii) other activators of inflammation such as C5a, the chemotactic cytokines MIP-1/2 and the tissue inhibitor of metalloproteinase TIMP-1.

In line with these observations, it has been reported that in several tissues and different cell types, including leukocytes, fibroblasts, osteoblasts and chondrocytes, mPGEs-1 expression is enhanced by a variety of inflammatory factors, including LPS, IL-1 β , TNF- α , and IL-17, the latter of which was targeted in this study [54, 55, 130]. COX-2/mPGEs-1 is a very complex enzymatic process that initiates the formation of PGE₂ and the lengthening of the pro-inflammatory and pro-nociceptive stimuli [45, 169]. The concept of a changeable PGs production pathway (including the modulation of both COX-2 and mPGEs-1) could have important implications for understanding the inflammatory events typical of certain illnesses, including gouty inflammation and/or arthritis. Interestingly, we have demonstrated that COX-2 and mPGEs-1 were up-regulated during MSU administration, and both decreased after IL-17Ab treatment. This finding was also confirmed by a strong reduction of PGE₂ levels in the IL-17Ab-treated group. The selective modulation of COX-2/mPGEs-1 pathway was also correlated with the observation that IL-17 receptor expression (increased in MSU-treated animals compared to the Ctrl

group) was not influenced by IL-17Ab administration. All these biochemical changes were consistent with those observed macroscopically. Indeed, administration of a neutralizing monoclonal antibody against IL-17 prevented the swelling of the inflamed joints between 18 and 24 h, but it failed to have a consistent effect at other time points of observation.

Successively, to investigate and compare the phenotype of the inflammatory leukocytes recruited by MSU injection into knee joints, we first gated on cells isolated from knee joints for B220⁻ population, followed by GR1-F480 expression to finally identify the level of CD115⁺, commonly correlated with the degree of maturation of inflammatory monocytes [131, 132]. Our results show that in MSU-injected mice, most of the cells recovered were inflammatory monocytes with a significant lower expression of mentioned markers in the IL-17Ab-treated group.

The inflammatory effects of MSU crystals have been recently suggested to involve the activation of the NLRP3 inflammasome and IL-1 β [170]. Furthermore, the role of this cytokine in the pathogenesis of inflammation in gout has been strengthened by studies showing that the biologic Anakinra (recombinant IL-1Ra) has beneficial therapeutic effects in gout [171, 172]. However, in the literature, the role of other specific inflammatory components necessary for gouty onset, such as IL-16, TREM-1, JE, Rantes and SDF-1 that we found up-regulated and modulated in MSU crystals and IL-17Ab-treated mice respectively, is less clear. In this context, the presence of IL-17 could justify the overproduction of these soluble mediators released from activated monocytes/macrophages in the later stage of gouty inflammation. In fact, an aspect that should not be omitted is that the presence of IL-17 at the

later stages of the inflammatory response has been proposed to be the main contributor to chronic inflammation due to its ability to sustain the recruitment of neutrophils and inflammatory monocytes [82, 173], mainly by the selective production of JE, IL-16 and TREM-1 [19, 56, 73, 74]. Given that this cytokine is thought to contribute to the pathogenesis of this disease, targeting the IL-17 axis could represent an attractive option for inflammatory-related diseases.

IL-16 and TREM-1 are classically considered key players in rheumatoid arthritis and inflammatory-related diseases due to their ability to modulate neutrophil migration across the epithelium [174] and macrophage infiltration at pathological sites [175, 176]. Recent studies also demonstrated that fibroblast-like synoviocytes from RA patients express higher levels of IL-16 compared to those from osteoarthritis patients [177] and that TREM-1 is involved in both neutrophil migration and macrophage infiltration in chronic inflammatory pathologies [174, 178] thus providing a possible explanation for the amplified inflammatory response we observed in our thesis.

Considering this scenario, it makes sense that patients with RA display a high level of IL-17 and are more sensitive to an anti-IL-17 inhibitor. Accordingly, in most of these patients, anti-IL-17 treatment reduces symptoms, inflammation, and bone destruction [179, 180]. Moreover, it should be noted that IL-17 has been shown to play a key role in other forms of arthritis, such as PsA, in which the induction of IL-17 cytokines axis (IL-17A, IL-17F and IL-22) promotes intra-and/or peri-articular inflammation [181-183]. To better understand this previous observation and to view the coin from another side, a flow cytometry bioassay was carried out on peripheral blood to evaluate the balance of Treg/Th17 after MSU crystals induction and IL-17Ab treatment. Interestingly, our results

show that IL-17Ab selectively reverted Th17 systemic positive cells “normally” up-regulated after MSU crystals injection without interfering with the Treg population.

2.1 Conclusions

Overall, our findings and previously reported evidence suggest that IL-17 may play a crucial role in joint pathology at the late phase of crystal-induced acute inflammation/arthritis. However, what we think as most interesting and novel in this thesis is the possibility of the existence of two mechanisms of inflammatory amplification during gouty inflammation: one local and the second systemic that, in turn, amplify and sustain the inflammatory onset but, intriguingly, both related to Th17 and IL-17 biology (Fig. 2). Future elucidation of the pathophysiological roles of IL-17 in gouty inflammation will be crucial in the understanding the precise mechanism of crystal-induced inflammation and will possibly provide a new strategy for the treatment of this pathology.

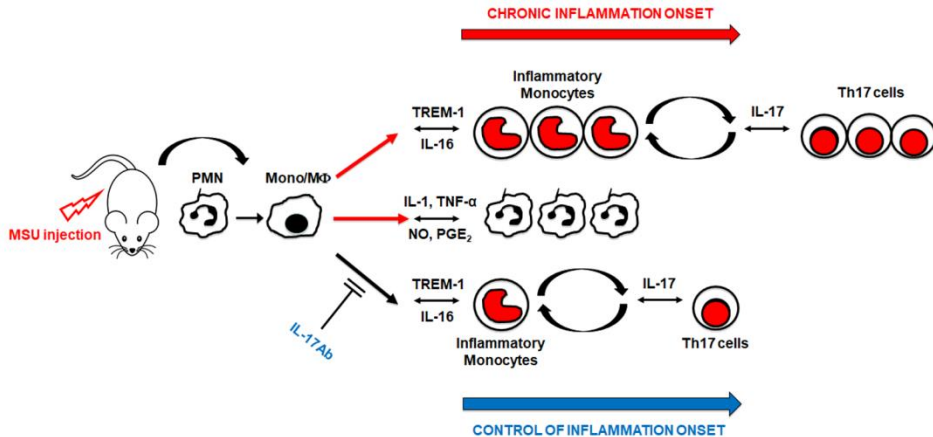


Fig. 2 Schematic representation of IL-17/COX-2/mPGES-1 axis involvement on the onset and resolution of gouty arthritis. Intra-articular injection of MSU crystals recruits infiltrating inflammatory monocytes and circulating Th17, but not Treg, producing a massive release of related pro-inflammatory cyto-chemokines. However, the administration of a neutralizing antibody against IL-17 (IL-17Ab) shifts this *equilibrium* attenuating joint symptoms, swelling and leukocyte infiltration. From Raucci *et al.* [86].

3. DESIGN OF THE MOST ACTIVE SEQUENCE OF IL-17A/F AND BIOLOGICAL CHARACTERIZATION OF A NOVEL MONOCLONAL NEUTRALIZING ANTIBODY

[REDACTED]

[Redacted text block]

[Redacted text block]

3.1 Conclusions

[Redacted text block]

[Redacted text block]

[Large redacted text block]



CHAPTER 5: GENERAL CONCLUSIONS

Rapid progress in both disease knowledge and biotechnology over the past three decades has led to an increasingly diverse armamentarium of therapies for IMIDs.

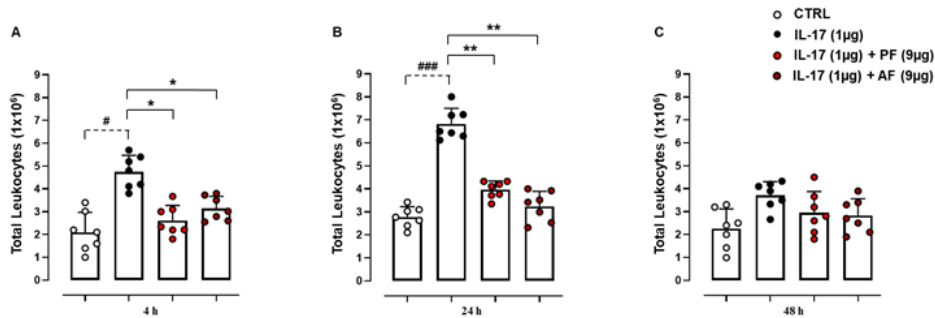
CD4⁺ T cells sit at the interface between innate and adaptive immunity and are considered the orchestrators of the adaptive immune response. Early studies of CD4⁺ T-cell biology described two mutually exclusive phenotypes, Th1 and Th2. Th1 cells promote cellular immunity against intracellular pathogens via the release of cytokines such as IFN γ , whereas Th2 cells promote humoral immunity and the response to helminth infections via the production of IL-4, IL-5 and IL-13. Th1 cells were initially regarded as the drivers of many IMIDs, including RA, although both animal and human data suggested that they were not always essential, catalysing the search for alternative subsets.

Th17 cells appeared to fill this gap, at least in some diseases. IL-17, one of the cytokines produced mainly by this subset, is a potent pro-inflammatory cytokine which, together with TNF α and IL-1 β , recruits neutrophils and macrophages as well as inhibits chondrocyte metabolism and promotes osteoclastogenesis. Since their discovery, Th17 cells have been implicated in various IMIDs, including RA, Ps, PsA, AS and IBDs. Blocking the Th17 axis, either by inhibiting IL-17 directly or via preventing Th17 cell differentiation, is now an area of intense therapeutic development.

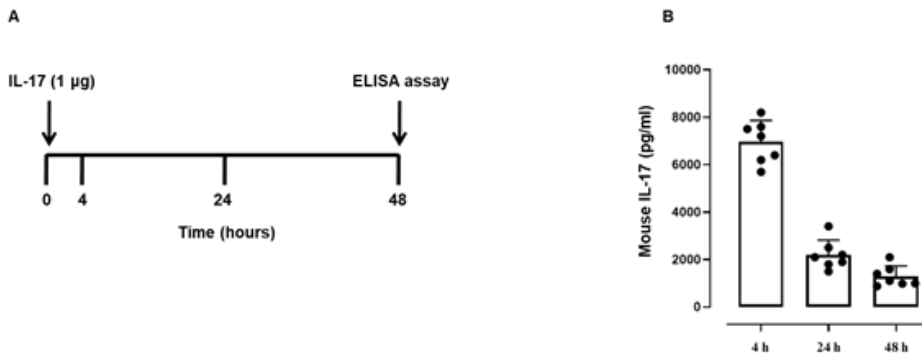
In this PhD thesis, we have highlighted a few examples of novel approaches, particularly where data have provided new downstream knowledge/s. We have demonstrated that IL-17 may constitute a specific modulator of inflammatory monocytes during later phases of the inflammatory response. The results of this thesis show, for the first time,

that the IL-17/mPGES-1/PPAR- γ pathway could represent a potential therapeutic target for inflammatory-based and immune-mediated diseases such as gouty arthritis. Contextually, we have identified the “essential” A.A. sequence responsible for both mouse and human IL-17A/F biological activity providing the biochemical basis and also preclinical evidence for the development of a “new generation” of IL-17-neutralizing antibodies.

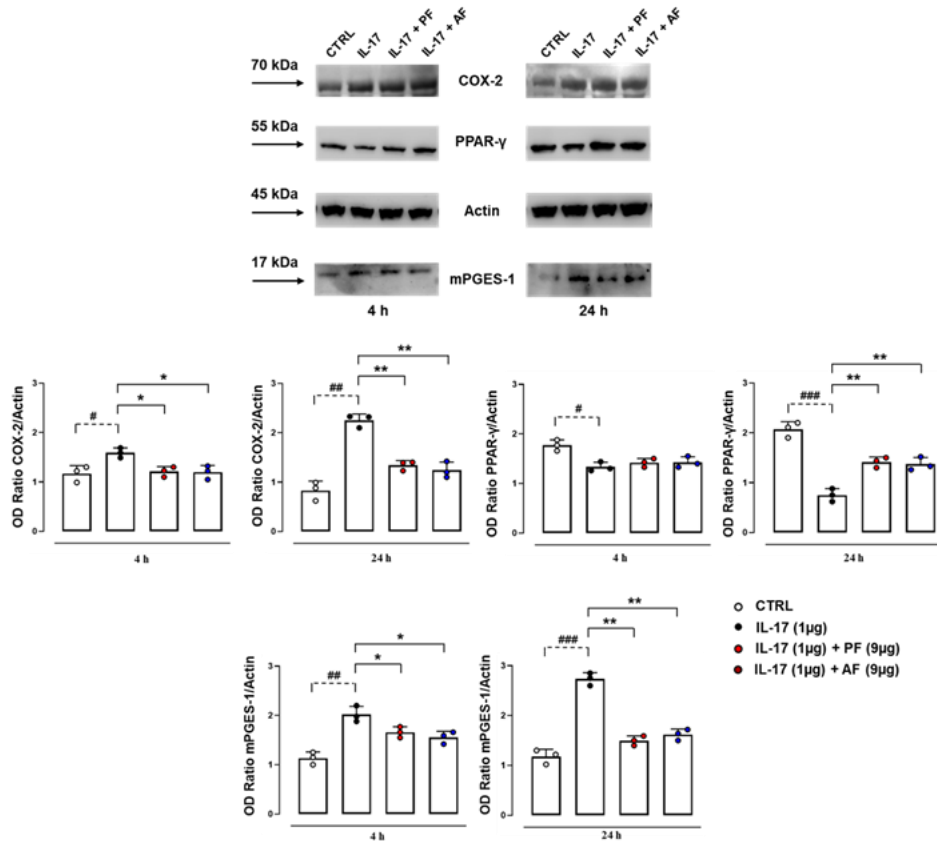
The future remains exciting for clinicians treating IMIDs and for their patients. Targeted therapies, as well as providing new treatment paradigms, continue to inform us about the pathogenesis of disease and its complications. Future studies and clinical trials will need to become increasingly sophisticated to address these varying requirements. We will see.

CHEPTER 6: SUPPLEMENTARY FIGURES

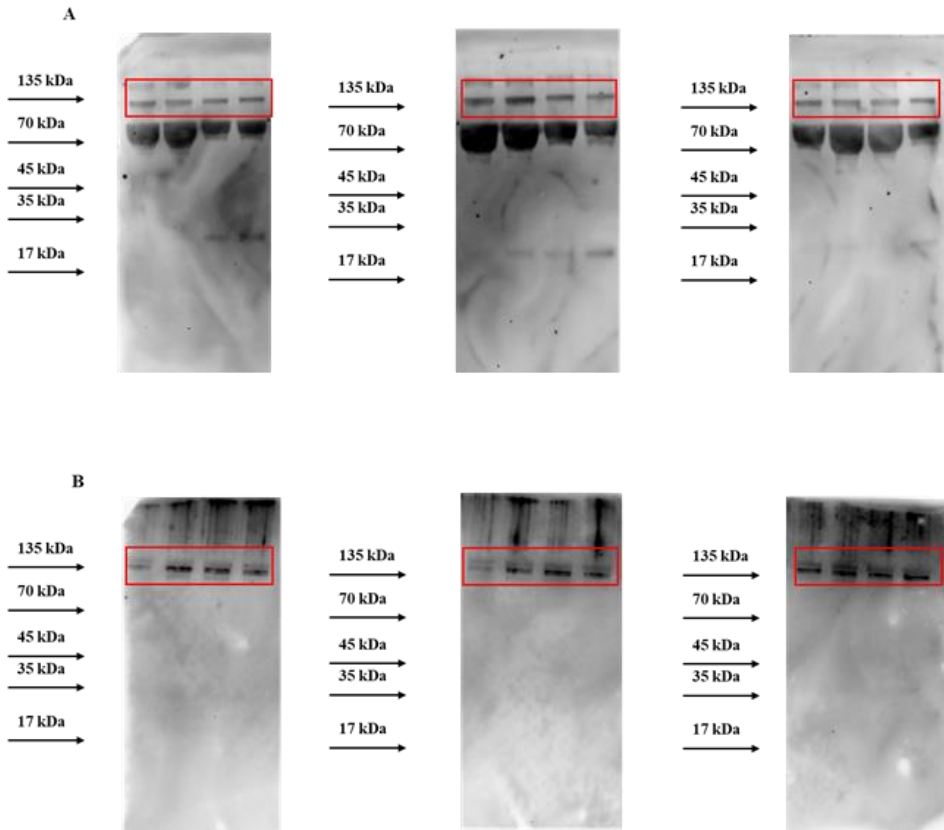
Supplementary Fig. 1. Mice were treated with IL-17 vehicle (CTRL), IL-17 (1 µg/pouch) alone (IL-17) or co-administrated with PF 9184 (PF, 9 µg/pouch) AF 3485 (AF, 9 µg/pouch) and, thereafter, total cell number from pouches' inflammatory exudates was evaluated at 4 (A), 24 (B) and 48 (C) h. Data were expressed as means ± S.D. of n=7 mice per group. Statistical analysis was conducted by one-way ANOVA followed by Bonferroni's for multiple comparisons. #P≤0.05, ###P≤0.005 vs CTRL group; *P≤0.05, **P≤0.01 vs IL-17 group. From Raucci *et al.* [29].



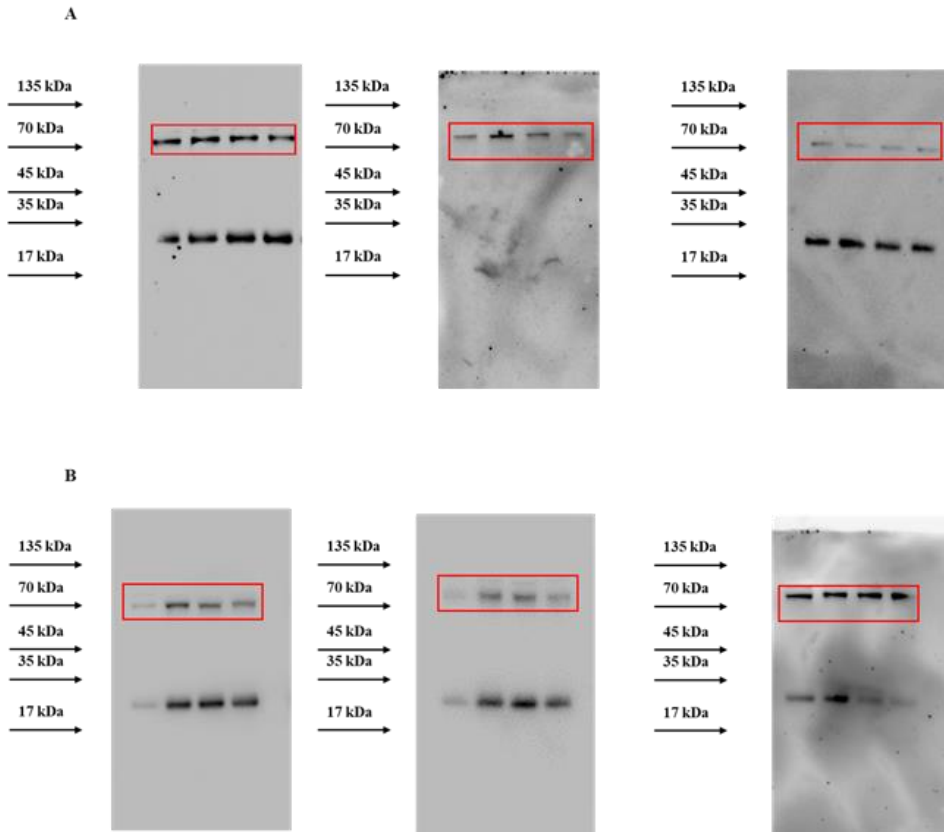
Supplementary Fig. 2. Mice received a single injection of IL-17 (1 µg in 0.5 ml of 0.5% CMC) as described in panel A. The inflammatory fluids collected from the air pouch at 4, 24 and 48 h were used to measure the levels of IL-17 (B). Values are presented as means ± S.D of n=7 mice per group. From Raucci *et al.* [29].



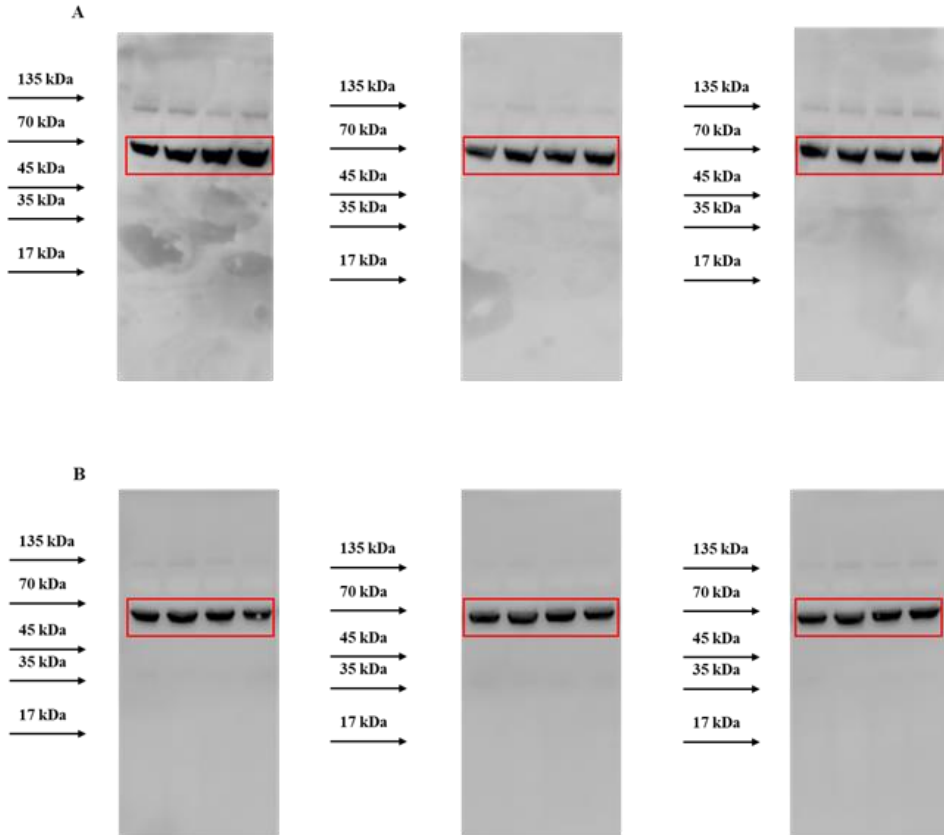
Supplementary Fig. 3. Whole cellular pellets homogenates from air pouch experiments in all experimental conditions (CTRL, IL-17, IL-17+PF, IL-17+AF from left to right respectively) were assayed by western blot for COX-2, PPAR- γ and mPGES-1 expression at 4 and 24 h. Western blot images are representative of three separate experiments with similar results. Cumulative densitometric values (at the bottom of the Figure) are expressed as OD Ratio with actin for both 4 and 24 h. Values are presented as means \pm S.D. of three separate independent experiments run each with $n=7$ mice per group pooled. Statistical analysis was conducted by one-way ANOVA followed by Bonferroni's for multiple comparisons. $\#P \leq 0.05$, $\#\#\#P \leq 0.005$ vs CTRL group; $*P \leq 0.05$, $**P \leq 0.01$ vs IL-17 group. From Raucci *et al.* [29].



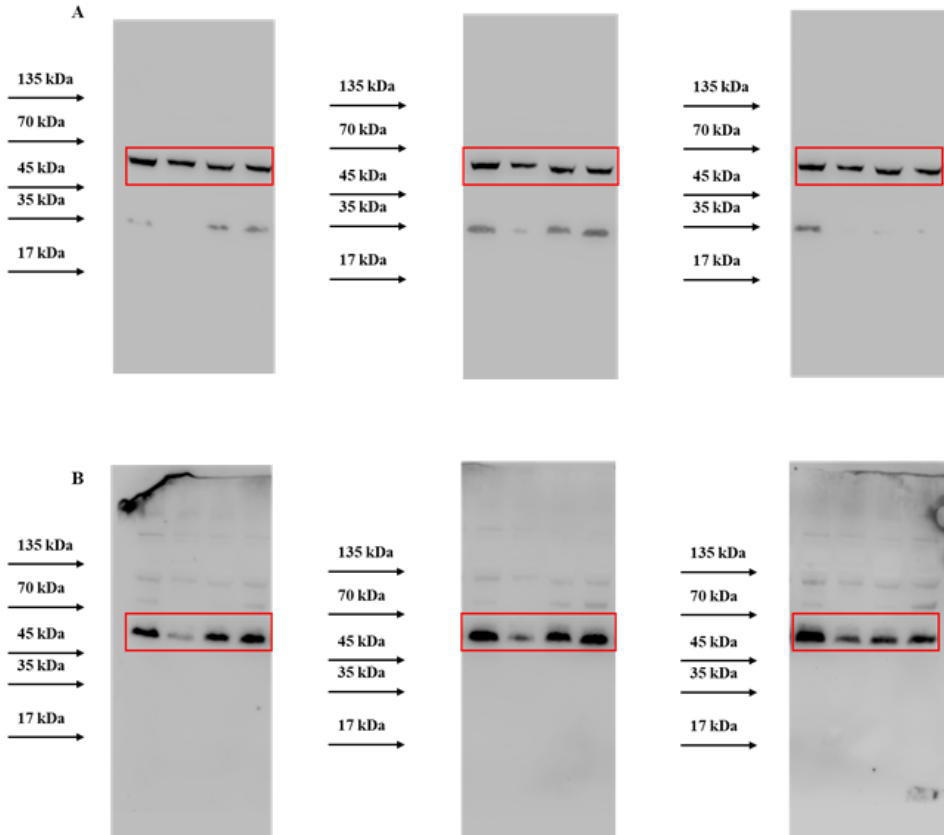
Supplementary Fig. 4. Uncropped original western blots for IL-17 Receptor at 4 (A) and 24 h (B) obtained from air pouch recruited cells in all experimental conditions (CTRL, IL-17, IL-17+PF, IL-17+TRO from left to right respectively). Images represent three separate independent experiments run each with n=7 mice per group pooled. From Raucci *et al.* [29].



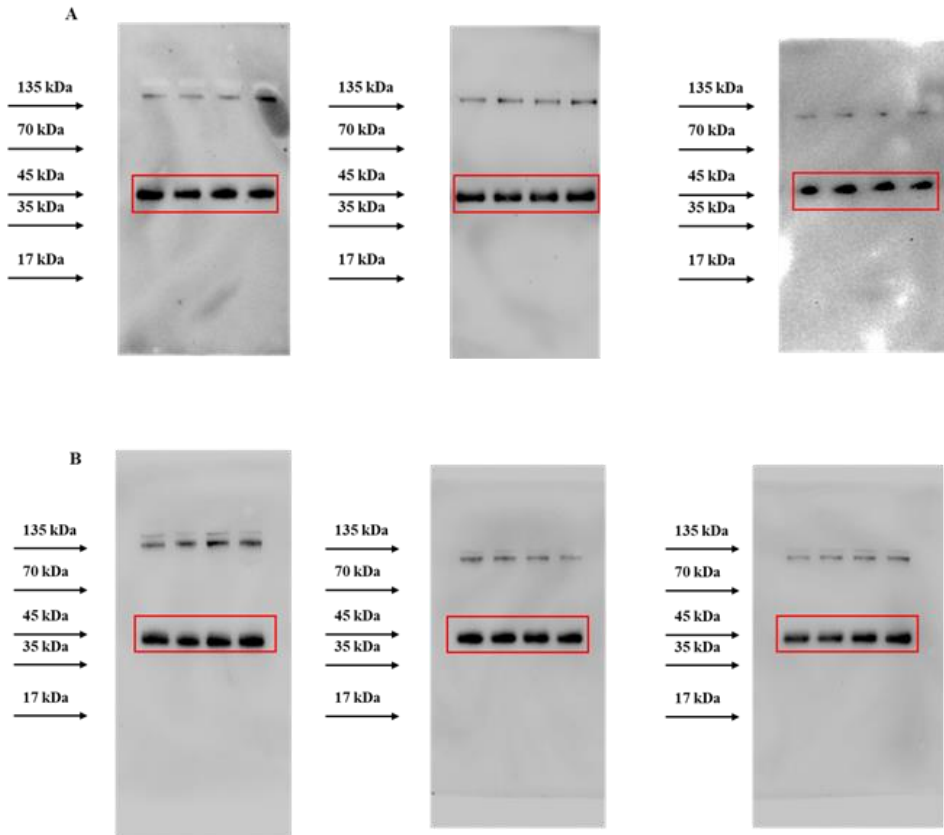
Supplementary Fig. 5. Uncropped original western blots for COX-2 at 4 (A) and 24 h (B) obtained from air pouch recruited cells in all experimental conditions (CTRL, IL-17, IL-17+PF, IL-17+TRO from left to right respectively). Images represent three separate independent experiments run each with n=7 mice per group pooled. From Raucci *et al.* [29].



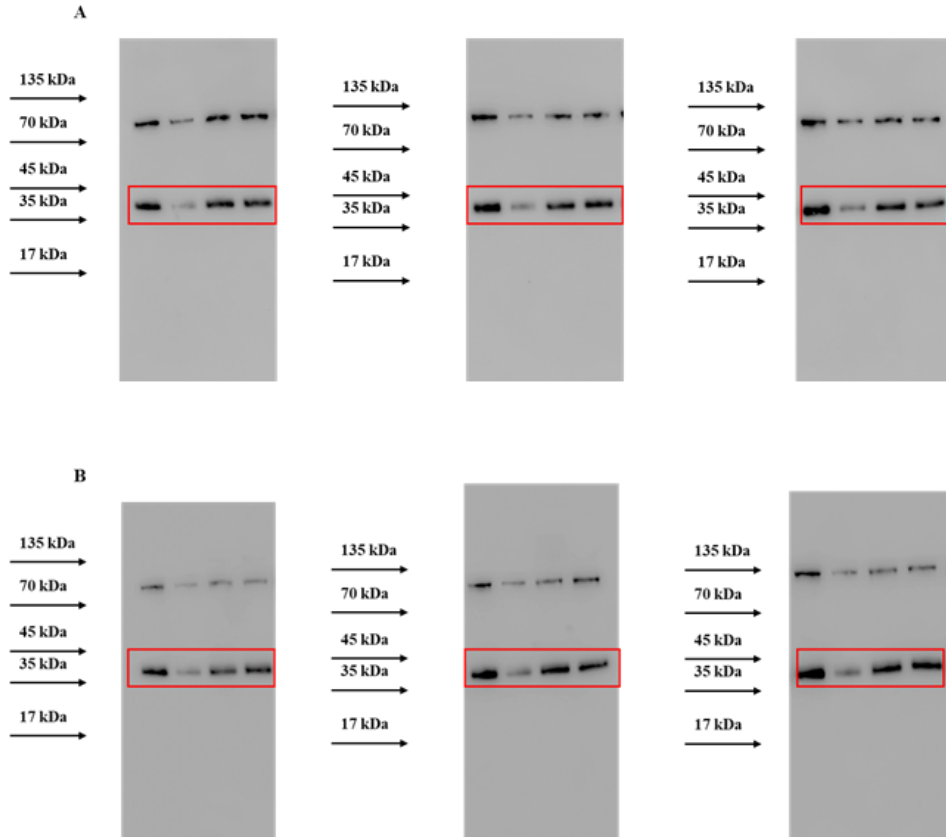
Supplementary Fig. 6. Uncropped original western blots for NF- κ B at 4 (A) and 24 h (B) obtained from air pouch recruited cells in all experimental conditions (CTRL, IL-17, IL-17+PF, IL-17+TRO from left to right respectively). Images represent three separate independent experiments run each with n=7 mice per group pooled. From Raucci *et al.* [29].



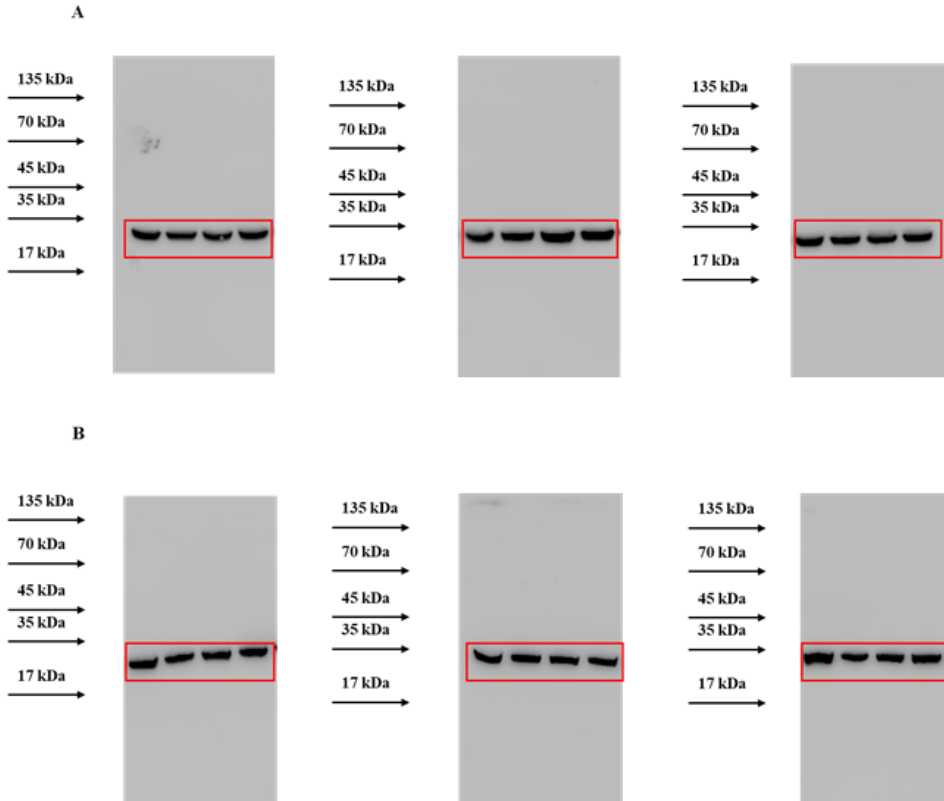
Supplementary Fig. 7. Uncropped original western blots for PPAR- γ at 4 (A) and 24 h (B) obtained from air pouch recruited cells in all experimental conditions (CTRL, IL-17, IL-17+PF, IL-17+TRO from left to right respectively). Images represent three separate independent experiments run each with n=7 mice per group pooled. From Raucci *et al.* [29].



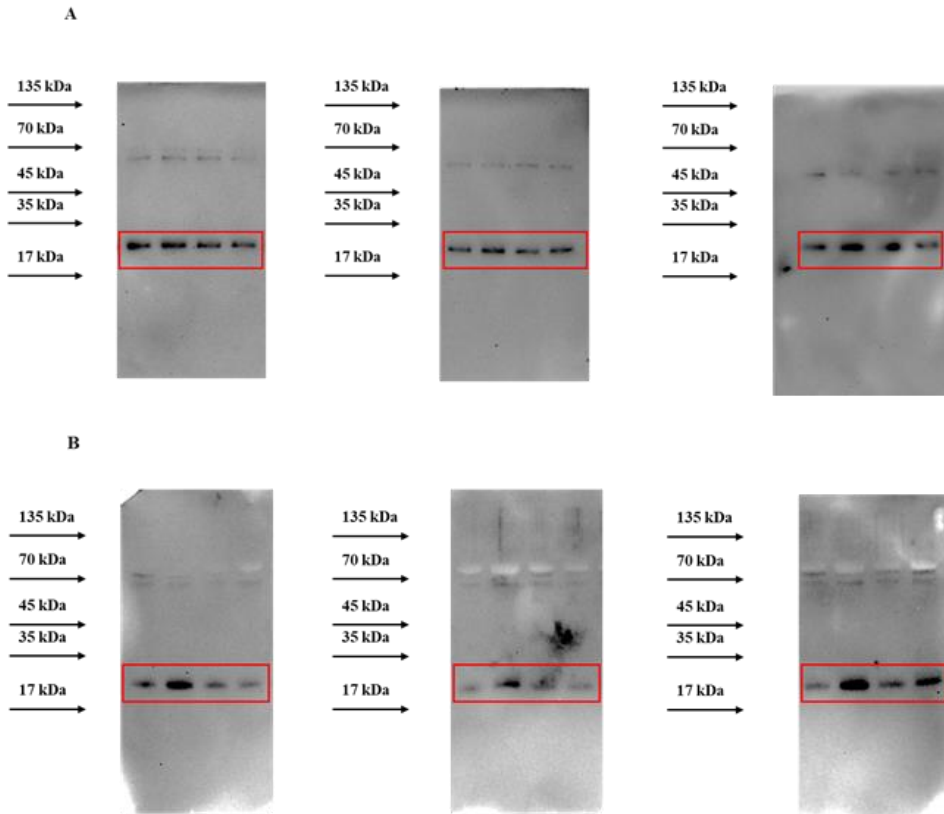
Supplementary Fig. 8. Uncropped original western blots for actin at 4 (A) and 24 h (B) obtained from air pouch recruited cells in all experimental conditions (CTRL, IL-17, IL-17+PF, IL-17+TRO from left to right respectively). Images represent three separate independent experiments run each with n=7 mice per group pooled. From Raucci *et al.* [29].



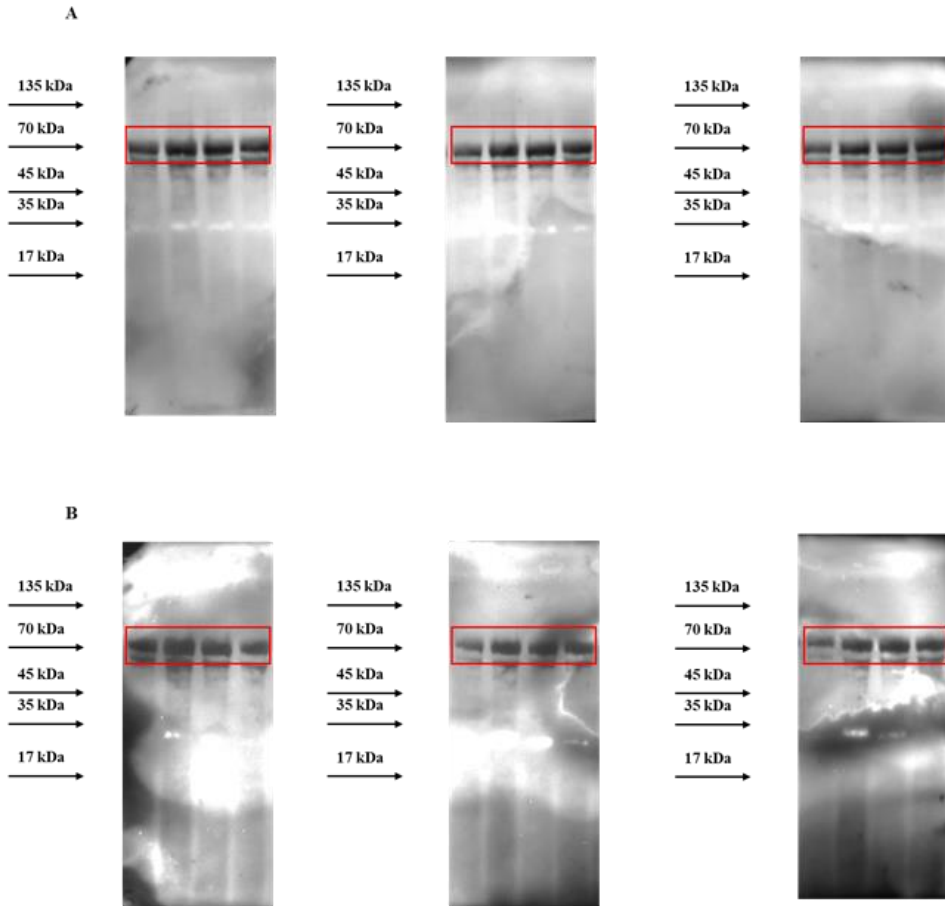
Supplementary Fig. 9. Uncropped original western blots for I κ B- α at 4 (A) and 24 h (B) obtained from air pouch recruited cells in all experimental conditions (CTRL, IL-17, IL-17+PF, IL-17+TRO from left to right respectively). Images represent three separate independent experiments run each with n=7 mice per group pooled. From Raucci *et al.* [29].



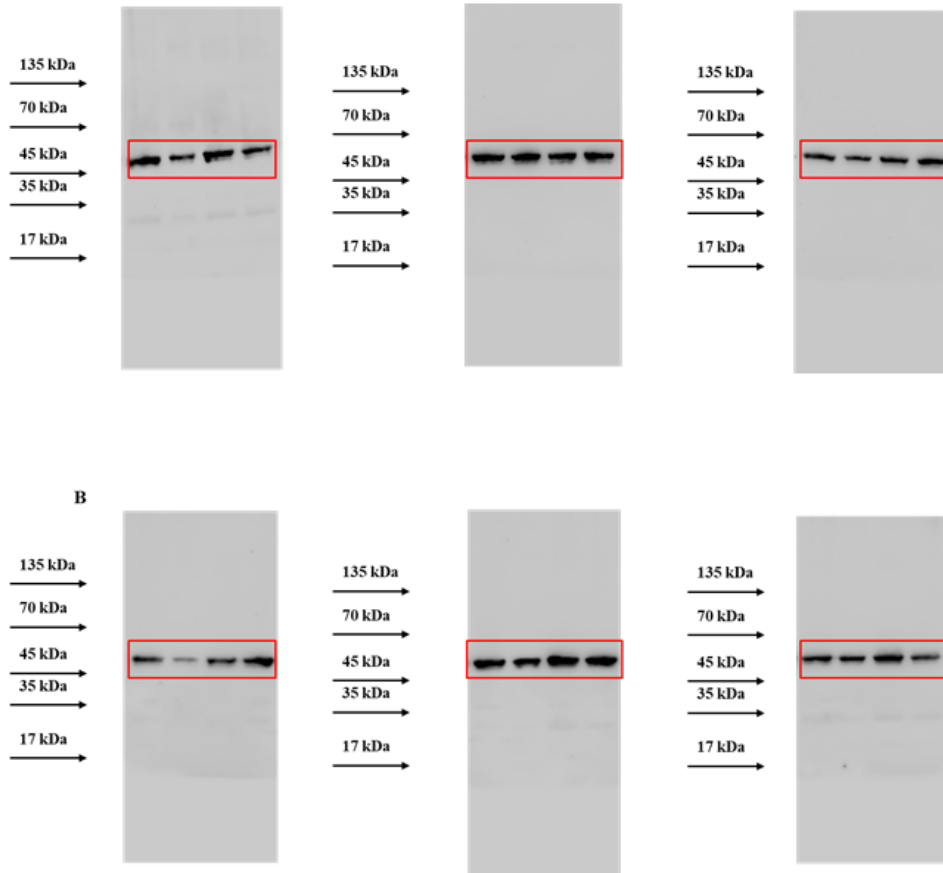
Supplementary Fig. 10. Uncropped original western blots for mPTGDS-1 at 4 (**A**) and 24 h (**B**) obtained from air pouch recruited cells in all experimental conditions (CTRL, IL-17, IL-17+PF, IL-17+TRO from left to right respectively). Images represent three separate independent experiments run each with n=7 mice per group pooled. From Raucci *et al.* [29].



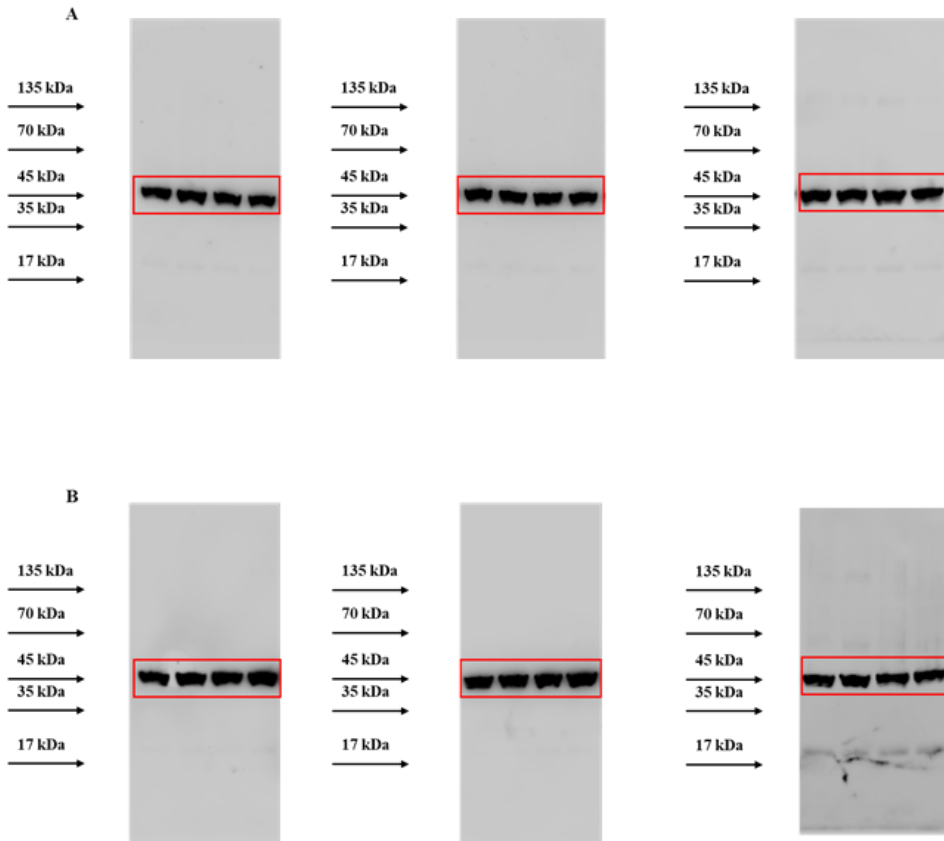
Supplementary Fig. 11. Uncropped original western blots for mPGES-1 at 4 (**A**) and 24 h (**B**) obtained from air pouch recruited cells in all experimental conditions (CTRL, IL-17, IL-17+PF, IL-17+TRO from left to right respectively). Images represent three separate independent experiments run each with n=7 mice per group pooled. From Raucci *et al.* [29].



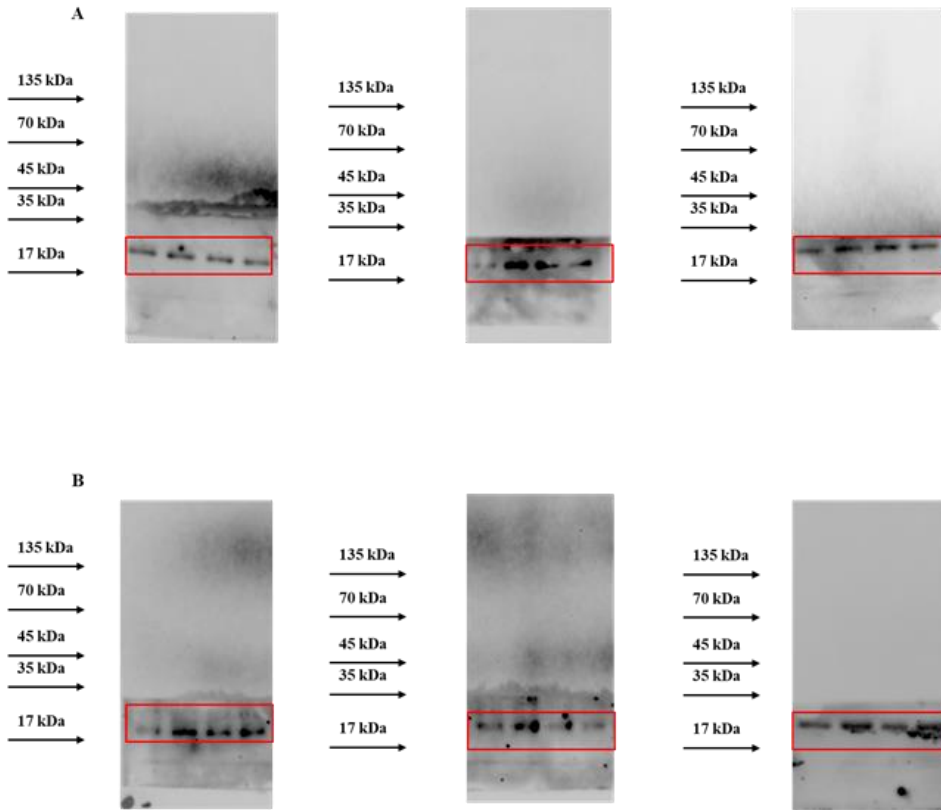
Supplementary Fig. 12. Uncropped original western blots for COX-2 at 4 (A) and 24 h (B) obtained from air pouch recruited cells in all experimental conditions (CTRL, IL-17, IL-17+PF, IL-17+AF from left to right respectively). Images represent three separate independent experiments run each with n=7 mice per group pooled. From Raucci *et al.* [29].



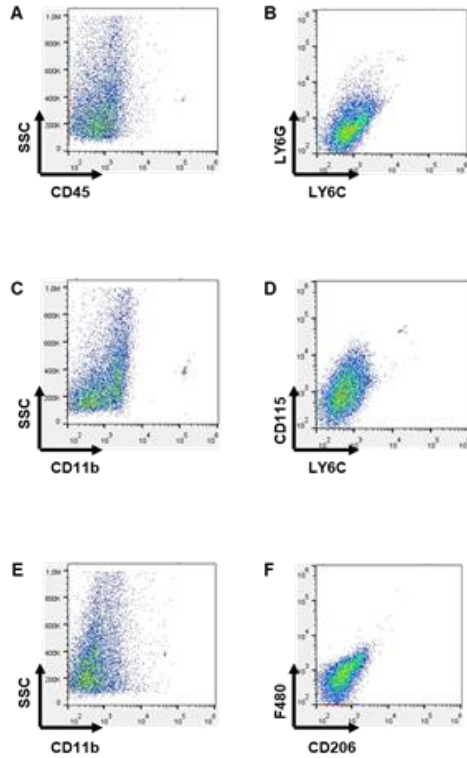
Supplementary Fig. 13. Uncropped original western blots for PPAR- γ at 4 (A) and 24 h (B) obtained from air pouch recruited cells in all experimental conditions (CTRL, IL-17, IL-17+PF, IL-17+AF from left to right respectively). Images represent three separate independent experiments run each with n=7 mice per group pooled. From Raucci *et al.* [29].



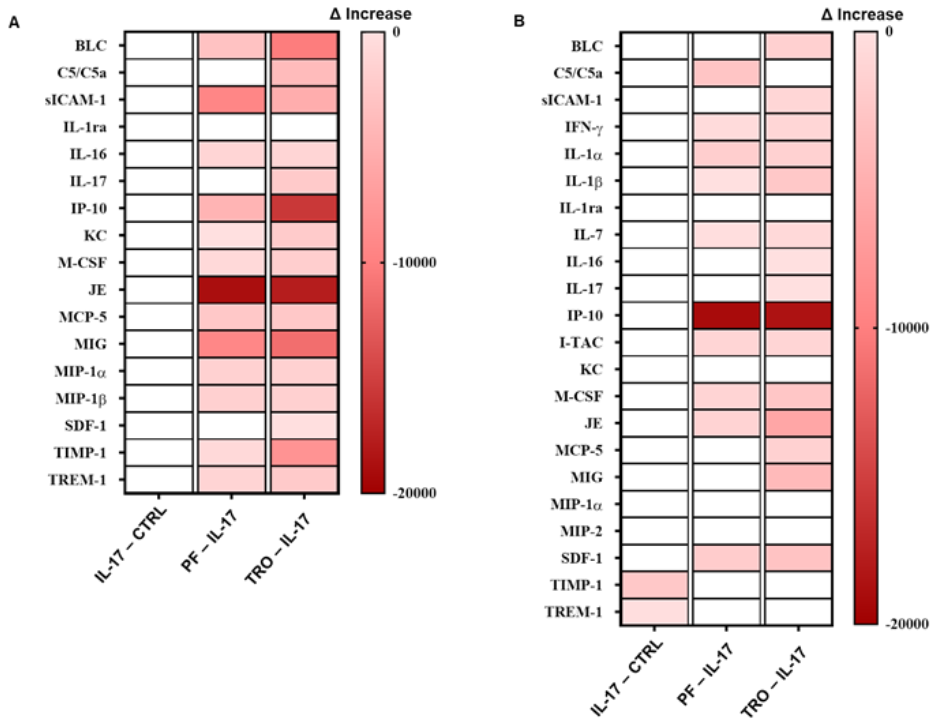
Supplementary Fig. 14. Uncropped original western blots for actin at 4 (A) and 24 h (B) obtained from air pouch recruited cells in all experimental conditions (CTRL, IL-17, IL-17+PF, IL-17+AF from left to right respectively). Images represent three separate independent experiments run each with n=7 mice per group pooled. From Raucci *et al.* [29].



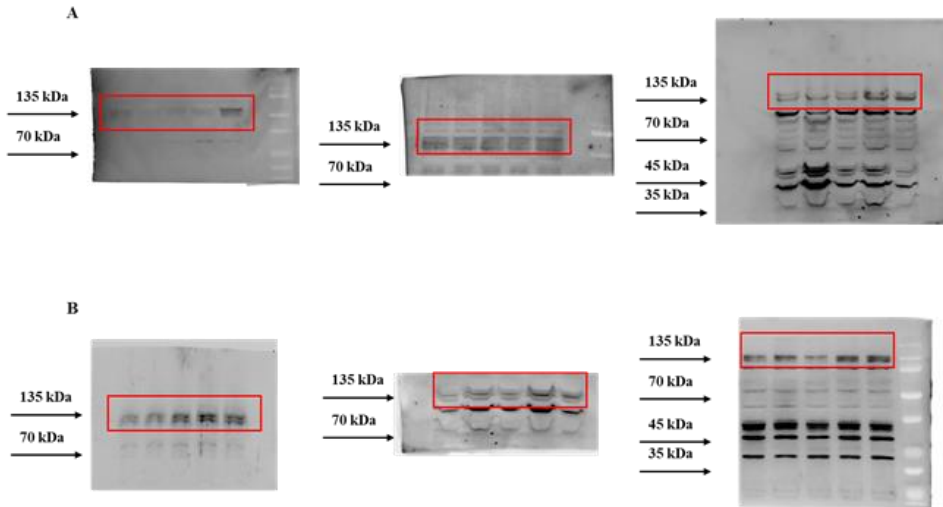
Supplementary Fig. 15. Uncropped original western blots for mPGES-1 at 4 (A) and 24 h (B) obtained from air pouch recruited cells in all experimental conditions (CTRL, IL-17, IL-17+PF, IL-17+AF from left to right respectively). Images represent three separate independent experiments run each with n=7 mice per group pooled. From Raucci *et al.* [29].



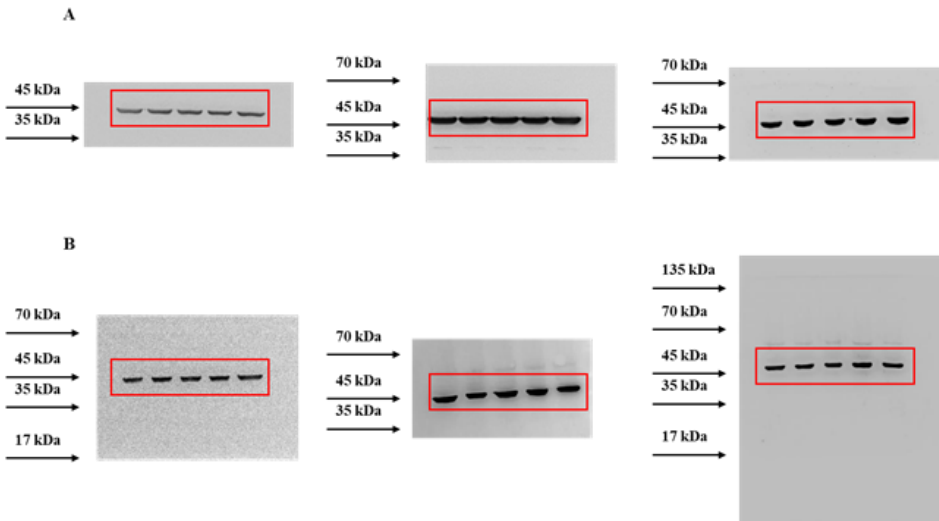
Supplementary Fig. 16. Quantification applied to identify potential $CD45^{+ve}/Ly6G^{+ve}/Ly6C^{+ve}$ (A-B), $CD11b^{+ve}/CD115^{+ve}/Ly6C^{+ve}$ (C-D) and $CD11b^{+ve}/CD206^{+ve}/F480^{+ve}$ (E-F) positive cells stained with isotype control antibodies. FACS pictures are representative of independent experiments with similar results with $n=7$ mice per group. From Raucci *et al.* [29].



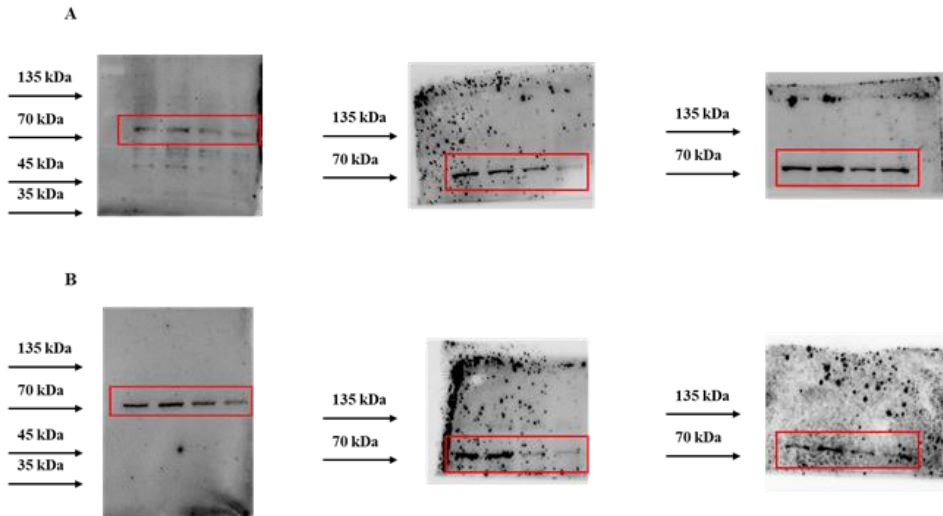
Supplementary Fig. 17. Inflammatory supernatants obtained from pouch cavities were assayed using a Proteome Profiler cytokine array at both 4 (A) and 24 h (B). Heat maps show Δ of increase/decrease between IL-17 (1 μ g/pouch) vs CTRL group (IL-17 vehicle), IL-17 (1 μ g/pouch) + PF 9184 (PF, 9 μ g/pouch) vs IL-17 (1 μ g/pouch) group, IL-17 (1 μ g/pouch) + Troglitazone (TRO, 9 μ g/pouch) vs IL-17 (1 μ g/pouch) group. Data (Δ increase/decrease) are presented as means \pm S.D. of positive spots of three separate independent experiments run each with n=7 mice per group pooled. From Raucci *et al.* [29].



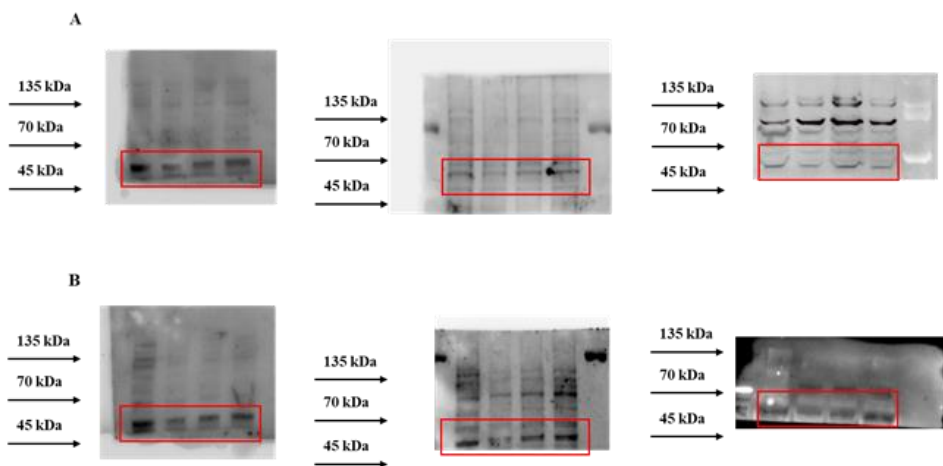
Supplementary Fig. 18. Original western blots for IL-17 Receptor at 4 (A) and 24 h (B) obtained from murine macrophages stimulated with increasing concentration of IL-17 (0.5-500 ng/ml). Images represent three separate independent experiments run each with n=7 mice per group pooled. From Raucci *et al.* [29].



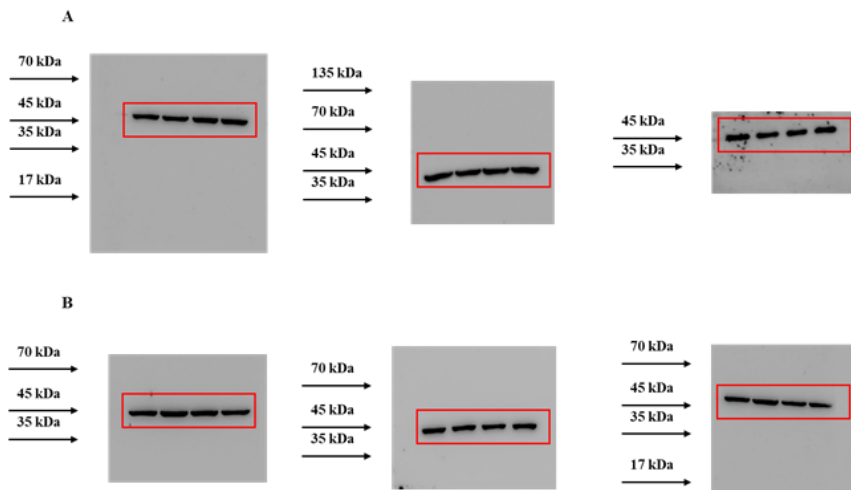
Supplementary Fig. 19. Original western blots for actin at 4 (A) and 24 h (B) obtained from murine macrophages stimulated with increasing concentration of IL-17 (0.5-500 ng/ml). Images represent three separate independent experiments run each with n=7 mice per group pooled. From Raucci *et al.* [29].



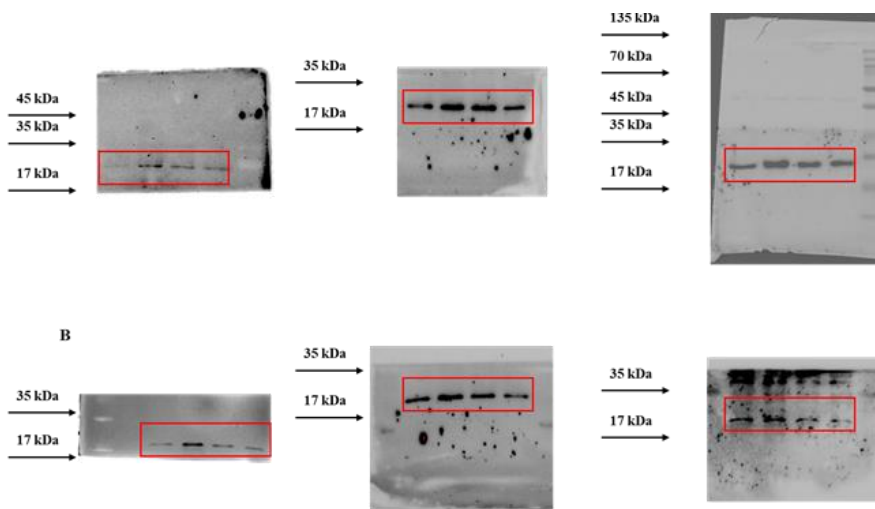
Supplementary Fig. 20. Original western blots for COX-2 at 4 (**A**) and 24 h (**B**) obtained from murine macrophages stimulated with IL-17 (50 ng/ml) in all experimental conditions (CTRL, IL-17, IL-17+PF, IL-17+TRO from left to right respectively). Images represent three separate independent experiments run each with n=7 mice per group pooled. From Raucci *et al.* [29].



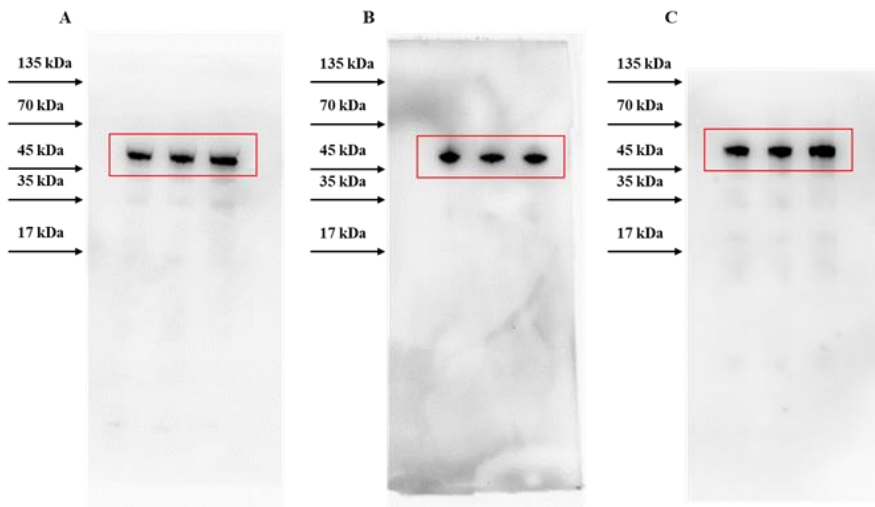
Supplementary Fig. 21. Original western blots for PPAR- γ at 4 (**A**) and 24 h (**B**) obtained from murine macrophages stimulated with IL-17 (50 ng/ml) in all experimental conditions (CTRL, IL-17, IL-17+PF, IL-17+TRO from left to right respectively). Images represent three separate independent experiments run each with n=7 mice per group pooled. From Raucci *et al.* [29].



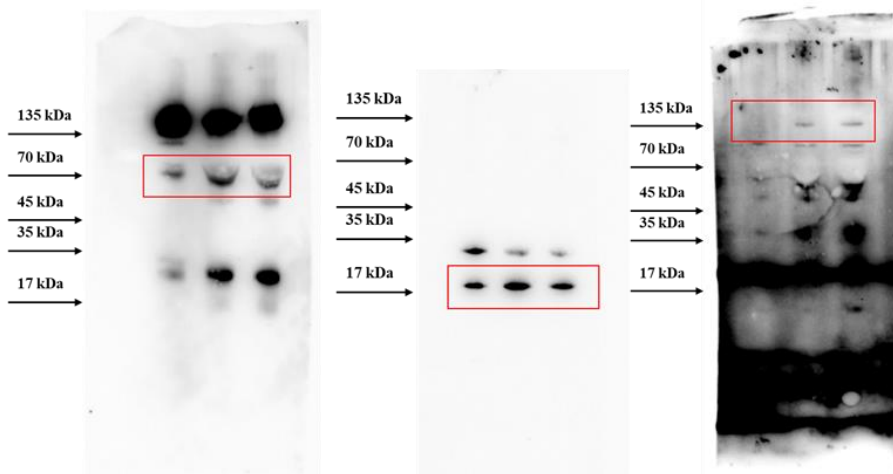
Supplementary Fig. 22. Original western blots for actin at 4 (**A**) and 24 h (**B**) obtained from murine macrophages stimulated with IL-17 (50 ng/ml) in all experimental conditions (CTRL, IL-17, IL-17+PF, IL-17+TRO from left to right respectively). Images represent three separate independent experiments run each with n=7 mice per group pooled. From Raucci *et al.* [29].



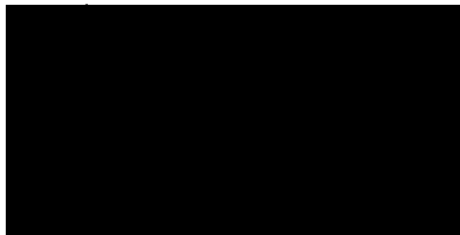
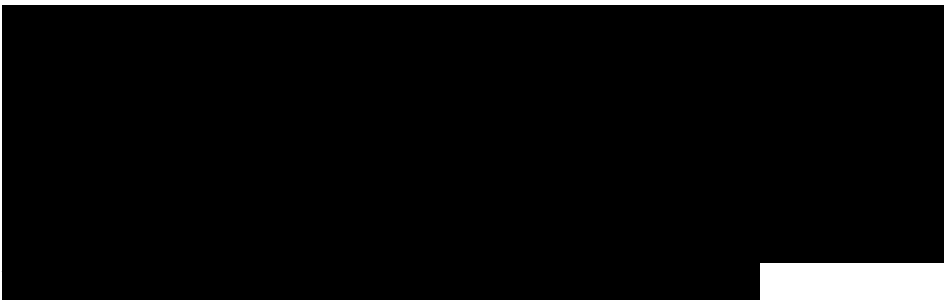
Supplementary Fig. 23. Original western blots for mPGES-1 at 4 (**A**) and 24 h (**B**) obtained from murine macrophages stimulated with IL-17 (50 ng/ml) in all experimental conditions (CTRL, IL-17, IL-17+PF, IL-17+TRO from left to right respectively). Images represent three separate independent experiments run each with n=7 mice per group pooled. From Raucci *et al.* [29].

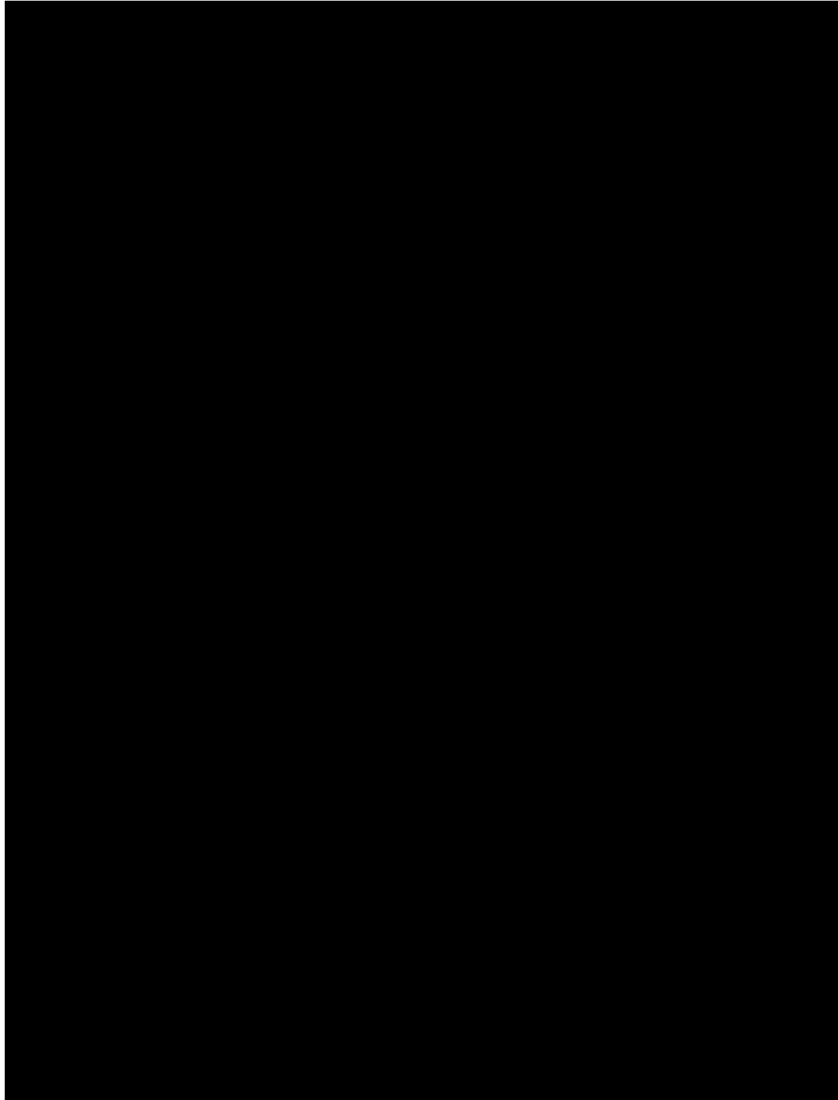


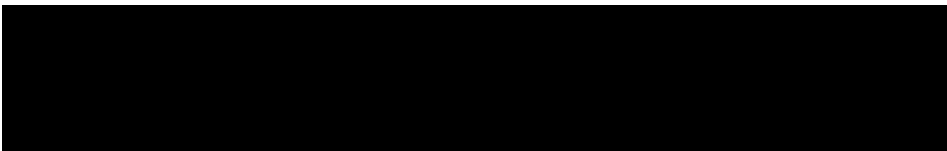
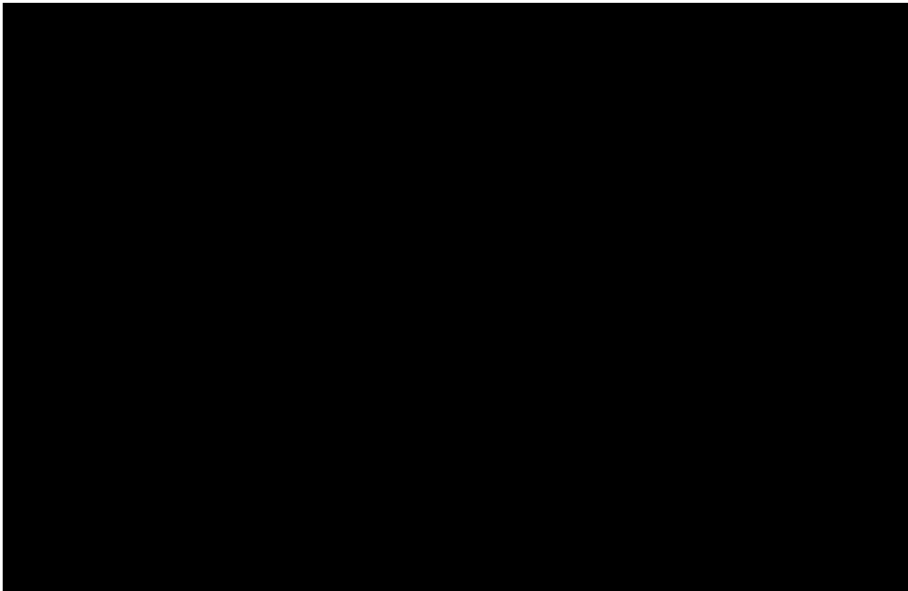
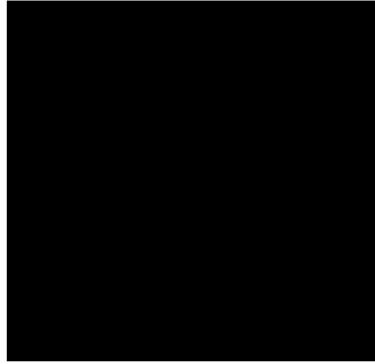
Supplementary Fig. 24. Original western blots for Actin respectively related to COX-2 (A), IL-17R (B) and mPGEs-1 (C). Red squares highlight cropped images reported into regular figures of the manuscript. From Raucci *et al.* [86].

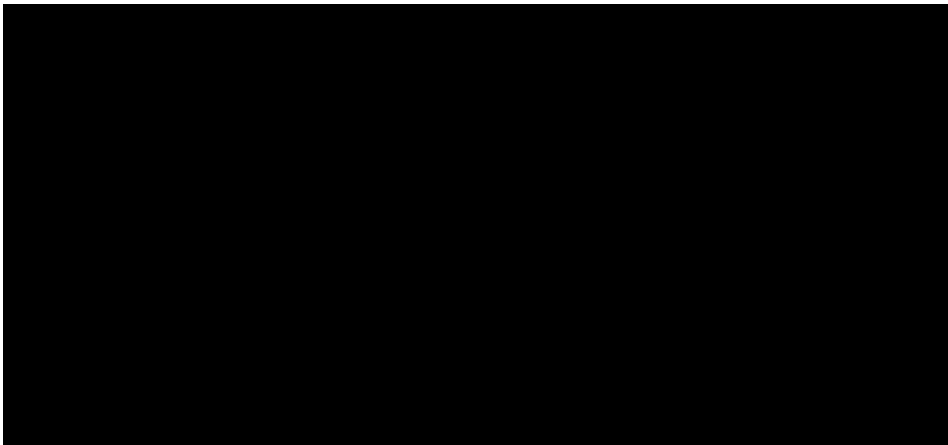
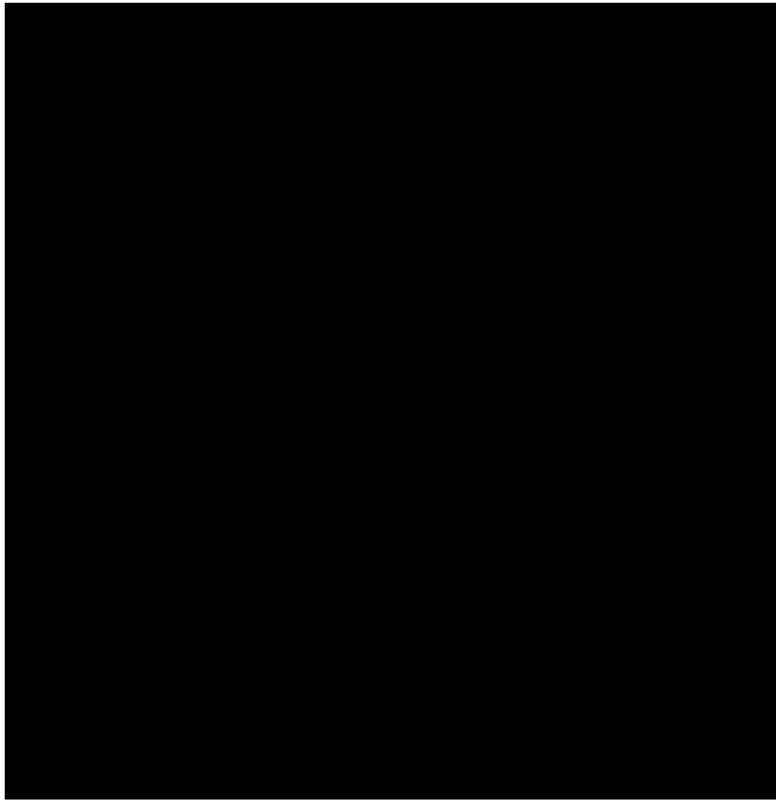


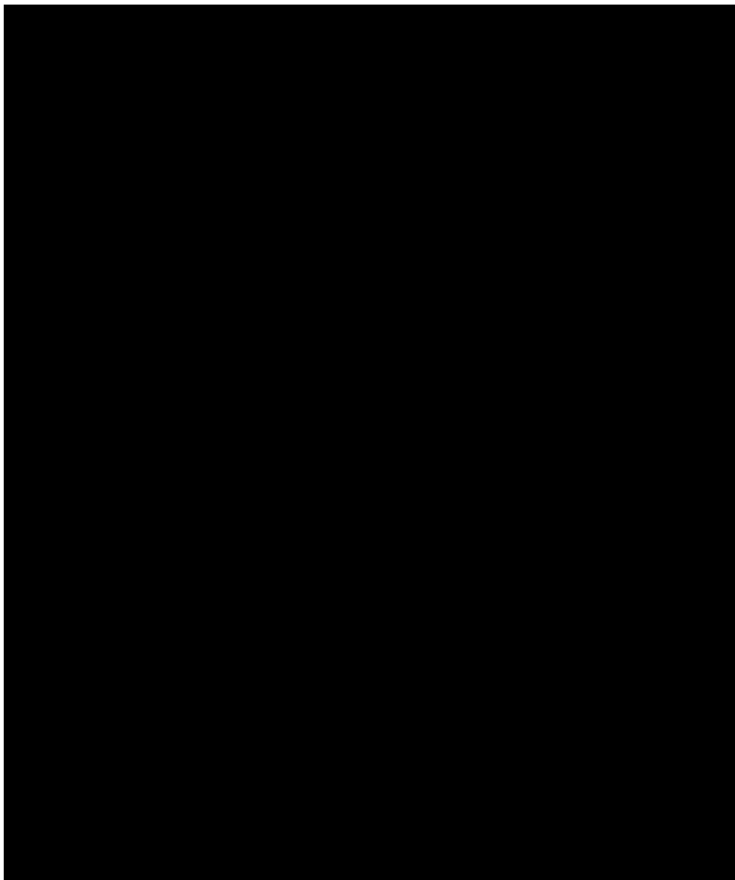
Supplementary Fig. 25. Original western blot for COX-2, mPGEs-1 and IL-17R. Red square highlights cropped image reported into regular figure of the manuscript. From Raucci *et al.* [86].

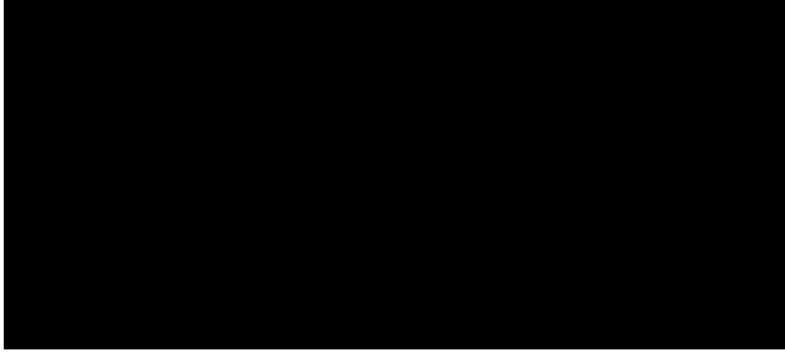






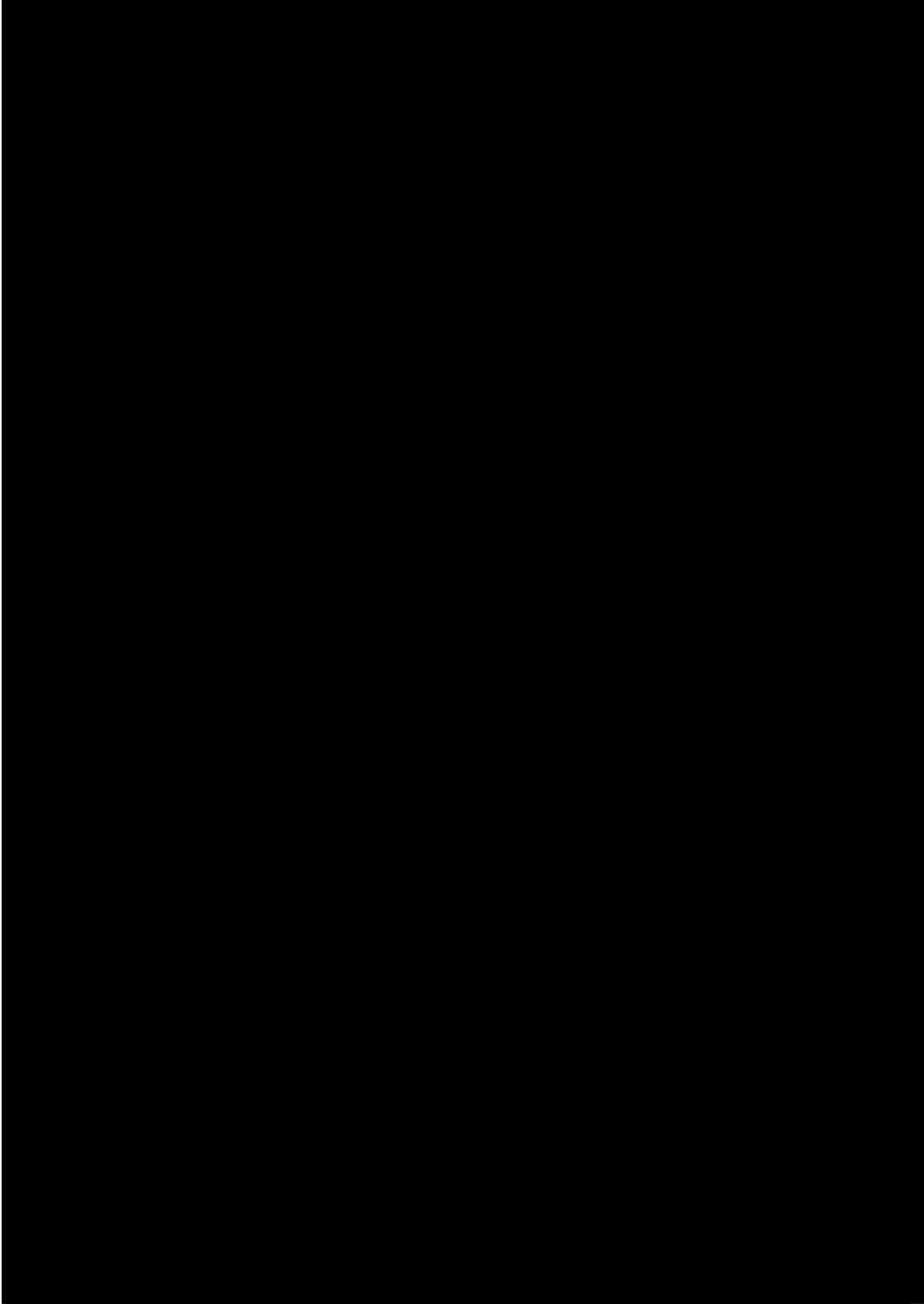


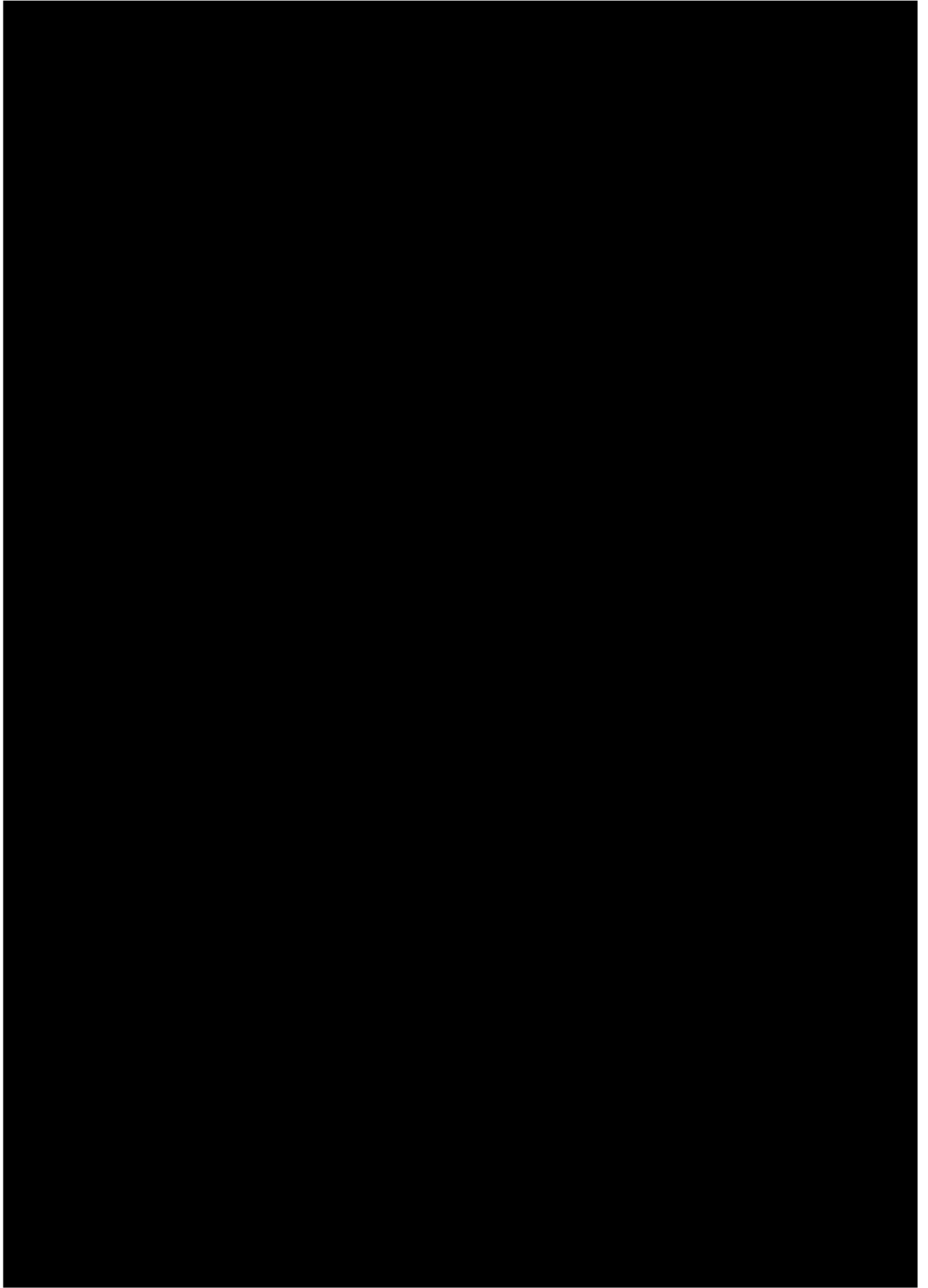


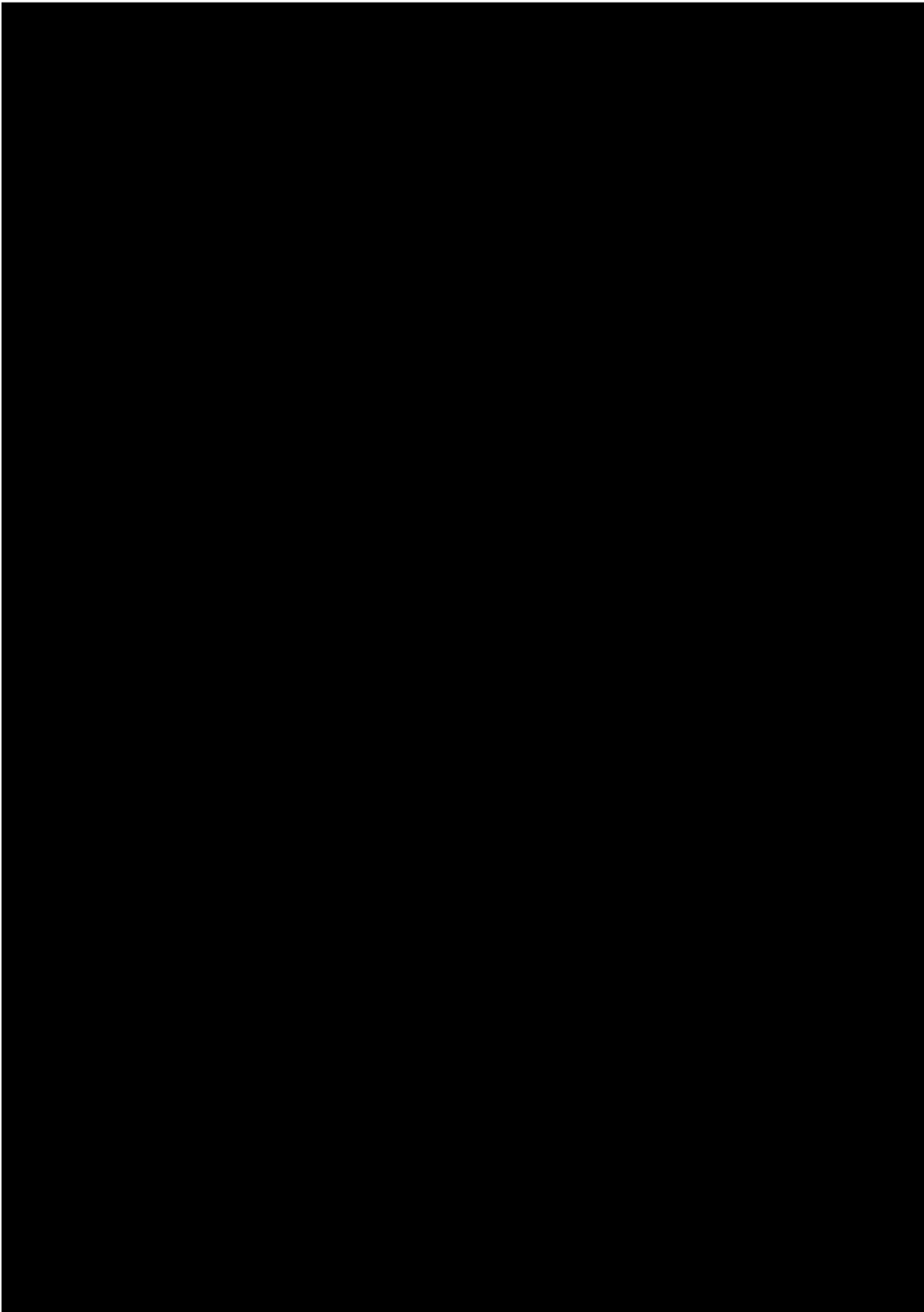


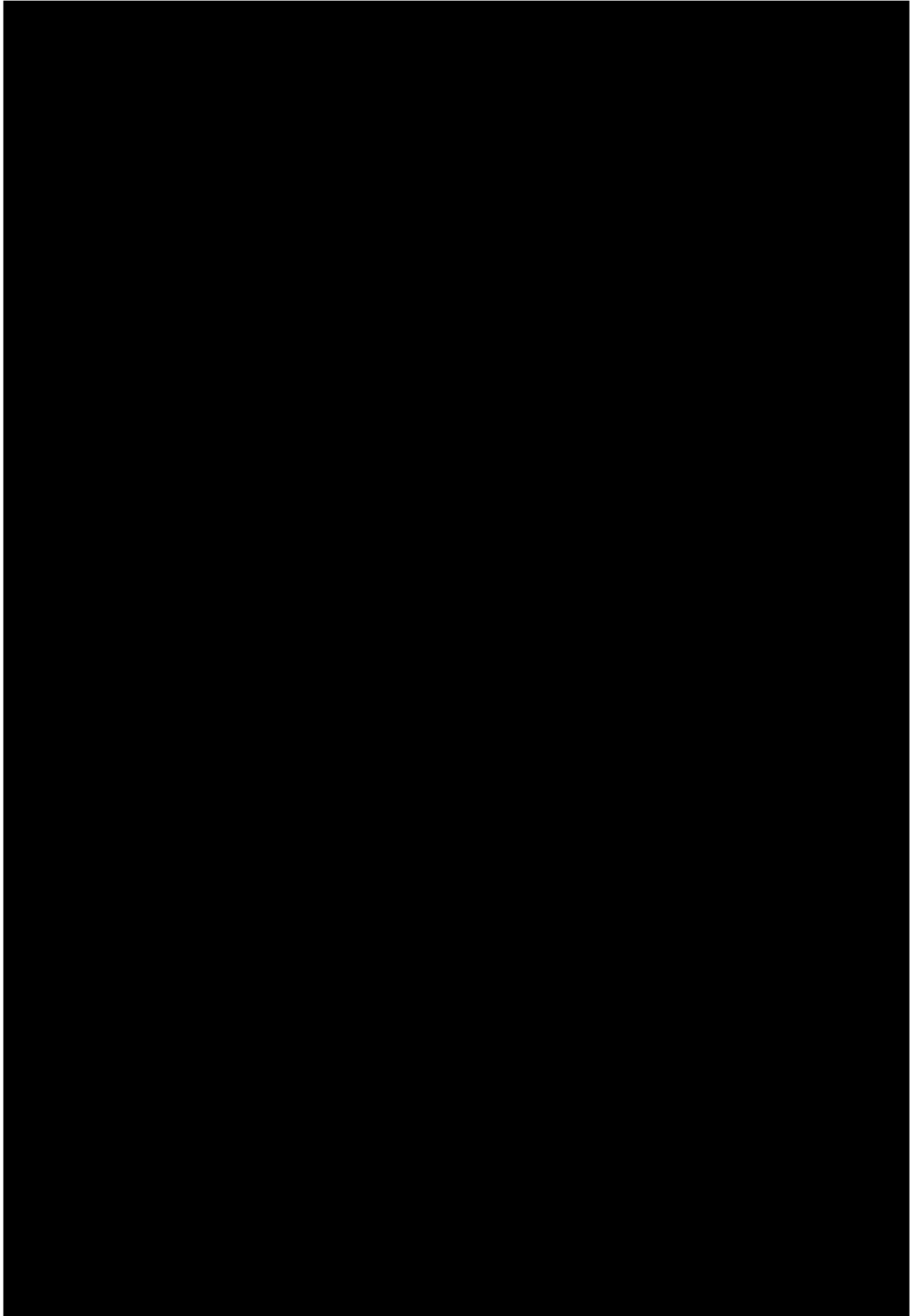
CHEPTER 7: SCIENTIFIC REPORTS

Scientific Report 1

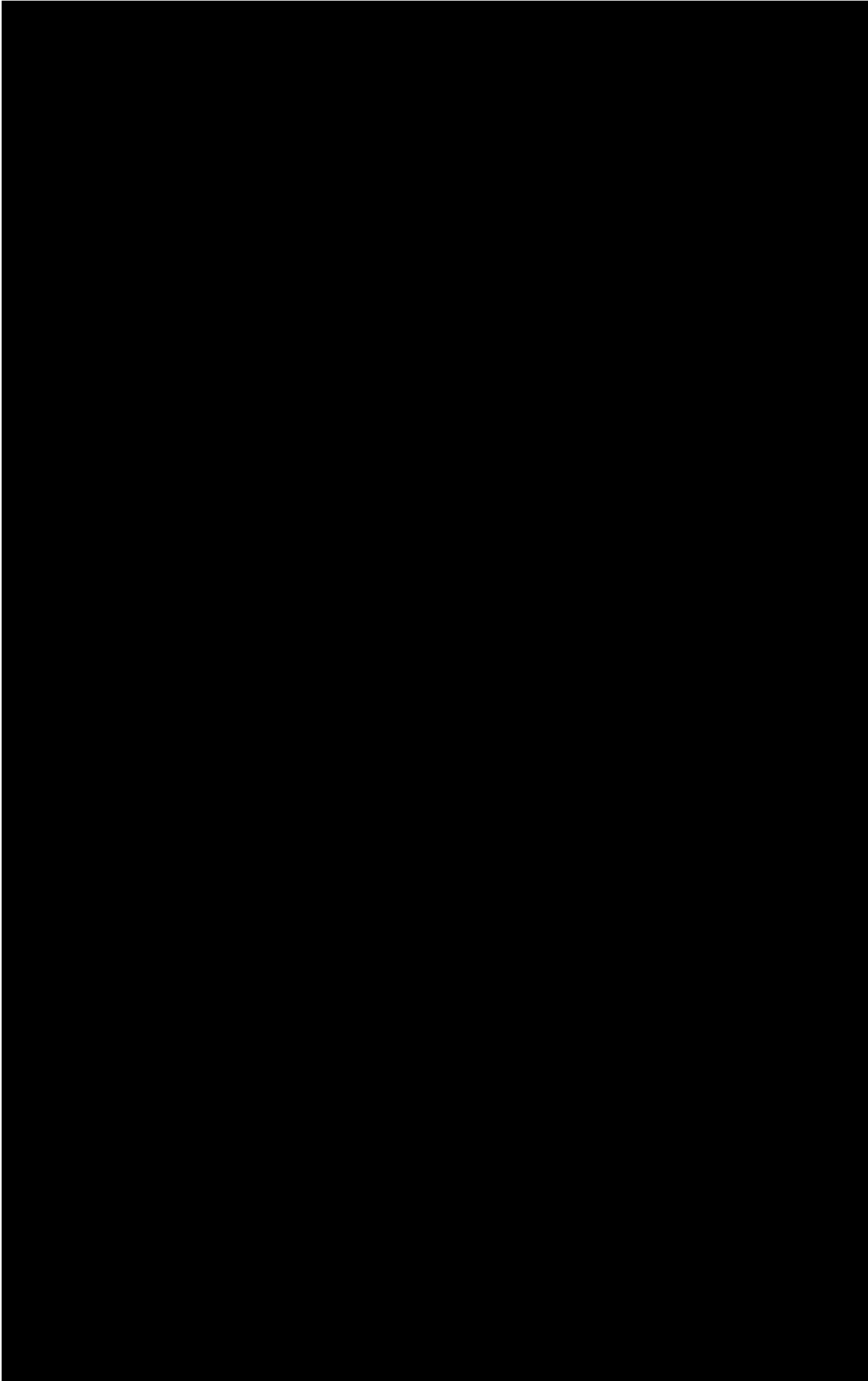


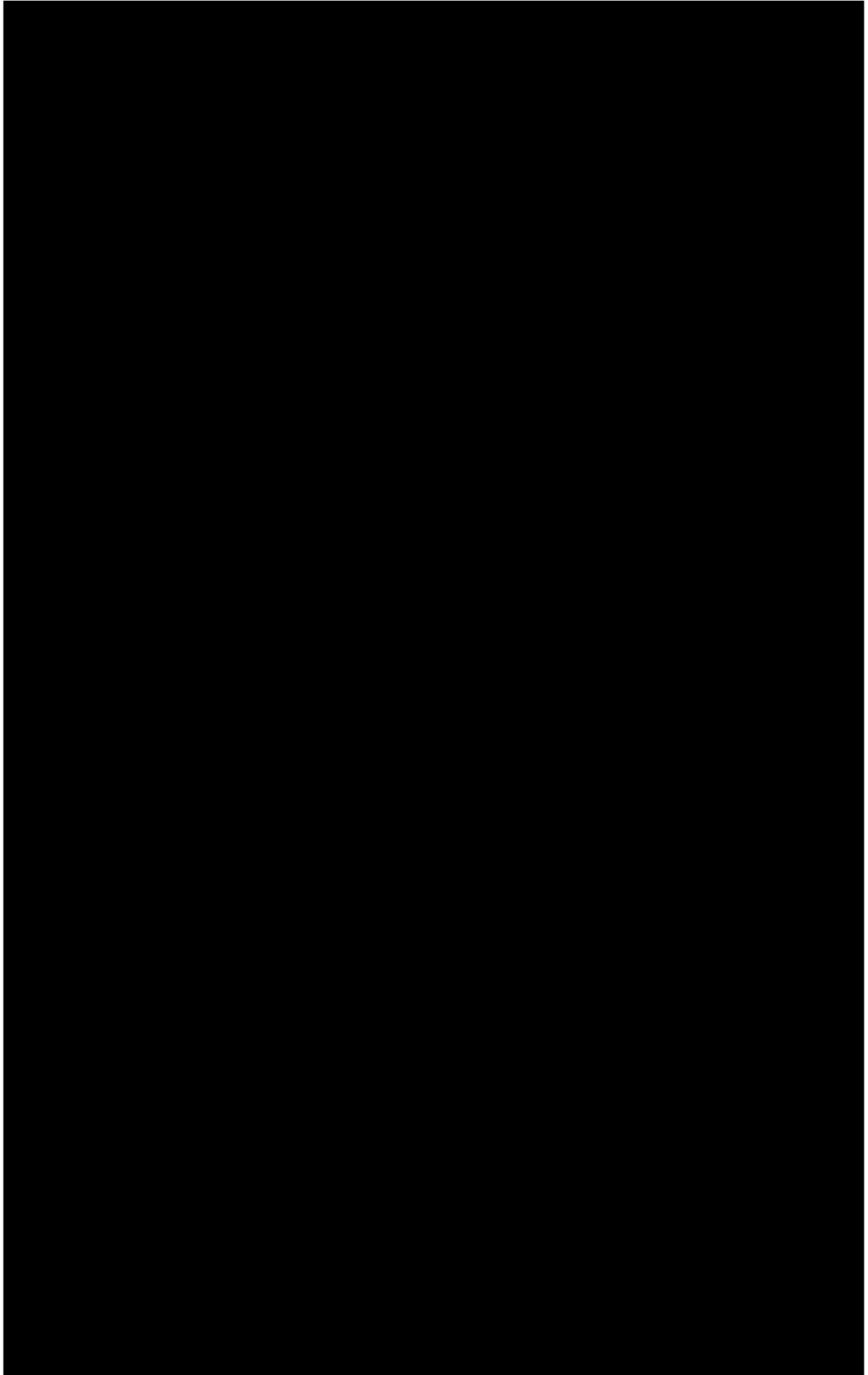


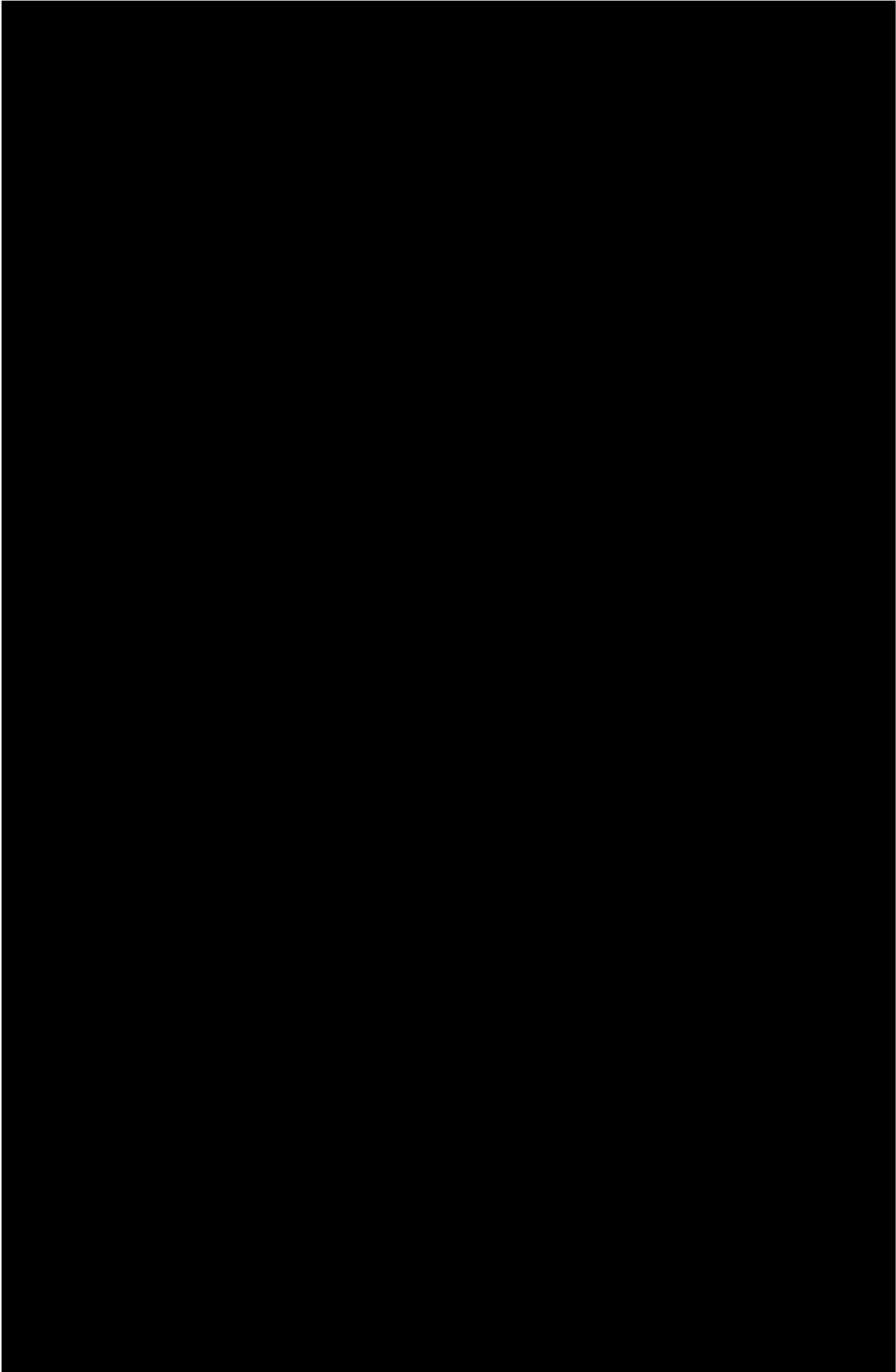


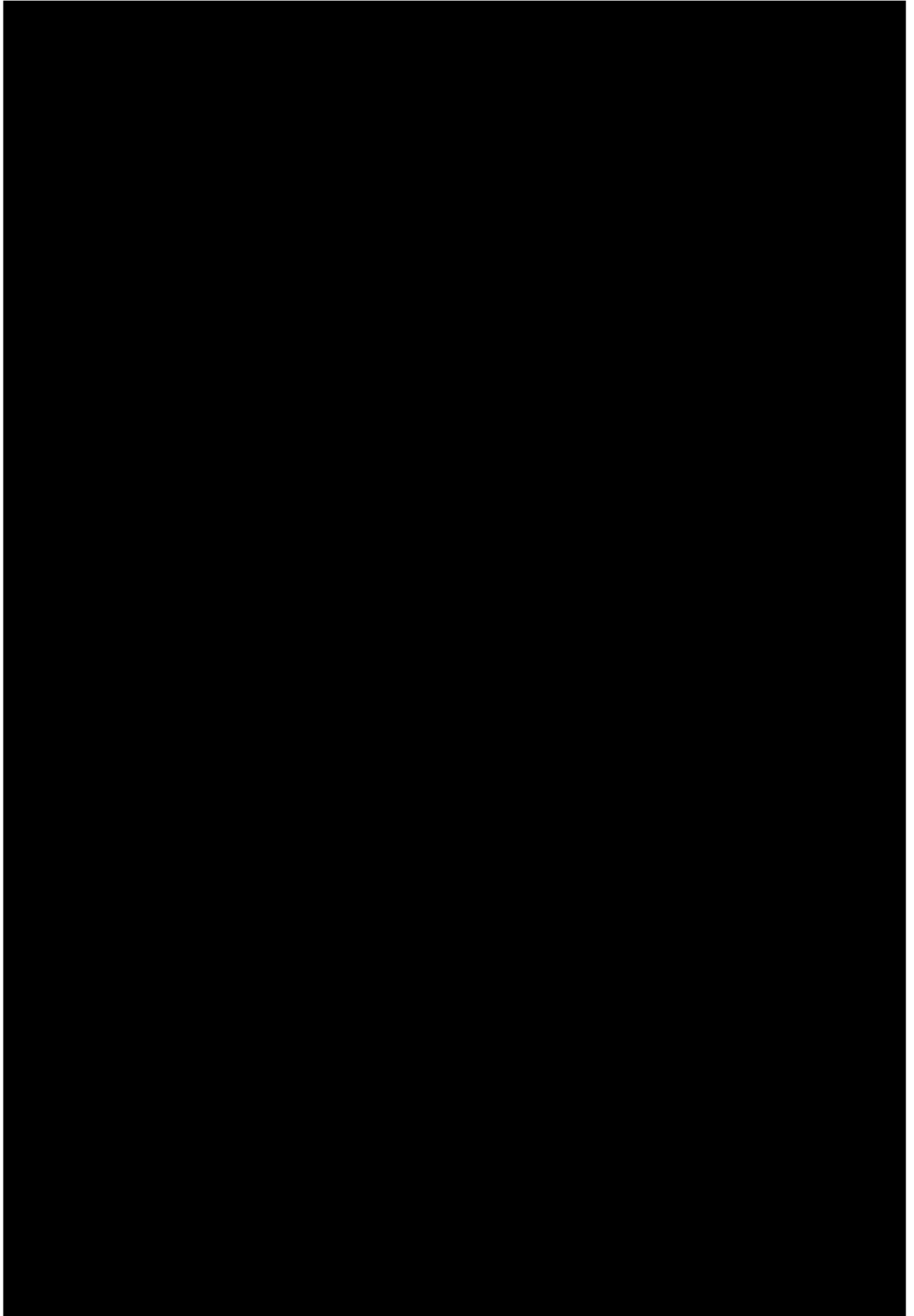


Scientific Report 2









ACKNOWLEDGEMENTS

This work was supported by MIUR (PRIN 2017; 2017A95NCJ/2017A95NCJ_002, “Stolen molecules - Stealing natural products from the depot and reselling them as new drug candidates”). Federica Raucci is supported by the University of Naples Federico II PhD scholarship in Pharmaceutical Sciences.

CONFLICT OF INTEREST

This article has been conducted and written in the absence of any commercial or financial relationships that could be construed as a potential conflict of interest. Part of the results of this thesis has been previously published [29, 86] by the Author of this PhD thesis.

DATA AVAILABILITY STATEMENT

The data that support this thesis's findings are available from Federica Raucci and the Supervisor of this PhD thesis (Prof Francesco Maione) upon reasonable request. Some data may not be made available because of privacy or ethical restrictions.

REFERENCES

1. Rouvier, E., et al., *CTLA-8, cloned from an activated T cell, bearing AU-rich messenger RNA instability sequences, and homologous to a herpesvirus saimiri gene.* J Immunol, 1993. 150(12): p. 5445-56.
2. Fossiez, F., et al., *T cell interleukin-17 induces stromal cells to produce proinflammatory and hematopoietic cytokines.* J Exp Med, 1996. 183(6): p. 2593-603.
3. Onishi, R.M. and S.L. Gaffen, *Interleukin-17 and its target genes: mechanisms of interleukin-17 function in disease.* Immunology, 2010. 129(3): p. 311-21.
4. Reynolds, J.M., P. Angkasekwinai, and C. Dong, *IL-17 family member cytokines: regulation and function in innate immunity.* Cytokine Growth Factor Rev, 2010. 21(6): p. 413-23.
5. Gaffen, S.L., *Structure and signalling in the IL-17 receptor family.* Nat Rev Immunol, 2009. 9(8): p. 556-67.
6. Kleinschek, M.A., et al., *IL-25 regulates Th17 function in autoimmune inflammation.* J Exp Med, 2007. 204(1): p. 161-70.
7. Yao, Z., et al., *Herpesvirus Saimiri encodes a new cytokine, IL-17, which binds to a novel cytokine receptor.* Immunity, 1995. 3(6): p. 811-21.
8. Gaffen, S.L., *Recent advances in the IL-17 cytokine family.* Curr Opin Immunol, 2011. 23(5): p. 613-9.
9. Liu, S., et al., *Crystal structures of interleukin 17A and its complex with IL-17 receptor A.* Nat Commun, 2013. 4: p. 1888.
10. Gaffen, S.L., et al., *The IL-23-IL-17 immune axis: from mechanisms to therapeutic testing.* Nat Rev Immunol, 2014. 14(9): p. 585-600.
11. Zrioual, S., et al., *IL-17RA and IL-17RC receptors are essential for IL-17A-induced ELR+ CXC chemokine expression in synoviocytes and are overexpressed in rheumatoid blood.* J Immunol, 2008. 180(1): p. 655-63.
12. Beringer, A., M. Noack, and P. Miossec, *IL-17 in Chronic Inflammation: From Discovery to Targeting.* Trends Mol Med, 2016. 22(3): p. 230-241.
13. D'Acquisto, F., F. Maione, and M. Pederzoli-Ribeil, *From IL-15 to IL-33: the never-ending list of new players in inflammation. Is it time to forget the humble aspirin and move ahead?* Biochem Pharmacol, 2010. 79(4): p. 525-34.

14. Lubberts, E., *The IL-23-IL-17 axis in inflammatory arthritis*. Nat Rev Rheumatol, 2015. 11(10): p. 562.
15. Gaffen, S.L., *Biology of recently discovered cytokines: interleukin-17--a unique inflammatory cytokine with roles in bone biology and arthritis*. Arthritis Res Ther, 2004. 6(6): p. 240-7.
16. Kehlen, A., et al., *Expression, modulation and signalling of IL-17 receptor in fibroblast-like synoviocytes of patients with rheumatoid arthritis*. Clin Exp Immunol, 2002. 127(3): p. 539-46.
17. Pedraza-Zamora, C.P., et al., *Th17 cells and neutrophils: Close collaborators in chronic Leishmania mexicana infections leading to disease severity*. Parasite Immunol, 2017. 39(4).
18. Wojkowska, D.W., et al., *Interactions between neutrophils, Th17 cells, and chemokines during the initiation of experimental model of multiple sclerosis*. Mediators Inflamm, 2014. 2014: p. 590409.
19. Maione, F., et al., *Interleukin 17 sustains rather than induces inflammation*. Biochem Pharmacol, 2009. 77(5): p. 878-87.
20. Witowski, J., et al., *IL-17 stimulates intraperitoneal neutrophil infiltration through the release of GRO alpha chemokine from mesothelial cells*. J Immunol, 2000. 165(10): p. 5814-21.
21. Ley, K., E. Smith, and M.A. Stark, *IL-17A-producing neutrophil-regulatory Tn lymphocytes*. Immunol Res, 2006. 34(3): p. 229-42.
22. Schwarzenberger, P., et al., *IL-17 stimulates granulopoiesis in mice: use of an alternate, novel gene therapy-derived method for in vivo evaluation of cytokines*. J Immunol, 1998. 161(11): p. 6383-9.
23. Albanesi, C., A. Cavani, and G. Girolomoni, *IL-17 is produced by nickel-specific T lymphocytes and regulates ICAM-1 expression and chemokine production in human keratinocytes: synergistic or antagonist effects with IFN-gamma and TNF-alpha*. J Immunol, 1999. 162(1): p. 494-502.
24. von Vietinghoff, S. and K. Ley, *Homeostatic regulation of blood neutrophil counts*. J Immunol, 2008. 181(8): p. 5183-8.
25. Xu, S. and X. Cao, *Interleukin-17 and its expanding biological functions*. Cell Mol Immunol, 2010. 7(3): p. 164-74.
26. Cray, C., J. Zaias, and N.H. Altman, *Acute phase response in animals: a review*. Comp Med, 2009. 59(6): p. 517-26.
27. Jovanovic, D.V., et al., *IL-17 stimulates the production and expression of proinflammatory cytokines, IL-beta and TNF-alpha, by human macrophages*. J Immunol, 1998. 160(7): p. 3513-21.
28. Wang, C.Q.F., et al., *IL-17 induces inflammation-associated gene products in blood monocytes, and treatment with ixekizumab*

- reduces their expression in psoriasis patient blood. J Invest Dermatol*, 2014. 134(12): p. 2990-2993.
29. Raucci, F., et al., *IL-17-induced inflammation modulates the mPGES-1/PPAR- γ pathway in monocytes/macrophages. Br J Pharmacol*, 2022. 179(9): p. 1857-1873.
 30. Hwang, S.Y., et al., *IL-17 induces production of IL-6 and IL-8 in rheumatoid arthritis synovial fibroblasts via NF-kappaB- and PI3-kinase/Akt-dependent pathways. Arthritis Res Ther*, 2004. 6(2): p. R120-8.
 31. Moseley, T.A., et al., *Interleukin-17 family and IL-17 receptors. Cytokine Growth Factor Rev*, 2003. 14(2): p. 155-74.
 32. Blauvelt, A. and A. Chiricozzi, *The Immunologic Role of IL-17 in Psoriasis and Psoriatic Arthritis Pathogenesis. Clin Rev Allergy Immunol*, 2018. 55(3): p. 379-390.
 33. Kehlen, A., et al., *Gene expression induced by interleukin-17 in fibroblast-like synoviocytes of patients with rheumatoid arthritis: upregulation of hyaluronan-binding protein TSG-6. Arthritis Res Ther*, 2003. 5(4): p. R186-92.
 34. Beringer, A. and P. Miossec, *Systemic effects of IL-17 in inflammatory arthritis. Nat Rev Rheumatol*, 2019. 15(8): p. 491-501.
 35. Hot, A., V. Lenief, and P. Miossec, *Combination of IL-17 and TNF α induces a pro-inflammatory, pro-coagulant and pro-thrombotic phenotype in human endothelial cells. Ann Rheum Dis*, 2012. 71(5): p. 768-76.
 36. Maione, F., et al., *IL-17A increases ADP-induced platelet aggregation. Biochem Biophys Res Commun*, 2011. 408(4): p. 658-62.
 37. Casillo, G.M., et al., *Could IL-17 represent a new therapeutic target for the treatment and/or management of COVID-19-related respiratory syndrome? Pharmacol Res*, 2020. 156: p. 104791.
 38. Raucci, F., et al., *Interleukin-17A (IL-17A), a key molecule of innate and adaptive immunity, and its potential involvement in COVID-19-related thrombotic and vascular mechanisms. Autoimmun Rev*, 2020. 19(7): p. 102572.
 39. Maione, F., et al., *Interleukin-17A (IL-17A): A silent amplifier of COVID-19. Biomed Pharmacother*, 2021. 142: p. 111980.
 40. Serhan, C.N., *Pro-resolving lipid mediators are leads for resolution physiology. Nature*, 2014. 510(7503): p. 92-101.
 41. Perretti, M., et al., *Immune resolution mechanisms in inflammatory arthritis. Nat Rev Rheumatol*, 2017. 13(2): p. 87-99.

42. Zhou, L., et al., *Monocytes and their pathophysiological role in Crohn's disease*. Cell Mol Life Sci, 2009. 66(2): p. 192-202.
43. Funk, C.D., *Prostaglandins and leukotrienes: advances in eicosanoid biology*. Science, 2001. 294(5548): p. 1871-5.
44. Hawkey, C.J., *COX-2 inhibitors*. Lancet, 1999. 353(9149): p. 307-14.
45. Koeberle, A. and O. Werz, *Perspective of microsomal prostaglandin E2 synthase-1 as drug target in inflammation-related disorders*. Biochem Pharmacol, 2015. 98(1): p. 1-15.
46. Samuelsson, B., R. Morgenstern, and P.J. Jakobsson, *Membrane prostaglandin E synthase-1: a novel therapeutic target*. Pharmacol Rev, 2007. 59(3): p. 207-24.
47. Cuzzocrea, S., et al., *The cyclopentenone prostaglandin 15-deoxy-Delta(12,14)-prostaglandin J(2) attenuates the development of acute and chronic inflammation*. Mol Pharmacol, 2002. 61(5): p. 997-1007.
48. Ricote, M., et al., *The peroxisome proliferator-activated receptor-gamma is a negative regulator of macrophage activation*. Nature, 1998. 391(6662): p. 79-82.
49. Tsai, J.S., et al., *Rosiglitazone inhibits monocyte/macrophage adhesion through de novo adiponectin production in human monocytes*. J Cell Biochem, 2010. 110(6): p. 1410-9.
50. Korbecki, J., R. Bobiński, and M. Dutka, *Self-regulation of the inflammatory response by peroxisome proliferator-activated receptors*. Inflamm Res, 2019. 68(6): p. 443-458.
51. Inada, M., et al., *Membrane-bound prostaglandin E synthase-1-mediated prostaglandin E2 production by osteoblast plays a critical role in lipopolysaccharide-induced bone loss associated with inflammation*. J Immunol, 2006. 177(3): p. 1879-85.
52. Uematsu, S., et al., *Lipopolysaccharide-dependent prostaglandin E(2) production is regulated by the glutathione-dependent prostaglandin E(2) synthase gene induced by the Toll-like receptor 4/MyD88/NF-IL6 pathway*. J Immunol, 2002. 168(11): p. 5811-6.
53. Trebino, C.E., et al., *Impaired inflammatory and pain responses in mice lacking an inducible prostaglandin E synthase*. Proc Natl Acad Sci U S A, 2003. 100(15): p. 9044-9.
54. Stichtenoth, D.O., et al., *Microsomal prostaglandin E synthase is regulated by proinflammatory cytokines and glucocorticoids in primary rheumatoid synovial cells*. J Immunol, 2001. 167(1): p. 469-74.

55. Li, X., et al., *Expression and regulation of microsomal prostaglandin E synthase-1 in human osteoarthritic cartilage and chondrocytes*. J Rheumatol, 2005. 32(5): p. 887-95.
56. Maione, F., *Commentary: IL-17 in Chronic Inflammation: From Discovery to Targeting*. Front Pharmacol, 2016. 7: p. 250.
57. Maione, F., et al., *The functional link between microsomal prostaglandin E synthase-1 (mPGES-1) and peroxisome proliferator-activated receptor γ (PPAR γ) in the onset of inflammation*. Pharmacol Res, 2020. 157: p. 104807.
58. Rchette, P. and T. Bardin, *Gout*. Lancet, 2010. 375(9711): p. 318-28.
59. Shi, Y., J.E. Evans, and K.L. Rock, *Molecular identification of a danger signal that alerts the immune system to dying cells*. Nature, 2003. 425(6957): p. 516-21.
60. Busso, N. and A. So, *Mechanisms of inflammation in gout*. Arthritis Res Ther, 2010. 12(2): p. 206.
61. Martinon, F. and L.H. Glimcher, *Gout: new insights into an old disease*. J Clin Invest, 2006. 116(8): p. 2073-5.
62. Martin, W.J., M. Walton, and J. Harper, *Resident macrophages initiating and driving inflammation in a monosodium urate monohydrate crystal-induced murine peritoneal model of acute gout*. Arthritis Rheum, 2009. 60(1): p. 281-9.
63. Di Giovine, F.S., et al., *Interleukin 1 (IL 1) as a mediator of crystal arthritis. Stimulation of T cell and synovial fibroblast mitogenesis by urate crystal-induced IL 1*. J Immunol, 1987. 138(10): p. 3213-8.
64. Schweyer, S., et al., *Continuous recruitment, co-expression of tumour necrosis factor-alpha and matrix metalloproteinases, and apoptosis of macrophages in gout tophi*. Virchows Arch, 2000. 437(5): p. 534-9.
65. Jania, L.A., et al., *Microsomal prostaglandin E synthase-2 is not essential for in vivo prostaglandin E2 biosynthesis*. Prostaglandins Other Lipid Mediat, 2009. 88(3-4): p. 73-81.
66. Mancini, J.A., et al., *Cloning, expression, and up-regulation of inducible rat prostaglandin e synthase during lipopolysaccharide-induced pyresis and adjuvant-induced arthritis*. J Biol Chem, 2001. 276(6): p. 4469-75.
67. Murakami, Y., et al., *Inhibition of monosodium urate monohydrate crystal-induced acute inflammation by retrovirally transfected prostaglandin D synthase*. Arthritis Rheum, 2003. 48(10): p. 2931-41.

68. Cleophas, M.C., T.O. Crişan, and L.A. Joosten, *Factors modulating the inflammatory response in acute gouty arthritis*. *Curr Opin Rheumatol*, 2017. 29(2): p. 163-170.
69. Terkeltaub, R., *What makes gouty inflammation so variable?* *BMC Med*, 2017. 15(1): p. 158.
70. Liu, Y., et al., *Serum levels of IL-17 are elevated in patients with acute gouty arthritis*. *Biochem Biophys Res Commun*, 2018. 497(3): p. 897-902.
71. Zhou, Z., et al., *Genetic Analysis of IL-17 Gene Polymorphisms in Gout in a Male Chinese Han Population*. *PLoS One*, 2016. 11(2): p. e0148082.
72. Dai, X.J., et al., *Changes of Treg/Th17 Ratio in Spleen of Acute Gouty Arthritis Rat Induced by MSU Crystals*. *Inflammation*, 2018. 41(5): p. 1955-1964.
73. Cristiano, C., et al., *Neutralization of IL-17 rescues amyloid- β -induced neuroinflammation and memory impairment*. *Br J Pharmacol*, 2019. 176(18): p. 3544-3557.
74. Maione, F., et al., *Repetitive Exposure of IL-17 Into the Murine Air Pouch Favors the Recruitment of Inflammatory Monocytes and the Release of IL-16 and TREM-1 in the Inflammatory Fluids*. *Front Immunol*, 2018. 9: p. 2752.
75. Allen, J.E., T.E. Sutherland, and D. Rückerl, *IL-17 and neutrophils: unexpected players in the type 2 immune response*. *Curr Opin Immunol*, 2015. 34: p. 99-106.
76. Ganesan, R. and M. Rasool, *Interleukin 17 regulates SHP-2 and IL-17RA/STAT-3 dependent Cyr61, IL-23 and GM-CSF expression and RANKL mediated osteoclastogenesis by fibroblast-like synoviocytes in rheumatoid arthritis*. *Mol Immunol*, 2017. 91: p. 134-144.
77. Matsuzaki, G. and M. Umemura, *Interleukin-17 family cytokines in protective immunity against infections: role of hematopoietic cell-derived and non-hematopoietic cell-derived interleukin-17s*. *Microbiol Immunol*, 2018. 62(1): p. 1-13.
78. Song, X., et al., *IL-17RE is the functional receptor for IL-17C and mediates mucosal immunity to infection with intestinal pathogens*. *Nat Immunol*, 2011. 12(12): p. 1151-8.
79. Sawada, Y., et al., *The Role of IL-17-Producing Cells in Cutaneous Fungal Infections*. *Int J Mol Sci*, 2021. 22(11).
80. Ishigame, H., et al., *Differential roles of interleukin-17A and -17F in host defense against mucoepithelial bacterial infection and allergic responses*. *Immunity*, 2009. 30(1): p. 108-19.

81. Das, S. and S. Khader, *Yin and yang of interleukin-17 in host immunity to infection*. F1000Res, 2017. 6: p. 741.
82. Miossec, P. and J.K. Kolls, *Targeting IL-17 and TH17 cells in chronic inflammation*. Nat Rev Drug Discov, 2012. 11(10): p. 763-76.
83. Noack, M. and P. Miossec, *Th17 and regulatory T cell balance in autoimmune and inflammatory diseases*. Autoimmun Rev, 2014. 13(6): p. 668-77.
84. Bettelli, E., et al., *Reciprocal developmental pathways for the generation of pathogenic effector TH17 and regulatory T cells*. Nature, 2006. 441(7090): p. 235-8.
85. Chang, S.H., et al., *Interleukin-17C promotes Th17 cell responses and autoimmune disease via interleukin-17 receptor E*. Immunity, 2011. 35(4): p. 611-21.
86. Raucci, F., et al., *IL-17A neutralizing antibody regulates monosodium urate crystal-induced gouty inflammation*. Pharmacol Res, 2019. 147: p. 104351.
87. Berry, S.P.D., et al., *The role of IL-17 and anti-IL-17 agents in the immunopathogenesis and management of autoimmune and inflammatory diseases*. Int Immunopharmacol, 2022. 102: p. 108402.
88. Dubash, S., et al., *The advent of IL-17A blockade in ankylosing spondylitis: secukinumab, ixekizumab and beyond*. Expert Rev Clin Immunol, 2019. 15(2): p. 123-134.
89. Messina, F. and S. Piaserico, *The dark side of the moon: the immune-mediated adverse events of IL-17A/IL-17R inhibition*. J Dermatolog Treat, 2022. 33(5): p. 2443-2454.
90. Baker, K.F. and J.D. Isaacs, *Novel therapies for immune-mediated inflammatory diseases: What can we learn from their use in rheumatoid arthritis, spondyloarthritis, systemic lupus erythematosus, psoriasis, Crohn's disease and ulcerative colitis?* Ann Rheum Dis, 2018. 77(2): p. 175-187.
91. Mills, K.H.G., *IL-17 and IL-17-producing cells in protection versus pathology*. Nat Rev Immunol, 2022: p. 1-17.
92. Álvarez-Coiradas, E., et al., *Discovery of novel immunopharmacological ligands targeting the IL-17 inflammatory pathway*. Int Immunopharmacol, 2020. 89(Pt A): p. 107026.
93. Adams, R., et al., *Bimekizumab, a Novel Humanized IgG1 Antibody That Neutralizes Both IL-17A and IL-17F*. Front Immunol, 2020. 11: p. 1894.

94. Krautter, F., et al., *Characterisation of endogenous Galectin-1 and -9 expression in monocyte and macrophage subsets under resting and inflammatory conditions*. Biomed Pharmacother, 2020. 130: p. 110595.
95. Mangan, P.R., et al., *Dual Inhibition of Interleukin-23 and Interleukin-17 Offers Superior Efficacy in Mouse Models of Autoimmunity*. J Pharmacol Exp Ther, 2015. 354(2): p. 152-65.
96. Yilmaz, Ş., et al., *Calcium hypochlorite on mouse embryonic fibroblast cells (NIH3T3) in vitro cytotoxicity and genotoxicity: MTT and comet assay*. Mol Biol Rep, 2020. 47(7): p. 5377-5383.
97. Martinez, F.O., et al., *Transcriptional profiling of the human monocyte-to-macrophage differentiation and polarization: new molecules and patterns of gene expression*. J Immunol, 2006. 177(10): p. 7303-11.
98. Jovanovic, D.V., et al., *Stimulation of 92-kd gelatinase (matrix metalloproteinase 9) production by interleukin-17 in human monocyte/macrophages: a possible role in rheumatoid arthritis*. Arthritis Rheum, 2000. 43(5): p. 1134-44.
99. Jovanovic, D.V., et al., *Modulation of TIMP-1 synthesis by antiinflammatory cytokines and prostaglandin E2 in interleukin 17 stimulated human monocytes/macrophages*. J Rheumatol, 2001. 28(4): p. 712-8.
100. Barbera, S., et al., *The small GTPase Rab5c is a key regulator of trafficking of the CD93/Multimerin-2/ β 1 integrin complex in endothelial cell adhesion and migration*. Cell Commun Signal, 2019. 17(1): p. 55.
101. Perretti, M., et al., *Selective inhibition of neutrophil function by a peptide derived from lipocortin 1 N-terminus*. Biochem Pharmacol, 1995. 50(7): p. 1037-42.
102. Kelly, S., et al., *Ultrasound-guided synovial biopsy: a safe, well-tolerated and reliable technique for obtaining high-quality synovial tissue from both large and small joints in early arthritis patients*. Ann Rheum Dis, 2015. 74(3): p. 611-7.
103. Filer, A., et al., *Utility of ultrasound joint counts in the prediction of rheumatoid arthritis in patients with very early synovitis*. Ann Rheum Dis, 2011. 70(3): p. 500-7.
104. Aletaha, D., et al., *2010 Rheumatoid arthritis classification criteria: an American College of Rheumatology/European League Against Rheumatism collaborative initiative*. Arthritis Rheum, 2010. 62(9): p. 2569-81.
105. Salmon, M., et al., *Inhibition of T cell apoptosis in the rheumatoid synovium*. J Clin Invest, 1997. 99(3): p. 439-46.

106. Kilkenny, C., et al., *Animal research: reporting in vivo experiments: the ARRIVE guidelines*. Br J Pharmacol, 2010. 160(7): p. 1577-9.
107. McGrath, J.C. and E. Lilley, *Implementing guidelines on reporting research using animals (ARRIVE etc.): new requirements for publication in BJP*. Br J Pharmacol, 2015. 172(13): p. 3189-93.
108. Bellavita, R., et al., *Temporin L-derived peptide as a regulator of the acute inflammatory response in zymosan-induced peritonitis*. Biomed Pharmacother, 2020. 123: p. 109788.
109. Ruiz-Miyazawa, K.W., et al., *Quercetin inhibits gout arthritis in mice: induction of an opioid-dependent regulation of inflammasome*. Inflammopharmacology, 2017.
110. Marchetti, C., et al., *NLRP3 inflammasome inhibitor OLT1177 suppresses joint inflammation in murine models of acute arthritis*. Arthritis Res Ther, 2018. 20(1): p. 169.
111. Akitsu, A., et al., *IL-1 receptor antagonist-deficient mice develop autoimmune arthritis due to intrinsic activation of IL-17-producing CCR2(+)V γ 6(+) γ δ T cells*. Nat Commun, 2015. 6: p. 7464.
112. Kapellos, T.S., et al., *Cannabinoid receptor 2 deficiency exacerbates inflammation and neutrophil recruitment*. Faseb j, 2019. 33(5): p. 6154-6167.
113. Podaru, M.N., et al., *Reparative macrophage transplantation for myocardial repair: a refinement of bone marrow mononuclear cell-based therapy*. Basic Res Cardiol, 2019. 114(5): p. 34.
114. Sunderkötter, C., et al., *Subpopulations of mouse blood monocytes differ in maturation stage and inflammatory response*. J Immunol, 2004. 172(7): p. 4410-7.
115. Raucci, F., et al., *In-depth immunophenotyping data relating to IL-17Ab modulation of circulating Treg/Th17 cells and of in situ infiltrated inflammatory monocytes in the onset of gouty inflammation*. Data Brief, 2019. 25: p. 104381.
116. Maione, F., et al., *Down regulation of pro-inflammatory pathways by tanshinone IIA and cryptotanshinone in a non-genetic mouse model of Alzheimer's disease*. Pharmacol Res, 2018. 129: p. 482-490.
117. Ting, J.P., et al., *Utilization of peptide phage display to investigate hotspots on IL-17A and what it means for drug discovery*. PLoS One, 2018. 13(1): p. e0190850.
118. Machado, I.D., et al., *Alterations in the profile of blood neutrophil membrane receptors caused by in vivo*

- adrenocorticotrophic hormone actions*. Am J Physiol Endocrinol Metab, 2014. 307(9): p. E754-63.
119. Eckardt, V., et al., *Chemokines and galectins form heterodimers to modulate inflammation*. EMBO Rep, 2020. 21(4): p. e47852.
 120. Mansour, A.A., et al., *Galectin-9 supports primary T cell transendothelial migration in a glycan and integrin dependent manner*. Biomed Pharmacother, 2022. 151: p. 113171.
 121. Merlino, F., et al., *Boosting Fmoc Solid-Phase Peptide Synthesis by Ultrasonication*. Org Lett, 2019. 21(16): p. 6378-6382.
 122. Cho, K., et al., *Introducing a checklist for manuscript submission to Pharmacological Research*. Pharmacol Res, 2015. 102: p. 319-21.
 123. Curtis, M.J., et al., *Experimental design and analysis and their reporting II: updated and simplified guidance for authors and peer reviewers*. Br J Pharmacol, 2018. 175(7): p. 987-993.
 124. Alexander, S.P.H., et al., *Goals and practicalities of immunoblotting and immunohistochemistry: A guide for submission to the British Journal of Pharmacology*. Br J Pharmacol, 2018. 175(3): p. 407-411.
 125. George, C.H., et al., *Updating the guidelines for data transparency in the British Journal of Pharmacology - data sharing and the use of scatter plots instead of bar charts*. Br J Pharmacol, 2017. 174(17): p. 2801-2804.
 126. de-Brito, N.M., et al., *Lipoxin-Induced Phenotypic Changes in CD115(+)/LY6C(hi) Monocytes TAM Precursors Inhibits Tumor Development*. Front Oncol, 2019. 9: p. 540.
 127. Ragab, G., M. Elshahaly, and T. Bardin, *Gout: An old disease in new perspective - A review*. J Adv Res, 2017. 8(5): p. 495-511.
 128. Amaral, F.A., et al., *Transmembrane TNF- α is sufficient for articular inflammation and hypernociception in a mouse model of gout*. Eur J Immunol, 2016. 46(1): p. 204-11.
 129. Fattori, V., F.A. Amaral, and W.A. Verri, Jr., *Neutrophils and arthritis: Role in disease and pharmacological perspectives*. Pharmacol Res, 2016. 112: p. 84-98.
 130. Saegusa, M., et al., *Contribution of membrane-associated prostaglandin E2 synthase to bone resorption*. J Cell Physiol, 2003. 197(3): p. 348-56.
 131. Geissmann, F., S. Jung, and D.R. Littman, *Blood monocytes consist of two principal subsets with distinct migratory properties*. Immunity, 2003. 19(1): p. 71-82.

132. Ingersoll, M.A., et al., *Comparison of gene expression profiles between human and mouse monocyte subsets*. *Blood*, 2010. 115(3): p. e10-9.
133. Dalbeth, N., T.R. Merriman, and L.K. Stamp, *Gout*. *Lancet*, 2016. 388(10055): p. 2039-2052.
134. Schindler, T.I., et al., *T(H)17 Cell Frequency in Peripheral Blood Is Elevated in Overweight Children without Chronic Inflammatory Diseases*. *Front Immunol*, 2017. 8: p. 1543.
135. Ye, J., et al., *Circulating Th1, Th2, Th9, Th17, Th22, and Treg Levels in Aortic Dissection Patients*. *Mediators Inflamm*, 2018. 2018: p. 5697149.
136. Ding, S., et al., *A protein structural classes prediction method based on PSI-BLAST profile*. *J Theor Biol*, 2014. 353: p. 19-23.
137. Park, J.Y., M.H. Pillinger, and S.B. Abramson, *Prostaglandin E2 synthesis and secretion: the role of PGE2 synthases*. *Clin Immunol*, 2006. 119(3): p. 229-40.
138. Kalinski, P., *Regulation of immune responses by prostaglandin E2*. *J Immunol*, 2012. 188(1): p. 21-8.
139. Sreeramkumar, V., M. Fresno, and N. Cuesta, *Prostaglandin E2 and T cells: friends or foes?* *Immunol Cell Biol*, 2012. 90(6): p. 579-86.
140. Sreeramkumar, V., et al., *Efficient T-cell priming and activation requires signaling through prostaglandin E2 (EP) receptors*. *Immunol Cell Biol*, 2016. 94(1): p. 39-51.
141. Westman, M., et al., *Expression of microsomal prostaglandin E synthase 1 in rheumatoid arthritis synovium*. *Arthritis Rheum*, 2004. 50(6): p. 1774-80.
142. Kojima, F., et al., *Defective generation of a humoral immune response is associated with a reduced incidence and severity of collagen-induced arthritis in microsomal prostaglandin E synthase-1 null mice*. *J Immunol*, 2008. 180(12): p. 8361-8.
143. Jakobsson, P.J., et al., *Identification of human prostaglandin E synthase: a microsomal, glutathione-dependent, inducible enzyme, constituting a potential novel drug target*. *Proc Natl Acad Sci U S A*, 1999. 96(13): p. 7220-5.
144. Korotkova, M., et al., *Effects of immunosuppressive treatment on microsomal prostaglandin E synthase 1 and cyclooxygenases expression in muscle tissue of patients with polymyositis or dermatomyositis*. *Ann Rheum Dis*, 2008. 67(11): p. 1596-602.
145. Jouzeau, J.Y., et al., *[Pathophysiological relevance of peroxisome proliferators activated receptors (PPAR) to joint diseases - the pro and con of agonists]*. *J Soc Biol*, 2008. 202(4): p. 289-312.

146. Navarini, L., et al., *Retention rates and identification of factors associated with anti-TNF α , anti-IL17, and anti-IL12/23R agents discontinuation in psoriatic arthritis patients: results from a real-world clinical setting*. Clin Rheumatol, 2020. 39(9): p. 2663-2670.
147. Kapoor, M., et al., *Microsomal prostaglandin E synthase-1 deficiency is associated with elevated peroxisome proliferator-activated receptor gamma: regulation by prostaglandin E2 via the phosphatidylinositol 3-kinase and Akt pathway*. J Biol Chem, 2007. 282(8): p. 5356-66.
148. García-Alonso, V., et al., *Coordinate functional regulation between microsomal prostaglandin E synthase-1 (mPGES-1) and peroxisome proliferator-activated receptor γ (PPAR γ) in the conversion of white-to-brown adipocytes*. J Biol Chem, 2013. 288(39): p. 28230-42.
149. Yousefnia, S., et al., *The influence of peroxisome proliferator-activated receptor γ (PPAR γ) ligands on cancer cell tumorigenicity*. Gene, 2018. 649: p. 14-22.
150. Thommesen, L., et al., *Selective inhibitors of cytosolic or secretory phospholipase A2 block TNF-induced activation of transcription factor nuclear factor-kappa B and expression of ICAM-1*. J Immunol, 1998. 161(7): p. 3421-30.
151. Afif, H., et al., *Peroxisome proliferator-activated receptor gamma1 expression is diminished in human osteoarthritic cartilage and is downregulated by interleukin-1beta in articular chondrocytes*. Arthritis Res Ther, 2007. 9(2): p. R31.
152. Korbecki, J., et al., *Cyclooxygenase pathways*. Acta Biochim Pol, 2014. 61(4): p. 639-49.
153. Murakami, M., *Lipid mediators in life science*. Exp Anim, 2011. 60(1): p. 7-20.
154. Chu, X., et al., *Suppression of adipogenesis program in cultured preadipocytes transfected stably with cyclooxygenase isoforms*. Biochim Biophys Acta, 2009. 1791(4): p. 273-80.
155. Pascual, G., et al., *A SUMOylation-dependent pathway mediates transrepression of inflammatory response genes by PPAR-gamma*. Nature, 2005. 437(7059): p. 759-63.
156. Zelcer, N. and P. Tontonoz, *SUMOylation and PPARgamma: wrestling with inflammatory signaling*. Cell Metab, 2005. 2(5): p. 273-5.
157. Di Francesco, L., et al., *Pharmacological Characterization of the Microsomal Prostaglandin E(2) Synthase-1 Inhibitor AF3485 In Vitro and In Vivo*. Front Pharmacol, 2020. 11: p. 374.

158. Tontonoz, P. and B.M. Spiegelman, *Fat and beyond: the diverse biology of PPARgamma*. *Annu Rev Biochem*, 2008. 77: p. 289-312.
159. Napimoga, M.H., et al., *Peroxisome proliferator-activated receptor-gamma ligand, 15-deoxy-Delta12,14-prostaglandin J2, reduces neutrophil migration via a nitric oxide pathway*. *J Immunol*, 2008. 180(1): p. 609-17.
160. Posadas, I., et al., *Co-regulation between cyclo-oxygenase-2 and inducible nitric oxide synthase expression in the time-course of murine inflammation*. *Naunyn Schmiedebergs Arch Pharmacol*, 2000. 361(1): p. 98-106.
161. Mosca, M., et al., *Regulation of the microsomal prostaglandin E synthase-1 in polarized mononuclear phagocytes and its constitutive expression in neutrophils*. *J Leukoc Biol*, 2007. 82(2): p. 320-6.
162. Kabala, P.A., et al., *Promotion of macrophage activation by Tie2 in the context of the inflamed synovia of rheumatoid arthritis and psoriatic arthritis patients*. *Rheumatology (Oxford)*, 2020. 59(2): p. 426-438.
163. Dhanasekar, C. and M. Rasool, *Morin, a dietary bioflavonol suppresses monosodium urate crystal-induced inflammation in an animal model of acute gouty arthritis with reference to NLRP3 inflammasome, hypo-xanthine phospho-ribosyl transferase, and inflammatory mediators*. *Eur J Pharmacol*, 2016. 786: p. 116-127.
164. Margalit, A., et al., *Altered arachidonic acid metabolism in urate crystal induced inflammation*. *Inflammation*, 1997. 21(2): p. 205-22.
165. Perez-Ruiz, F., N. Dalbeth, and T. Bardin, *A review of uric acid, crystal deposition disease, and gout*. *Adv Ther*, 2015. 32(1): p. 31-41.
166. Cunha, T.M., et al., *Crucial role of neutrophils in the development of mechanical inflammatory hypernociception*. *J Leukoc Biol*, 2008. 83(4): p. 824-32.
167. Hainer, B.L., E. Matheson, and R.T. Wilkes, *Diagnosis, treatment, and prevention of gout*. *Am Fam Physician*, 2014. 90(12): p. 831-6.
168. Staurengo-Ferrari, L., et al., *Trans-Chalcone Attenuates Pain and Inflammation in Experimental Acute Gout Arthritis in Mice*. *Front Pharmacol*, 2018. 9: p. 1123.
169. Maione, F., et al., *Anti-inflammatory and analgesic activity of carnosol and carnosic acid in vivo and in vitro and in silico*

- analysis of their target interactions.* Br J Pharmacol, 2017. 174(11): p. 1497-1508.
170. Martinon, F., et al., *Gout-associated uric acid crystals activate the NALP3 inflammasome.* Nature, 2006. 440(7081): p. 237-41.
171. Dinarello, C.A., *Blocking IL-1 in systemic inflammation.* J Exp Med, 2005. 201(9): p. 1355-9.
172. So, A., et al., *A pilot study of IL-1 inhibition by anakinra in acute gout.* Arthritis Res Ther, 2007. 9(2): p. R28.
173. Miossec, P., *Update on interleukin-17: a role in the pathogenesis of inflammatory arthritis and implication for clinical practice.* RMD Open, 2017. 3(1): p. e000284.
174. Klesney-Tait, J., et al., *Trans epithelial migration of neutrophils into the lung requires TREM-1.* J Clin Invest, 2013. 123(1): p. 138-49.
175. Bouchon, A., J. Dietrich, and M. Colonna, *Cutting edge: inflammatory responses can be triggered by TREM-1, a novel receptor expressed on neutrophils and monocytes.* J Immunol, 2000. 164(10): p. 4991-5.
176. Kageyama, Y., et al., *Interleukin-16 in synovial fluids from cases of various types of arthritis.* Joint Bone Spine, 2000. 67(3): p. 188-93.
177. Cho, M.L., et al., *IL-17 induces the production of IL-16 in rheumatoid arthritis.* Exp Mol Med, 2008. 40(2): p. 237-45.
178. Bosco, M.C., F. Raggi, and L. Varesio, *Therapeutic Potential of Targeting TREM-1 in Inflammatory Diseases and Cancer.* Curr Pharm Des, 2016. 22(41): p. 6209-6233.
179. Glatt, S., et al., *Dual IL-17A and IL-17F neutralisation by bimekizumab in psoriatic arthritis: evidence from preclinical experiments and a randomised placebo-controlled clinical trial that IL-17F contributes to human chronic tissue inflammation.* Ann Rheum Dis, 2018. 77(4): p. 523-532.
180. Robert, M. and P. Miossec, *IL-17 in Rheumatoid Arthritis and Precision Medicine: From Synovitis Expression to Circulating Bioactive Levels.* Front Med (Lausanne), 2018. 5: p. 364.
181. Fiocco, U., et al., *JAK/STAT/PKC δ molecular pathways in synovial fluid T lymphocytes reflect the in vivo T helper-17 expansion in psoriatic arthritis.* Immunol Res, 2014. 58(1): p. 61-9.
182. Fiocco, U., et al., *Quantitative imaging by pixel-based contrast-enhanced ultrasound reveals a linear relationship between synovial vascular perfusion and the recruitment of pathogenic IL-*

- 17A-F(+)*IL-23(+) *CD161(+)* *CD4(+)* *T helper cells in psoriatic arthritis joints*. Clin Rheumatol, 2017. 36(2): p. 391-399.
183. Costa, L., et al., *Small molecule therapy for managing moderate to severe psoriatic arthritis*. Expert Opin Pharmacother, 2017. 18(15): p. 1557-1567.
184. Roussel, L., et al., *IL-17 promotes p38 MAPK-dependent endothelial activation enhancing neutrophil recruitment to sites of inflammation*. J Immunol, 2010. 184(8): p. 4531-7.
185. Hueber, W., et al., *Secukinumab, a human anti-IL-17A monoclonal antibody, for moderate to severe Crohn's disease: unexpected results of a randomised, double-blind placebo-controlled trial*. Gut, 2012. 61(12): p. 1693-700.
186. Schmidt, C., *Suicidal thoughts end Amgen's blockbuster aspirations for psoriasis drug*. Nat Biotechnol, 2015. 33(9): p. 894-5.
187. Reich, K., et al., *Bimekizumab versus Secukinumab in Plaque Psoriasis*. N Engl J Med, 2021. 385(2): p. 142-152.
188. Warren, R.B., et al., *Bimekizumab versus Adalimumab in Plaque Psoriasis*. N Engl J Med, 2021. 385(2): p. 130-141.
189. Lucaciu, L.A., et al., *Real-world experience with tofacitinib in ulcerative colitis: a systematic review and meta-analysis*. Therap Adv Gastroenterol, 2021. 14: p. 17562848211064004.

PERSONAL ACKNOWLEDGEMENTS

Writing these thank-you sentences is the concluding piece of my thesis. It has been a journey of intense scientific and personal learning, so I would like to say a few words of gratitude to all the people who have supported and helped me during this period.

First, I want to thank the person who allowed me to be here today, **Francesco**. Thank you very much, Boss, for all the opportunities you have offered me, the tolerance you have had, and the teachings you have given me. You've educated me over these years not as a boss, but as a friend, an experimental dad and an older brother. There are no words that sum up all the esteem I have for you and for us: this wonderful group. Thank you **Nella, Noemi and Giammi**, for supporting me and, above all, tolerated me on this wonderful journey together. You will always be my F62 family... Thank you.

This journey was also enriched by a wonderful experience in Birmingham, with the support and help of my second boss **Asif**. Thank you for all the lessons you have given me, the beautiful Lab experience you have allowed me, and the wonderful people you introduced me. I will always carry you and all the guys in your Lab in my heart, especially **Adel and Jennifer**: I am a big fan of yours beyond any distance.

I also wanted to thank Prof **Cirino**, Prof **Bucci**, Prof **Vellecco**, and all the other **Profs** in the Department of Pharmacy who contributed directly or indirectly to the realisation of this project.

To **Mum and Dad**, for their constant support and their teachings, without which I would not be what I am today. Without you, none of this would have been possible, and I am immensely grateful for that. Sooner or later, all the anxieties and worries I kindly gave you had to be repaid! I do not have money, so I hope that these words can begin to repay all that you have given me. I love you.

Thank you **Pati, Alberto**, and my loves: **Antonia and Biagio**. Thank you for your smiles, suggestions, caresses, lightheartedness and kisses full of immense love. You are and always will be my fixed point.

Paolo, in this journey, you have been fundamental to me. Your "know that I love you, and I will always be there for you" have made me

stronger in facing everything... Despite every distance, you are a point of reference for me.

Thank you **Aunty Maghi**, who always supported me like a mother and advised me like a sister. For me, you're a stone, always there to support me, and you've been like that throughout my journey.

Thank you beautiful **Granny**, who, with your loving eyes and proud hug, made me the person I am today. I will never stop thanking you for genuinely teaching me the meaning of pure love.

Thank you to all **my Family**, irreplaceable and indissoluble sustainers. Without your support and love, I would never have reached so high without fear of heights. You are my stable point.

Thank you **Imma** and thank you **Sasi**. With you I started and finished this journey... With you I laughed, cried, and talked about every fear, joy, worry and satisfaction I had... Your advice and your constant presence have allowed me to reach this goal... Thank you for always believing in me. And I thank you to that ugly Vincenzo Diamare Street that I bless every day because it could not give me the most beautiful gift: true friends like you.

Thank you to my 3B (**Fede, Ioli and Dali**), who became 4B (**Ceci**) in the meantime, to your **mates/husbands** and to our little **Giulia**. Thank you for always being there for me, supporting me in every choice and decision, and always giving me a smile, a laugh and kindness... You have been and will always be my strength.

Thank you **Lulla**, that "senz e te Nun pozz sta perché tu m appartien". Thank you always because you never made your physical distance a real distance. Thank you for all the love and goodness you give me, even with a single look on video call. And thank you always for the constant support and love you gave me.

Thank you to my **aMica**. My great supporter from beginning to end... and by beginning, I mean beginning, well, almost 10 years have passed. You are an infinite certainty for me, and with one look, you have always given me more than a thousand words.... Thank you for always being there and remember that I am and will be there for you as long as you will return to speaking Neapolitan.

Thank you **Corte**. With you, my post-work evenings and weekends have always been lighter. Your smile, harmony and joy have made me a better person, and for that, I am immensely grateful to our little house. So we sing in choir: Brazilll la la la la la laaaaaa...

No less lucky I have been in my **new little house**. And so, thank you Lilli, my pole dancer, Rossana, our mommy, Ivan, our break-dermatologist, Marco and Rita. Thank you for your constant support and assistance, but, above all, for our tidy sandwiches, burnt schnitzels and many, many laughs.

Thank you **Nerea and Gina**, that have been with me during these six months in the UK. Thank you for the amazing laughs, the fantastic food and, above all, as actual British citizens, the incredible drinks. You have been an essential part of this journey for me, so I must give you great recognition.

Last/s, but not least, I wanted to thank **Dario** and our greatest fans, **Caterina and Gaspare**.

You, that from nothing have coloured this picture that was only drafted in the best possible way. You, that have given me strength, support, and courage in every difficult and joyful moment of this journey. To you who believe in me more than anyone else, I simply wanted to say: Thank you for constantly being there. "Always and forever on the same side, you will find me".

And finally, I would like to dedicate a super and well-deserved Thank You to **Myself**. To me, that with great love and passion have faced this journey... To me, that with so many tears but also so many joys and satisfactions have become an adult in these four walls. To me, that believed in this journey, achieved it, and concluded it in the best possible way.

I am proud of myself...

... that myself who with the help of all of you has become a beautiful person.

PERSONAL ACKNOWLEDGEMENTS (ITALIAN VERSION)

Scrivere queste frasi di ringraziamento è il tocco finale della mia tesi. È stato un percorso di profondo apprendimento sia scientifico che personale, pertanto, vorrei spendere due parole di ringraziamento nei confronti di tutte le persone che mi hanno sostenuto ed aiutato durante questo periodo.

Primo tra tutti volevo ringraziare la persona che mi ha permesso di arrivare oggi qui, **Francesco**. Grazie mille Boss, per tutte le opportunità che mi hai dato, per tutta la pazienza che hai avuto e per tutti gli insegnamenti che mi hai regalato. Mi hai cresciuto in questi anni non da capo, ma da amico, da papà sperimentale e da fratello maggiore. Non ci sono parole che riassumono tutta la stima che ho di te, e che ho di noi: questo meraviglioso gruppo. Grazie **Nella, Noemi e Giammi** per avermi supportato e, soprattutto, sopportato in questo meraviglioso percorso insieme. Resterete per sempre la mia famiglia F62... Grazie.

Questo percorso inoltre è stato arricchito da un'esperienza bellissima a Birmingham, con il supporto ed il sostegno del mio secondo boss **Asif**. Grazie per tutti gli insegnamenti che mi hai dato, della bella esperienza in lab che mi hai permesso di vivere, e delle bellissime persone che mi hai fatto conoscere. Porterò sempre nel cuore te e tutti i ragazzi del tuo Lab, in particolare **Adel e Jennifer**: sono una vostra grande fan, oltre ogni distanza.

Volevo, inoltre, ringraziare il Prof **Cirino**, la Prof, **Bucci**, la Prof **Vellecco**, nonché tutti gli altri **Proff** del Dipartimento di Farmacia che, in maniera diretta o indiretta, hanno contribuito alla realizzazione di questo percorso.

A **Mamma e Papà**, al loro costante sostegno ed ai loro insegnamenti senza i quali oggi non sarei ciò che sono. Senza di voi, tutto questo non sarebbe stato possibile, e per questo ve ne sono immensamente grata. Prima o poi tutte le ansie e le preoccupazioni che vi ho gentilmente donato dovevano essere ripagate! Soldi non ne ho, quindi spero che queste parole possano iniziare a ricompensare tutto quello che mi avete donato. Vi voglio bene.

Grazie a voi **Pati, Alberto**, ed amori miei: **Antonia e Biagio**. Grazie ai vostri sorrisi, ai vostri suggerimenti, alle vostre carezze, alla vostra

spensieratezza ed ai vostri baci pieni di amore immenso. Siete e sarete sempre il mio punto fermo.

Paolo, in questo percorso tu per me sei stato fondamentale. I tuoi "sappi che ti voglio bene e ci sarò sempre per te" mi hanno resa più forte nell'affrontare ogni cosa. Nonostante ogni distanza, sei un punto di riferimento per me.

Grazie **zia Maghi** che mi hai sempre sostenuto come una mamma e consigliato come una sorella. Per me sei una roccia sempre lì pronta a sorreggermi, e tale sei stata in tutto questo mio percorso.

Grazie **Nonnina** bella, che con quel tuo sguardo pieno d'amore e quel tuo abbraccio pieno di orgoglio, mi hai reso la persona che oggi sono. Non smetterò mai di ringraziarti per avermi insegnato davvero cos'è l'amore puro.

Grazie a tutta la **mia famiglia**, sostenitrice insostituibile ed indissolubile. Senza il vostro sostegno ed il vostro amore non sarei mai arrivata così in alto senza paura dell'altezza. Siete il mio punto stabile.

Grazie **Imma** e grazie **Sasi**. Con voi ho iniziato e terminato questo percorso. Con voi ho riso, pianto e parlato di ogni paura, gioia, preoccupazione e soddisfazione avuta. I vostri consigli e la vostra presenza costante mi hanno permesso di raggiungere questo obiettivo. Grazie per aver creduto sempre in me. E dico grazie a quella bruttissima Via Vincenzo Diamare che ogni giorno benedico, perché non poteva farmi regalo più grande e più bello: veri amici come voi.

Grazie alle mie 3B (**Fede, Ioli e Dali**) che in corso d'opera sono diventate 4B (**Ceci**), ai vostri **compagni/mariti** ed alla nostra piccola **Giulia**. Grazie di essere stati sempre presenti, di avermi supportato in ogni mia scelta e decisione, di avermi sempre dedicato un sorriso, una risata ed una carezza... Siete stati e sarete sempre la mia forza.

Grazie **Lulla**, che "senz e te Nun pozz sta perché tu m appartien". Grazie sempre perché non hai mai reso la tua lontananza fisica, una distanza reale. Grazie di tutto l'amore ed il bene che mi trasmetti anche con un solo sguardo in videochiamata. E grazie sempre del supporto costante e dell'amore che mi hai regalato.

Grazie a **Mica** mia. Mia grande sostenitrice dall'inizio alla fine... e per inizio intendo inizio inizio, bhe quasi 10 anni sono passati. Sei un'infinita certezza per me, e con uno sguardo mi hai sempre trasmesso più di mille parole. Grazie di esserci sempre e ricorda che io per te ci sono e ci sarò, a patto che tornerai a parlare napoletano.

Grazie **Corte**, con voi le mie serate post lavoro ed i miei weekend sono stati sempre più leggeri. Il vostro sorriso, la vostra armonia e la vostra gioia mi hanno reso una persona migliore, e di questo sono immensamente grata alla nostra casetta. Quindi cantiamo in coro: Brazilll la la la la la la laaaaaa...

Non meno fortunata sono stata nella mia **nuova casetta**. E quindi grazie Lilli, la mia pole dancer, Rossana, la nostra mamma, Ivan, il nostro rompi-dermatologo, Marco e Rita. Grazie per il supporto e sostegno costante, ma soprattutto per i nostri panini ordinati, cotolette bruciate e tante tante risate.

Grazie a voi **Nerea** e **Gina**, che mi avete accompagnato in questi sei mesi in UK. Grazie delle immense risate, delle grandi mangiate e soprattutto, da veri cittadini british, delle grandi bevute. Siete state per me un tassello importante di questo percorso, quindi a voi devo un grandissimo riconoscimento.

Per ultimo/i, ma assolutamente non per importanza, volevo ringraziare te **Dario** ed i nostri più grandi sostenitori, **Caterina** e **Gaspere**. Te che dal nulla hai colorato nel miglior modo possibile questo quadro che era solo abbozzato. Te che mi hai dato forza, sostegno e coraggio in ogni momento di difficoltà e di gioia di questo percorso. A te che credi in me più di ogni altra persona, volevo semplicemente dire: Grazie di esserci stato e di esserci costantemente. "Sempre e per sempre dalla stessa parte mi troverai".

Ed infine, vorrei dedicare un super e meritato Grazie a **Me stessa**. A me che con grande amore, e passione ho affrontato questo percorso... A me che con tanti pianti ma anche tantissime gioie e soddisfazioni sono diventata grande in queste quattro mura. A me che ho creduto in questo percoso, e l'ho ottenuto, raggiunto e concluso nel migliore di modi. Sono fiera di me stessa...
... quella me stessa che con l'aiuto di tutti voi è diventata una grande persona.